БЕЗОПАСНОСТЬ ТЕХНОГЕННЫХ И ПРИРОДНЫХ СИСТЕМ

№1 2023

SAFETY OF TECHNOGENIC AND NATURAL SYSTEMS

n.1 2023

ISSN 2541-9129

DOI 10.23947/2541-9129

Сетевой электронный теоретический и научно - практический журнал

Network Electronic Journal

https://www.bps-journal.ru

Safety of Technogenic and Natural Systems

No. 1, 2023

Online electronic journal

Published since 2017

Quarterly
(February, May, August, November)
December 2022 – February 2023

ISSN 2541-9129
DOI: 10.23947/2541-9129

Founder and publisher ─ Don State Technical University (DSTU), Rostov-on-Don, Russia

Included in the list of peer-reviewed scientific editions where the basic research results of doctoral, candidate's theses should be published (State Commission for Academic Degrees and Titles List) in the following research areas:

2.1.16. Labor Protection in Construction (Engineering Sciences)
2.5.11. Ground Transport and Technological Means and Complexes (Engineering Sciences)
2.5.21. Machines, Aggregates and Technological Processes (Engineering Sciences)
2.6.1. Metallurgical Science and Heat Treatment of Metals and Alloys (Engineering Sciences)
2.6.5. Powder Metallurgy and Composite Materials (Engineering Sciences)
2.6.17. Materials Science (Engineering Sciences)
2.10.1. Fire Safety (Engineering Sciences)
2.10.2. Environmental Safety (Engineering Sciences)
2.10.3. Occupational Safety (Engineering Sciences)

The journal is indexed and archived in the Russian Science Citation Index (RSCI), CyberLeninka, ROAD, GoogleScholar.

he journal is a member, Association of Science Editors and Publishers (ASEP) and CrossRef.

Certificate of mass media registration ЭЛ № ФС 77 – 66531 of 21.07.2016 is issued by the Federal Service for Supervision of Communications, Information Technology, and Mass Media

The issue is prepared by:
Inna V. Boyko, Daliya S. Bogatyreva (English version)

Founder's, Publisher's and Printery Address:
Gagarin Sq. 1, Rostov-on-Don, 344003, Russia. Phone: +7 (863) 2-738-372
E-mail: spu-10.2.3@donstu.ru https://btps.elpub.ru/

CONTENTS

TECHNOSPHERE SAFETY

MACHINE BUILDING

CHEMICAL TECHNOLOGIES, MATERIALS SCIENCES, METALLURGY

TECHNOSPHERE SAFETY

Original article
UDC 519.6:616-036.2
https://doi.org/10.23947/2541-9129-2023-1-4-15

Statistical Assessment of Biogenic Risk for the Human Population from New Viral Infections Based on COVID-19

Nataliya N. Azimova ✉, **Maria V. Bedoidze**, **Svetlana N. Kholodova**, **Tatyana A. Mokina**, **Dzhakhangul Kh. Zairova**, **Aleksandr S. Ermakov**
Don State Technical University, 1, Gagarin Sq., Rostov-on-Don, Russian Federation
✉ arkomaazimov@mail.ru

Abstract
Introduction. Understanding the epidemic curve and spatiotemporal dynamics of SARS-CoV-2 virus is of fundamental importance for the work of the health system during epidemic and pandemic periods. Firstly, the data obtained allow us to assess the epidemiological characteristics of the virus. Secondly, it becomes possible to develop and coordinate measures to counter the spread of COVID-19, to allocate resources reasonably. The work objective is to create and initialize a mathematical model of the epidemic process, which makes it possible to explain the observed dynamics, to predict its development and to assess the reliability of such forecasts.
Materials and Methods. Scientific research was based on the statistical data analysis. A hierarchy of mathematical models describing the dynamics of the spread of a new coronavirus infection (COVID-19) and the mortality of COVID-positive patients from 12.02.2020 to 22.09.2021 has been constructed. The incidence submodel reflects regular (aperiodic and periodic), as well as random components. To study and predict the processes, the classical technique of time series research, correlation and Fourier analysis were used. This approach allowed using the method of moments to identify the statistical properties of the scientific research object, and then visualize the stages and algorithm of work.
Results. An optimistic, pessimistic and intermediate scenario of infection spread has been mathematically investigated. Their strengths and weaknesses are noted. Numerical characteristics of the trend model and the model of fluctuations in the incidence of COVID-19 are systematized in the form of tables. Based on these data, a conclusion is formulated about the optimality of the pessimistic model: after the highest possible indicators, the infection curve reaches a plateau, and the virus remains in the population. It has been established that the spread of a new coronavirus infection has a pronounced seasonal character with a period of 1/3 of the year. Mathematical analysis and modeling of the mortality dynamics of COVID-positive patients revealed weekly fluctuations in the level of deaths. At the same time, it turned out that the maximum risk corresponds to the 15th and 22nd day of infection. According to the hypothesis proposed by the authors, this virus will be characteristic of the human population. The mortality rate is expected to be 1.75 %. The calculations have shown that the influence of random components of morbidity and mortality will correspond to seasonal fluctuations.
Discussion and Conclusion. The probable frequency of the epidemic has been established — three times a year. The potential mortality rate is determined as constant. It is caused by epidemiological and organizational reasons, i.e. the work of medical institutions and authorities. Taking into account the features of the new coronavirus strain (omicron), it is possible to predict the further dynamics of the pandemic and make recommendations regarding its prevention. The authors believe that vaccination should be carried out three times a year. Optimal periods of vaccination campaigns: 05.02–15.02, 17.05–28.05, 24.09–5.10.

Keywords: epidemic, pandemic, new coronavirus infection, SARS-CoV-2, COVID-19, mortality of COVID-positive patients, epidemiological characteristics of the virus, counter the spread of COVID-19, mathematical model of the epidemic process, infection spread scenario, COVID-19 trend model, COVID-19 incidence fluctuation model, omicron, recommended vaccination periods, vaccination campaigns.

Acknowledgements. The authors would like to thank the scientific project consultant O. V. Yatsenko, associate professor, Cand. Sci. (Eng.), who made a significant contribution to the construction of a mathematical model of COVID-19 spread and made valuable comments in the design of this work.

For citation. N. N. Azimova, M. V. Bedoidze, S. N. Kholodova, T. A. Mokina, Dz. Kh. Zairova, A. S. Ermakov. Statistical Assessment of Biogenic Risk for the Human Population from New Viral Infections Based on COVID-19. Safety of Technogenic and Natural Systems, 2023, no.1, pp. 4–15. https://doi.org/10.23947/2541-9129-2023-1-4-15

Introduction. Understanding the epidemic curve and spatiotemporal dynamics of SARS-CoV-2 virus spread is necessary, firstly, to assess its epidemiological characteristics. In addition, it allows us to work out and implement measures to counter the spread of coronavirus infection (COVID-19), rationally allocate resources. The work objective is to create a mathematical model of the epidemic process, which makes it possible to explain the observed dynamics, predict the spread of infection and assess the reliability of such forecasts. COVID-19 is a new disease, so it is being studied through detailed monitoring of infections and mortality. The results are interpreted using mathematical models and related analytical approaches [1–2]. Knowledge of the evolutionary patterns and numerical indicators of epidemic diseases makes it possible to stop the process in a timely manner, using official medical and other organizational resources [3–4]. Reliable factual information on the incidence of COVID-19 and related mortality on a global scale [5] is published on worldometers.info[1] (the period from 12.02.2020 to 22.09.2021 is considered). The use of these data reduces the errors of regional and time monitoring to some extent, but may prevent the identification of local dynamic parameters of the process. However, the duration of the observations recorded in [5] allows us to hope that this disadvantage is offset by the time series analysis technique [6].

The available data on the dynamics of morbidity and mortality of Covid-positive patients from 12.02.2020 to 22.09.2021 are taken from worldometers.info. Based on them, the authors have constructed the diagrams (Fig. 1–2).

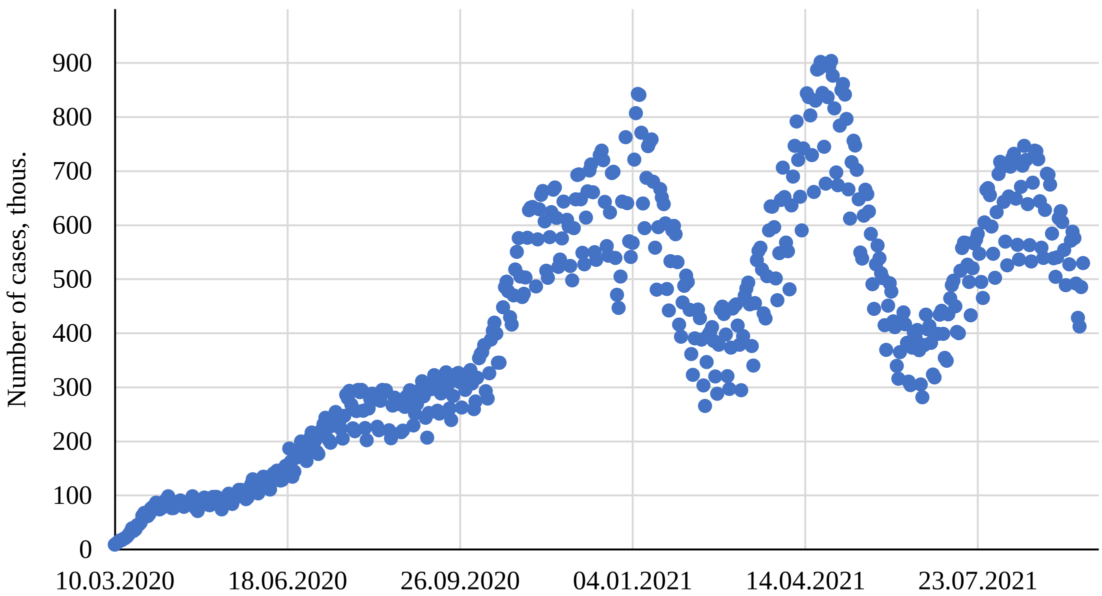

Fig. 1. Data on the incidence of COVID-19

[1] Covid-19 coronavirus pandemic. International team of developers, researchers, and volunteers. Available from: https://www.worldometers.info/coronavirus/ (accessed 10.01.2023).

The authors set the task to analyze the relationship of mortality (recorded subsequently) with the stage of the pandemic and the level of morbidity. To do this, the initial data were grouped by quarters (3 months). In Figure 2, they are indicated by dots of a certain color. This approach visualizes the representation of transformed mortality data, in which the moments of death do not explicitly appear.

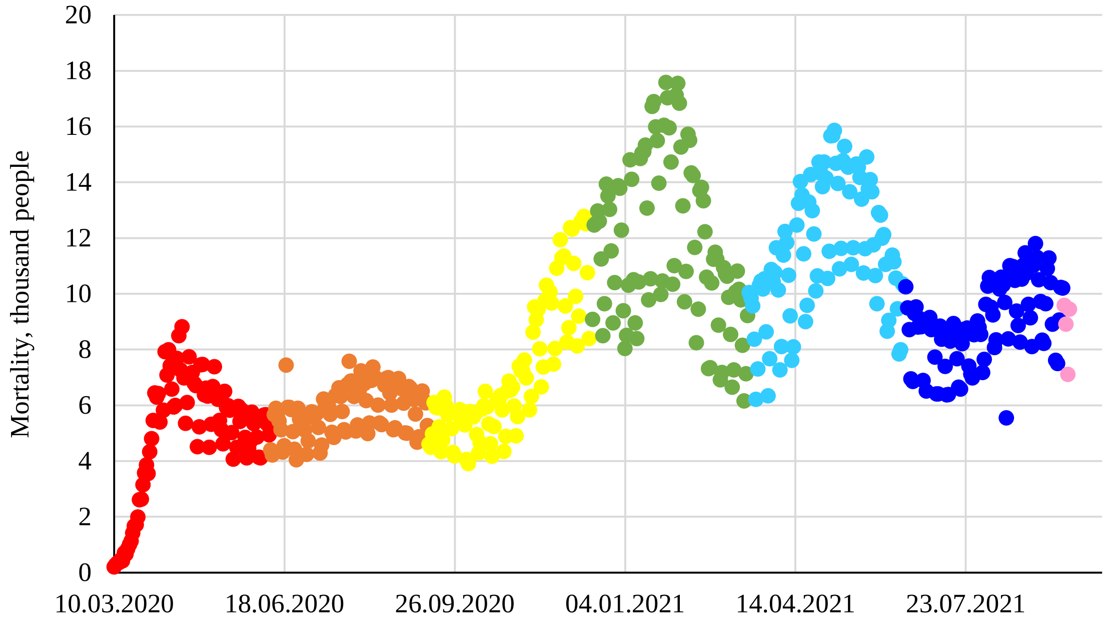

Fig. 2. Actual data on mortality of Covid-positive patients. The red dots indicate the pandemic period from 12.02.20 to 9.06.20; orange — from 10.06.20 to 10.09.20; yellow — from 11.09.20 to 14.12.20; green — from 16.12.20 to 17.03.21; light blue — from 18.03.21 to 17.06.21; blue — from 18.06.21 to 18.09.21; lilac — from 19.09.21 to 22.09.21

Materials and Methods. The data considered are a composition of regular and random components. In the regular ones, aperiodic and periodic components are distinguished. Accordingly, the analysis, interpretation and forecasting in this case are performed by classical means of time series research [6]. We are talking about the sequential allocation of the trend (aperiodic component), cyclic and noise (random) components. Each of them is mathematically characterized by amplitude and (or) time parameters [7]. We will sequentially isolate these components from the actual data, and then describe the results.

The classical technique of studying time series $\Phi(t)$ was chosen as a mathematical tool for analyzing and predicting the dynamics of COVID-19 [6]. It is implemented in several stages, which are aimed at consistently identifying regular $P(t)$, oscillatory $\Pi(t)$ and random $\xi(t)$ components of the trend. In this case, as a rule, the hypothesis is taken into account that the time average value of the last two components of the time series is zero

$$\Phi(t) = P(t) + \Pi(t) + \xi(t), \tag{1}$$

that is , the ratio is fulfilled:

$$\lim_{T\to\infty}\frac{1}{T}\int_0^T f(t)\,dt = \lim_{T\to\infty}\frac{1}{T}\int_0^T \xi(t)\,dt = 0. \tag{2}$$

The regular component $P(t)$ is extracted first. The algorithmic basis here is the theory of function approximation [7]. It is based on the idea of finding a curve of a given type, as close as possible to a cloud of points displaying a time series. In this case, it is required to successfully choose a template for approximating a series function. On the one hand, this is an exceptionally creative task. On the other hand, it requires deep knowledge in the field of mathematical analysis. Then the regular component is excluded from (1) and the combination $\Phi(t) - P(t) = \Pi(t) + \xi(t)$ is analyzed.

Important characteristics of such a residual term are period and form [8]. The technique of correlation and Fourier analysis is used to identify the period of the leaving $\Pi(t)$. In the framework of autocorrelation analysis, the period of the function $\Pi(t)$ is the value τ satisfying the condition

$$\frac{1}{T}\int_0^T \Pi(t)\cdot\Pi(t+\tau)\,dt \to \max, \quad (3)$$

where $[0\ldots T]$ — $\Pi(t)$ value observation interval.

The use of a discrete Fourier transform for the same purpose makes it possible to localize the value of τ in a narrow interval. Knowing τ, it is possible to identify the form of the periodic component, but often researchers limit themselves to the first harmonic.

The final stage is the identification of statistical properties $\xi(t) = \Phi(t) - P(t) - \Pi(t)$. For this, the method of moments is the most convenient one [9]. It works like this: the actual noise moments of the series $\xi(t)$ are compared with the moments of the model noise given by the known distribution functions $F(\xi)$. The described scheme for analyzing the time series $\Phi(t)$ is shown in Fig. 3.

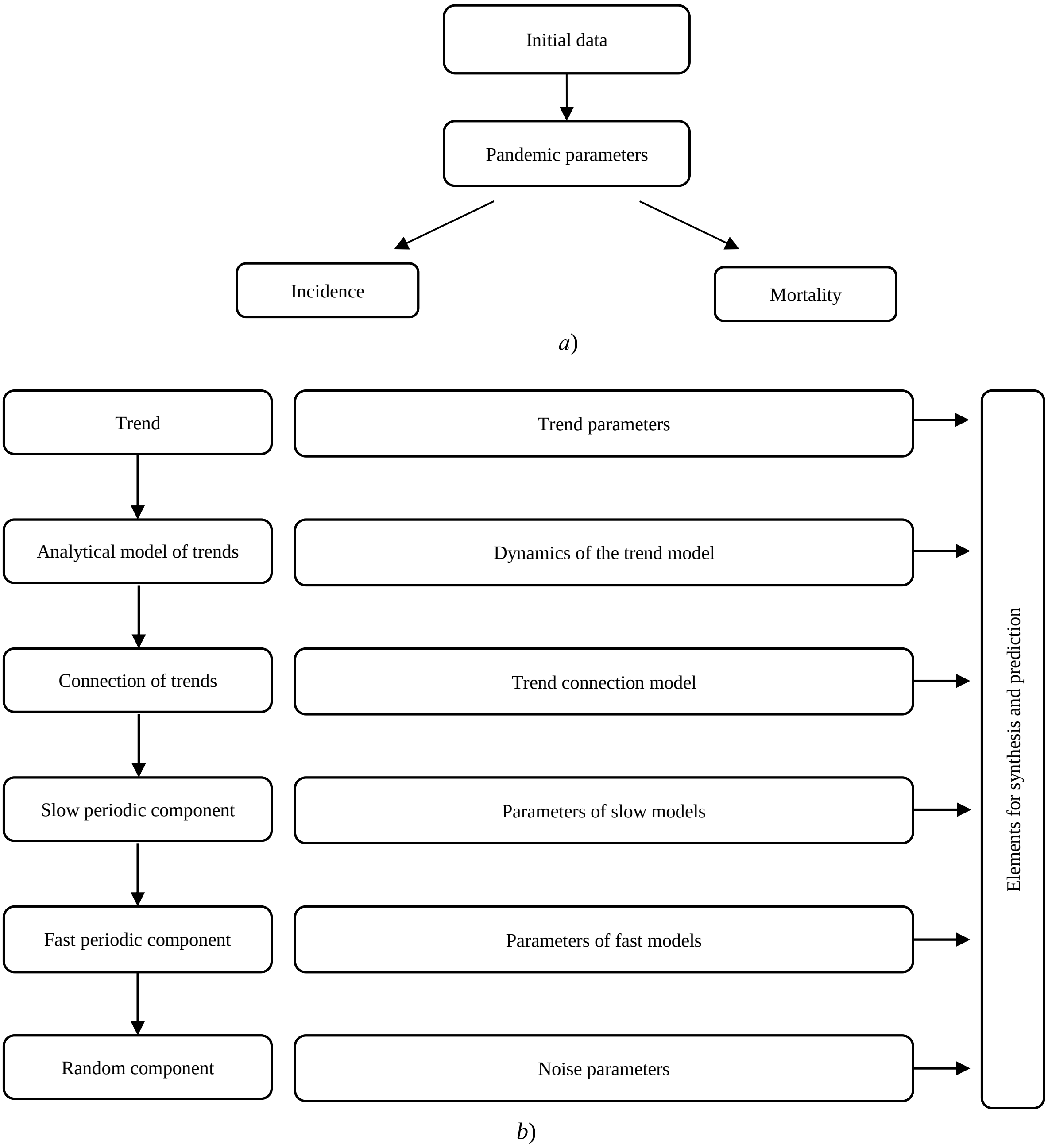

Fig. 3. Analysis of the time series of morbidity and mortality of Covid-positive patients: a — stages according to the focus of research; b — the study algorithm

Results. It is known that any epidemic process in the initial stage is characterized by exponential dynamics in time [10], i.e.

$$N(t) = A\cdot e^{Bt}, \quad (4)$$

where N — number of cases; A and B — some positive numbers.

Further development of the epidemic may occur according to an optimistic or pessimistic scenario. In the first case, the epidemic reaches a certain peak and comes to naught. The dependence of the number of cases at some point has the form:

$$N_{opt}(t) = \frac{A}{ch^2(Bt+C)}, \tag{5}$$

where *A*, *B*, *C* — coefficients of the model; ch — hyperbolic cosine.

This scenario corresponds to the differential equation:

$$\frac{dN_{opt}(t)}{dt} = \pm 2BN_{opt}(t)\sqrt{1-\frac{N_{opt}(t)}{A}}. \tag{6}$$

Here the plus sign is implemented at $N_{opt}(t) < A$ up to the t^* moment, at which $N_{opt}(t^*) = A$. Starting from this moment, the minus sign is implemented in formula (6). According to (6), upon reaching a certain critical number of cases A, the incidence will begin to decrease monotonously.

The pessimistic scenario implies that the epidemic, which initially develops exponentially, also reaches a plateau exponentially over time, i.e. the pathogen remains in the affected population. This can be described by evolutionary dependence

$$N_{pess}(t) = 2A\big(1 + th(Bt + C)\big), \tag{7}$$

which corresponds to the differential equation:

$$\frac{dN_{pess}(t)}{dt} = 2AB\left(1-\left(1-\frac{N_{pess}(t)}{A}\right)^2\right). \tag{8}$$

Here th — hyperbolic tangent. In (7) and (8), the multiplier 2 is added for reasons of coincidence of the starting asymptotics, i.e. to fulfill the natural relation:

$$\lim_{t=t_0(\to-\infty)} \frac{N_{opt}(t)}{N_{pess}(t)} = 1. \tag{9}$$

The intermediate epidemic scenario combines the elements of the two considered ones and assumes the following stages:

1) primary exponential growth;

2) saturation and subsequent decline;

3) exit to a non-zero plateau.

The dynamics of morbidity in this case is described by the linear conjugation of formulas (5) and (7) with weight *D*:

$$N(t) = \frac{AD}{ch^2(Bt+C)} + 2A(1-D)\big(1 + th(Bt + C)\big), \tag{10}$$

where *D* — the coefficient reflecting the contribution of an optimistic and pessimistic scenario to the overall process..

Solution (10) corresponds to nonlinear high-order differential equation [11], which we omit because of its bulkiness.

To find the coefficients *A*, *B*, *C*, *D*, it is necessary to solve mathematical programming problem [12] in its general form:

$$\sum_{i=1}^{I}\left(N(t_i) - N_i^{fact}\right)^2 = \sum_{i=1}^{I}\left(\frac{AD}{ch^2(Bt_i+C)} + 2A(1-D)\big(1 + th(Bt_i + C)\big) - N_i^{fact}\right)^2 \to \min, \tag{11}$$

where N_i^{fact} and t_i are, respectively, the incidence and the moment of its fixation.

Extremum condition (11) corresponds to the generalized epidemic scenario. In particular cases of models (5) and (7), constraints *D* = 1 or *D* = 0 should be added to (11).

$$\begin{cases} \frac{\partial}{\partial A}\sum_{i=1}^{I}\left(\frac{AD}{ch^2(Bt_i+C)} + 2A(1-D)\big(1 + th(Bt_i + C)\big) - N_i^{fact}\right)^2 = 0, \\ \frac{\partial}{\partial B}\sum_{i=1}^{I}\left(\frac{AD}{ch^2(Bt_i+C)} + 2A(1-D)\big(1 + th(Bt_i + C)\big) - N_i^{fact}\right)^2 = 0, \\ \frac{\partial}{\partial C}\sum_{i=1}^{I}\left(\frac{AD}{ch^2(Bt_i+C)} + 2A(1-D)\big(1 + th(Bt_i + C)\big) - N_i^{fact}\right)^2 = 0, \\ \left[\begin{array}{l} \frac{\partial}{\partial D}\sum_{i=1}^{I}\left(\frac{AD}{ch^2(Bt_i+C)} + 2A(1-D)\big(1 + th(Bt_i + C)\big) - N_i^{fact}\right)^2 = 0, \\ D = 1, \\ D = 0. \end{array}\right. \end{cases} \tag{12}$$

Here ∂ denotes the partial differential. It can also be strictly proved that system (12) is equivalent to an overdetermined system of algebraic equations:

$$\begin{cases} \frac{AD}{ch^2(Bt_i+C)} + 2A(1-D)\big(1+th(Bt_i+C)\big) = N_i^{fact}, \quad i = 1,2,\dots I \\ \begin{bmatrix} D = 1, \\ D = 0, \\ D \in \mathbb{R}, \end{bmatrix} \end{cases} \quad (13)$$

the variants of which correspond to the described scenarios.

The results of identifying the trend dependence $P(t)$ using the built-in MS Excel functions [13] for all scenarios of epidemic dynamics are shown in Figure 2 and in Table 1.

Table 1

Numerical characteristics of the trend model of COVID-19 morbidity

Models and indicators	*A*	B	C	*D*	σ, thous. people	ξ
Optimistic	615.1483	0.003842	–1.55037	1	138.7840681	0.8058189
Pessimistic	142.9481	0.009928	–1.5551	0	116.8074635	0.8522902
Generalized	353.0566	0.007984	–1.87759	0.613561	113.4654191	0.8612546

As it can be seen from the data in the table, generalized model (10) describes the real situation better. However, it has a significant drawback. This is the comparative complexity and inability to explicitly write out nonlinear differential equations that correspond to the dynamics of COVID-19. In this respect, the pessimistic model attracts with its simplicity and, accordingly, the possibilities of improvement.

To identify the oscillatory component in the mortality data for COVID-19 (Fig. 3), we choose the following model. Let us assume that the real data fluctuates near the trend line. In our case, these are models (5)–(6), (7)–(8) and (10) with an amplitude α, a circular frequency β and an initial phase γ. Such a regular model of epidemic dynamics is decomposed and described by equation:

$$\tilde{N}(t) = N(t) \cdot [1 + \alpha \cdot \sin(\beta \cdot t + \gamma)],$$

$$\text{where } N(t) = \begin{bmatrix} N(t)_{opt} \text{ according to } (5)\text{–}(6), \\ N(t)_{pess} \text{ according to } (7)\text{–}(8), \\ N(t)_{gen} \text{ according to } (10). \end{bmatrix} \quad (14)$$

To find the parameters of oscillatory model (14), it is necessary to solve the following optimization problem [12] :

$$\sum_{i=1}^{I} (1 + \alpha \cdot \sin(\beta \cdot t_i + \gamma) - \frac{N_i^{fact}}{N(t_i)})^2 \to \min. \quad (15)$$

If we consider (15) as a function of the variables α, β, γ, the necessary condition of the extremum takes the form [8]:

$$\begin{cases} \frac{\partial}{\partial\alpha} \sum_{i=1}^{I} (1 + \alpha \cdot \sin(\beta \cdot t_i + \gamma) - \frac{N_i^{fact}}{N(t_i)})^2 = 0, \\ \frac{\partial}{\partial\beta} \sum_{i=1}^{I} (1 + \alpha \cdot \sin(\beta \cdot t_i + \gamma) - \frac{N_i^{fact}}{N(t_i)})^2 = 0, \\ \frac{\partial}{\partial\gamma} \sum_{i=1}^{I} (1 + \alpha \cdot \sin(\beta \cdot t_i + \gamma) - \frac{N_i^{fact}}{N(t_i)})^2 = 0. \end{cases} \quad (16)$$

The solution of problem (16) coincides with the solution of the overdetermined system of equations:

$$1 + \alpha \cdot \sin(\beta \cdot t_i + \gamma) = \frac{N_i^{fact}}{N(t_i)}, \quad i = 1,2,\dots I. \quad (17)$$

However, the practical implementation of algorithms (16) and (17) is hampered by their instability due to the peculiarities of problem [7]. In this case, the algorithm based on finding the model parameters that provide the best correlation between actual data [9] and the model function $\tilde{N}(t)$ is more stable:

$$\mathrm{Corr}(\tilde{N}(t_i),\ N_i^{fact}) \to \max. \quad (18)$$

Solution (18) obtained by means of Excel [9] for variants of model $N(t)$ (5)–(6), (7)–(8) and (10) are given in Table 2.

Table 2

Numerical characteristics of the COVID-19 incidence fluctuation model

Models and indicators	α	β	γ	ξ	σ, thous. people
Optimistic	0.339708	0.049332	0.760834	0.912426	102.0689
Pessimistic	0.264411	0.049207	0.840402	0.928869	83.29141
Generalized	0.273133	0.049298	7.08885	0.94078	76.13293

Numerical indicators of the adequacy of models ξ and σ presented in Table 2 indicate that the generalized model better corresponds to the actual data. At the same time, it is much more difficult than the pessimistic one with an insignificant improvement in accuracy. Thus, the advantage of the pessimistic model should be recognized. It has the optimal complexity of the mathematical description of the COVID-19 epidemic, allowing for simple interpretation and ease of improvement.

It is important to note that any trend is characterized by a periodicity of 127 ± 0.5 days. This result is in good agreement with the data of autocorrelation and spectral analysis of the oscillation component of $\tilde{N}(t)$ function (Fig. 4). Thus, it is recorded that outbreaks of the disease occur after 124 and 110 days. This means that the disease is seasonal with a period of 1/3 of the year.

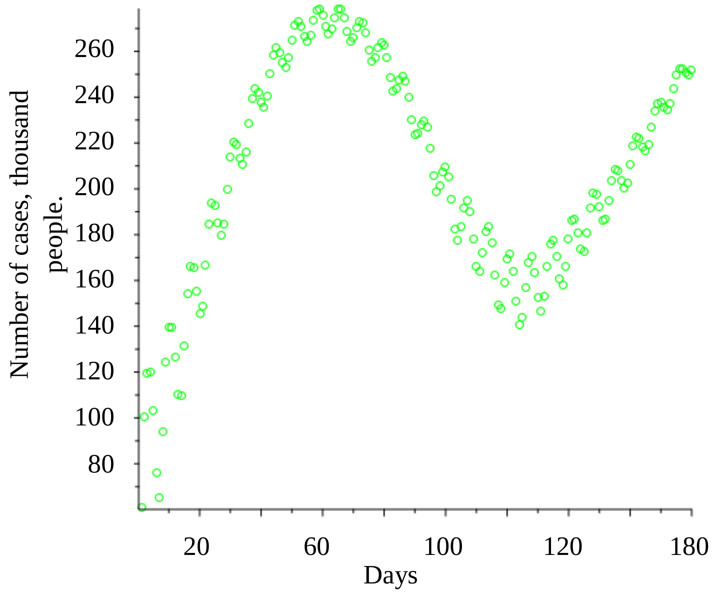

a)

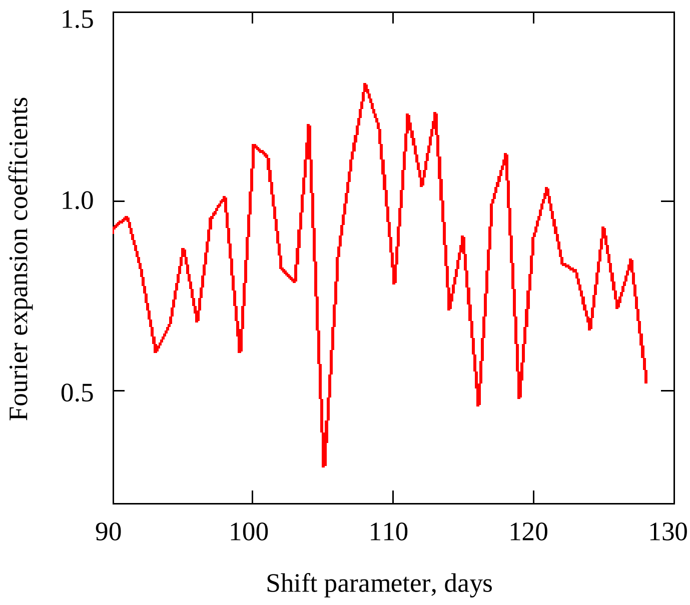

b)

Fig. 4. Data of autocorrelation and spectral analysis of the oscillation component: a — difference in the dynamics of morbidity with a shift by a different number of days; b — coefficients of spectral decomposition of morbidity

Data comparison in Tables 1 and 2 allows us to assess the relative role of the oscillation and noise components. If we consider them independent (orthogonal) and use the well-known ratio $\sigma_\Sigma = \sqrt{\sigma_1^2 + \sigma_2^2}$, we can make sure that the contributions of the periodic and random components are comparable.

Subtracting the model values of morbidity $\widetilde{N}(t_i)$ from the observed ones N_i^{fact} (or vice versa), we allocate the remaining noise component of the model. Figure 5 provides the result for the pessimistic scenario.

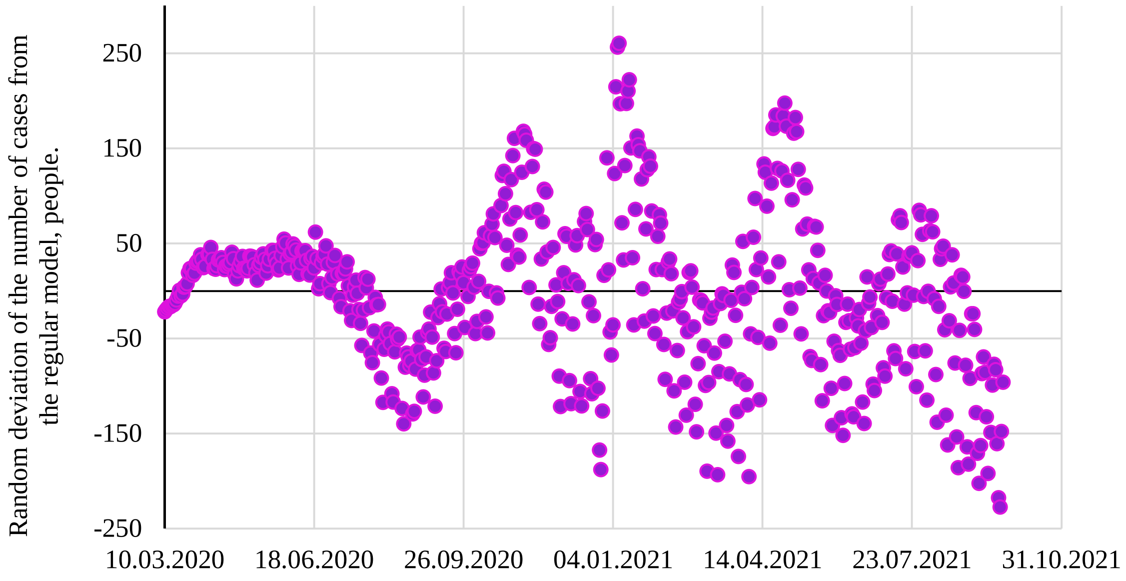

Fig. 5. Noise component in the pessimistic model

Numerical characteristics of data shown in the figure correspond to a normal Gaussian distribution [9] with a mathematical expectation of "zero" and a standard deviation of 80 thousand cases per day, which is confirmed by numerical identification data:

– mathematical expectation *M* = –2.87;

– standard deviation σ = 79.9;

– Skewness asymmetry = 0.0085;

– Kurtosis excess = 3.51.

Thus, the identification of the mathematical model $\widetilde{N}(t) + N_{cases}$ performed in this work, presumably, allows predicting morbidity for the entire duration of the epidemic [5].

Similarly, the dynamics of mortality among Covid-positive patients was analyzed from 12.02.2020 to 22.09.2021 (Fig. 3). Given that the lethal outcome is a likely result of infection, it is logical to present a mortality model:

$$M_{fact}(t+\tau) = k_{leth} \cdot N_{fact}(t). \tag{19}$$

Or taking into account the approximation of morbidity:

$$\widetilde{M}(t+\tau) + M_{cases} = k_{leth} \cdot \left(\widetilde{N}(t) + N_{cases}\right). \tag{20}$$

Here *M* denotes mortality; k_{leth} — the probability of dying from this disease; τ — the most likely time from infection of a person to his death. We find numeric parameters k_{leth} and τ, that appear in mortality patterns (19), by minimizing the functional deviations:

$$\Phi(\tau,\ k_{leth}) = \sum_{i=I_{\min}}^{I_{\max}-\tau}[M_{fact_{i+\tau}} - k_{leth} \cdot N_{\mathrm{fact}_i}]^2 \to \min \tag{21}$$

taking into account natural constraints $0 \leq k_{leth} \leq 1, \tau \in \mathbb{N}, 1 \leq \tau \leq 30$.

The peculiarity of the solution to problem (21) is that one of the desired variables appears in the upper index of summation. Therefore, we will get the solution to the optimization problem in two stages. The first one is based on a necessary condition for the extremum $\Phi(\tau,\ k_{leth})$:

$$k_{leth}(\tau) = \sum_{i=I_{\min}}^{I_{\max}-\tau}(M_{fact_{i+\tau}} N_{\text{fact}_i}) \cdot \left[\sum_{i=I_{\min}}^{I_{\max}-\tau} N_{fact_{i+\tau}}{}^2\right]^{-1} \quad (22)$$

for the entire range of τ. Then we choose a pair of values $\{\tau,\ k_{leth}\}$, that provides the minimum value (21).

It is important to mention that $I_{\min}$ is assumed to be equal to 150 days. The assumption is due to the fact that the first months of morbidity and mortality statistics [5] do not seem to be sufficiently complete and reliable.

Having solved problem (21), we get: $k_{leth} = 0{,}0184 \pm 0{,}0003$ and $\tau = 21$ days. The correlation of mortality with morbidity is demonstrated in more detail by the correlogram of the data $M_{fact}(t+\tau)$ and $k_{leth} \cdot N_{fact}(t)$ (Fig. 6).

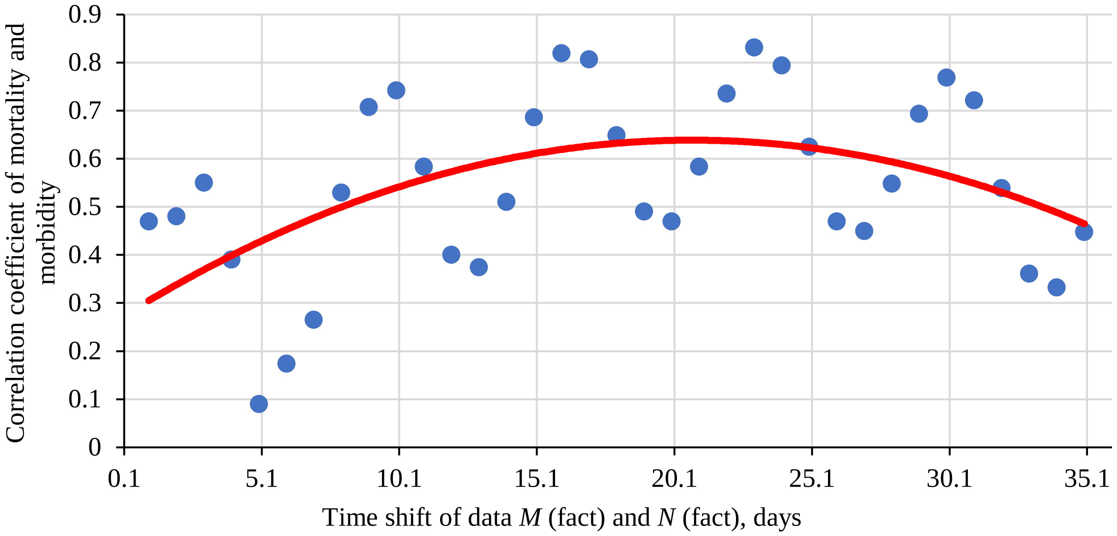

Fig. 6. Correlogram of mortality and morbidity depending on the shift parameter τ

Trend analysis shows the probability of death from COVID-19 on the 21st day after infection. In addition, the frequency of the risk of death is obvious. Trend-free variations of the risk of death are visualized in Fig. 7.

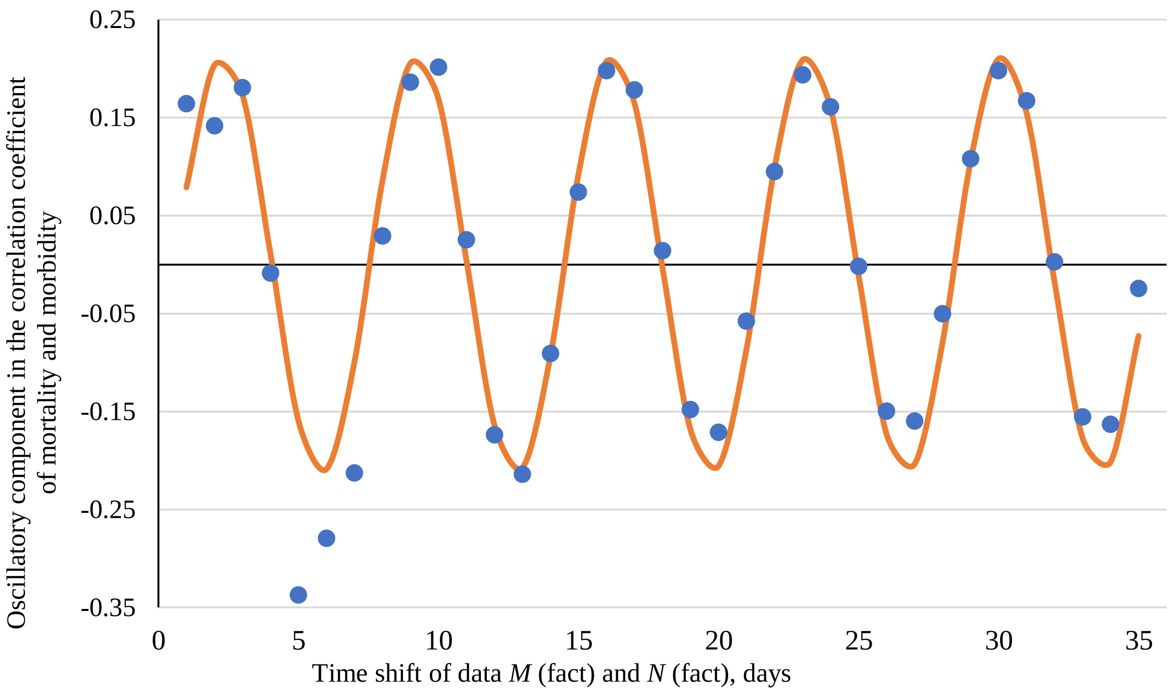

Fig. 7. Fast oscillation component in the correlogram of mortality and morbidity

According to Fig. 7, the risk of death in COVID-19 fluctuates around the above average value with a period of 7 days, which fully corresponds to the cyclical work of medical institutions around the world. The analytical dependence approximating the data in Fig. 7 has the form:

$$\mu(\tau) = 0{,}212 \cdot \sin(0{,}902 \cdot \tau - 0{,}522), \quad (23)$$

where μ — the fast component of mortality.

Discussion and Conclusion. The main results of the work are listed below.

1. Models of morbidity and mortality in COVID-19 have been constructed and initialized.

2. It has been established that the spread of coronavirus infection is repeated three times a year.

3. Mortality is constant on average and contains two oscillation components. The frequency of the first one corresponds to the frequency of morbidity, and the frequency of the second one corresponds to the regulations of medical institutions.

4. Based on the observation interval from 12.02.2020 to 22.09.2021, it can be concluded that the scenario of the epidemic is close to pessimistic.

5. Random component in the morbidity and mortality models turned out to be at the level of seasonal fluctuations.

Statistical data that appeared in December 2021 showed that the known COVID-19 strains were practically replaced by a new one — omicron. Its contagiousness is 3/5 times higher; mortality is 3/5 times lower. This circumstance dictates the need to improve the proposed dynamic models of the epidemic, taking into account the virus-competitive effect. This is the objective of the following research by the team of authors.

The obtained results allow us not only to predict further dynamics of the pandemic, but also to formulate practically significant recommendations. For example, the following intervals are proposed as the optimal timing of anti-Covid vaccination by Sputnik V (annually): 05.02–15.02, 17.05–28.05, 24.09–5.10.

References

1. Janyce E. G., Kolawole V. S., Gaeetan B. K., Romain G. K. On the reliability of predictions on Covid-19 dynamics: A systematic and critical review of modelling techniques. Infectious Disease Modelling. 2021;6:258–272. https://doi.org/10.1016/j.idm.2020.12.008

2. Hermanowicz S. W. Forecasting the Wuhan coronavirus (2019-nCov) epidemics using a simple (simplistic) model. MedRxiv. 2020. 10 p. https://doi.org/10.1101/2020.02.04.20020461

3. Lalmuanawma S., Hussain J., Chhakchhuack L. Applications of machine learning and artificial intelligence for COVID-19 (SARS-CoV-2) pandemic: A review. Chaos, Solitons & Fractals. 2020;139:110059. https://doi.org/10.1016/j.chaos.2020.110059

4. Postniko E. B. Estimation of COVID-19 dynamics «on a back-of-envelope»: Does the simplest SIR model provide quantitative parameters and predictions? Chaos, Solitons & Fractals. 2020;135:109841. https://doi.org/10.1016/j.chaos.2020.109841

5. Brunton S. L., Kutz J. N. Data-Driven Science and Engineering. Moscow: DMK Press, 2021. 574 p. (In Russ.).

6. Vinogradov A. Yu. Numerical methods for solving rigid and nonrigid boundary value problems. Moscow: National Research, 2017. 112 p. (In Russ.).

7. Pugh Ch. C. Real Mathematical Analysis. Second Edition. Cham: Springer, 2015. https://doi.org/10.1007/978-3-319-17771-7

8. Maheshwari A. Data Analytics Made Accessible. Bellevue: Kindle Edition, 2023. 156 p.

9. Gribova E. Z., Saichev A. I. Fizicheskii podkhod k analizu diffuzii chastits. Nizhny Novgorod: N. I. Lobachevsky State University of Nizhny Novgorod, 2012. 232 p. (In Russ.).

10. Egorov A. I. Obyknovennye differentsial'nye uravneniya s prilozheniyami. 2nd ed., rev. Moscow: Fizmatlit, 2003. 384 p. (In Russ.).

11. Nesterov Yu. E. Metody vypukloi optimizatsii. Moscow: Moscow center for continuous mathematical education, 2010. 281 p. (In Russ.).

12. Ben-Tal A., Nemirovski A. Lectures on Modern Convex Optimization Analysis, Alogorithms, and Engineering Applications. Philadelphia: SIAM, 2001. 537 p.

13. Kryanev A. V., Lukin G. V. Matematicheskie metody obrabotki neopredelennykh dannykh. Moscow: Fizmatlit, 2006. 216 p. (In Russ.).

Received 02.11.2022.

Revised 09.12.2022.

Accepted 09.01.2023.

About the Authors:

Azimova, Nataliya N., associate professor of the Applied Mathematics Department, Don State Technical University (1, Gagarin sq., Rostov-on-Don, 344003, RF), ORCID, arkomaazimov@mail.ru

Bedoidze, Maria V., senior lecturer of the Applied Mathematics Department, Don State Technical University (1, Gagarin sq., Rostov-on-Don, 344003, RF), ORCID, masha.bedoidze@gmail.com

Kholodova, Svetlana N., associate professor of the Life Safety and Environmental Protection Department, Don State Technical University (1, Gagarin sq., Rostov-on-Don, 344003, RF), Cand. Sci. (Eng.), ORCID, holls9@mail.ru

Mokina, Tatyana A., Bachelor's degree student, Don State Technical University (1, Gagarin sq., Rostov-on-Don, 344003, RF), ORCID, mokinat337@gmail.com

Zairova, Dzhakhangul Kh., Bachelor's degree student, Don State Technical University (1, Gagarin sq., Rostov-on-Don, 344003, RF), ORCID, gulyazair@gmail.com

Ermakov, Aleksandr S., Bachelor's degree student, Don State Technical University (1, Gagarin sq., Rostov-on-Don, 344003, RF), ORCID, ermakov_sahsa11@mail.ru

Claimed contributorship

N. N. Asimova: development and implementation of a dynamic epidemic model, development of computational algorithms. M. V. Bedoidze: development of statistical analysis methods, preparation of the text of the article. S. N. Kholodova: selection of statistical data, formulation of the conclusions and recommendations, revision of the text. T. A. Mokina: verification of statistical data, comparison of the results of the simulation experiment on forecasting the dynamics of the epidemic with real data. Dz. Kh. Zairova: allocation of regular and random components of the model, calculations based on the model of the epidemic dynamics. A. S. Ermakov: parametric identification of the regular and random components of the model, implementation of the simulation experiment to predict the epidemic dynamics.

Conflict of interest statement

The authors do not have any conflict of interest.

All authors have read and approved the final manuscript.

TECHNOSPHERE SAFETY

Original article
UDC 504.064.2+504.064.36
https://doi.org/10.23947/2541-9129-2023-1-16-27

Study of the Influence of Forest and Peat Fires on the Radiation Situation in the South-Western Regions of the Bryansk Region

Oleg N. Apanasyuk ✉, **Sergey L. Gavrilov**, **Sergey A. Shikin**, **Artem E. Pimenov**

Nuclear Safety Institute of the Russian Academy of Sciences, Moscow, Russian Federation

✉ aon@ibrae.ac.ru

Abstract

Introduction. The paper considers the influence of radiation forest and peat fires on the spread of radioactive contamination, which affects the well-being of thousands of people. The state of the environment in vast territories is deteriorating; negative socio-economic processes are developing. This is a serious problem of two states: the Russian Federation and the Republic of Belarus. The objectives of the presented work are to study the radiation situation in forests and peat bogs located in the border areas of the Bryansk region, as well as to study the possibility of transferring radioactive materials during forest and peat fires.

Materials and Methods. The facts that clarified the theoretical basis of the presented research are highlighted in the scientific literature. The authors took into account, in particular, that:

– the activity of radionuclides in the soil decreases in direct proportion to the depth;

– a peat fire is an uncontrolled burning;

– emissions of caesium-137 fractions (^{137}Cs) during a fire can reach 3-4 %.

We know the areas of forests in radiation-contaminated territories (RCT) of the Bryansk region from the applied literature and official sources. The most problematic areas from this point of view have been identified.

A mobile radiometric laboratory, a scintillation gamma-ray spectrometer MKS-AT6101S were involved in the expedition research. The results of field gamma-ray spectrometry were recorded in three localities. The calculations for a hypothetical fire were carried out using the SAUR AIUS RSCHS 2030 software tool.

Results. The consequences of large and prolonged fires in the exclusion zone of the Chernobyl nuclear power plant are analyzed. It is established that the incidents did not lead to dangerous consequences for the population. The total effective dose of inhalations was ~0.003 % of the permissible level of irradiation. It is noted, however, that the forest soil of the Bryansk region has received significant damage from ^{137}Cs pollution. The density of such pollution exceeded 5 Ci/km^2 in 40 % of the affected forests. Of these, an indicator of 15-40 Ci/km^2 and more was recorded in 16 %, in some quarters — up to 200 Ci/km^2. It is established that zones with a high contamination density (40 Ci/km^2) will remain in the region until 2026. Five districts are particularly problematic: Gordeevsky, Zlynkovsky, Klintsovsky, Krasnogorsky and Novozybkovsky.

When fixing and predicting harm, the authors of the presented work proceeded from the following fact: during fires, the combustion products (forest litter, grass and undergrowth) contain more radioactive substances than the crowns of trees. In this regard, measurements were not made at a significant height.

The field study route was chosen based on the available data on the maximum level of radioactive contamination. The ambient dose equivalent rate (ADER) of gamma radiation recorded at 2,757 points did not exceed 1.2 μSv/h (with an average value of 0.2-0.3 μSv/h). Measurements in the marshes did not reveal traces of ^{137}Cs at a depth of more than 40 cm. The maximum activity of ^{137}Cs was observed in the upper (0–4 cm) soil layer (up to 65 %). Taking into account the data obtained, the possibility of radioactive contamination in the event of a forest fire was assessed. According to the calculations in the software environment, radioactive contamination will spread to 348 hectares. The density of

radioactive contamination of the area may increase by 5–10 % (from the initial one). 33 people will suffer; there is a threat of death of 1 person.
It has been established that a burning peat bog is the most powerful and long-term source of radioactive contamination, therefore it is important to prevent peat and forest fires. This will reduce the transfer of radionuclides and emissions of radioactive fumes. Remote and surface radiation monitoring facilities should be developed.
***Discussion and Conclusion*.** The registered ADER is not dangerous for the health of the population of the Bryansk region. However, frequent fires significantly increase the likelihood of transferring active ^{137}Cs to residential areas. In this sense, timely monitoring and forecasting of fires is relevant. The authors formulated proposals to improve the technical and technological components of the solution of the considered problem.
1. To clarify the radiation situation, all-terrain vehicles should be equipped with:
– means of registering the radiation situation;
– software and hardware complex for automatic collection, analysis of information and its fixation in databases.
2. There should be a reliable cellular communication between all rapid response units in the emergency zone.
Further research is focused on the creation of fast-deployable radiation monitoring modules and mobile aerial photography complexes using drones in the emergency zone.

Keywords: forest fires, peat fires, radioactively contaminated territory, Chernobyl accident, radioactive contamination zones, radiation survey, radiation control, radiation risks for the population.

Acknowledgements. The authors express their gratitude to their colleagues — Simonov A. V., Dolgov V. N., Klemin A. S., Yakovlev V. Yu. and Shvedov A. M. for their direct participation in the organization and conduct of field studies of radioactively contaminated territories of the south-western regions of the Bryansk region.

For citation. O. N. Apanasyuk, S. L. Gavrilov, S. A. Shikin, A. E. Pimenov. Study of the Influence of Forest and Peat Fires on the Radiation Situation in the South-Western Regions of the Bryansk Region. Safety of Technogenic and Natural Systems, 2023, no.1, pp. 16–27. https://doi.org/10.23947/2541-9129-2023-1-16-27

Introduction. The data of scientific and applied literature allow us to get an idea of the radiation situation in forests and peat bogs located on radiation-contaminated territories (RCT) of the border areas of the Bryansk region. A number of works have studied the environmental impact of large forest fires in the exclusion zone (EZ) of the Chernobyl Nuclear Power Plant (Chernobyl NPP).

It follows from the materials of the Atlas of the consequences of the Chernobyl accident[1] that forests were exposed to radioactive contamination on the territory of more than 3 million hectares in 15 subjects of the Russian Federation and six regions of the Republic of Belarus. The accident at the Chernobyl nuclear power plant caused the contamination of more than 1.5 million hectares of Russian[2] and 292.1 thousand hectares of Bryansk forests with radionuclides. It is worth clarifying that the last figure is about 30 % of the forest fund of the Bryansk region.

Fires in forests and peat bogs on the RCT increase radiation risks for the population of adjacent territories, including the south-western districts of the Bryansk region. This determines the relevance of the problem under consideration.

The objectives of scientific research is to study the radiation situation in forests and peat bogs located in the border areas of the Bryansk region, as well as to study the possibility of transferring radioactive materials during forest and peat fires.

Main tasks:

– analysis of the content of ^{137}Cs in forest combustible materials in the event of fires;

– assessment of the danger of fires in forests and peat bogs with high levels of radioactive contamination to the health of the population living on the RCT;

– preparation of proposals for improving technical and technological components of the solution to the problem under study;

– determination of the direction of further research in this area.

[1] Izrael Yu. A. (Ed.), Bogdevich I. M. (Ed.) The atlas of recent and predictable aspects of consequences of Chernobyl accident on polluted territories of Russia and Belarus (ARPA — Belarus). Moscow; Minsk, 2009. 140 p. (In Russ.).
[2] Voronov S. I. et al. 30 let chernobyl'skoi avarii. Itogi i perspektivy preodoleniya ee posledstvii v Rossii 1986–2016. Rossiiskii natsional'nyi doklad. Moscow, 2016. 202 p. (In Russ.).

Materials and Methods. A significant number of studies have been devoted to assessing the environmental impact of fires in forests and peat bogs of the RCT[3] [3–12]. A number of scientists note that the smoke of forest fires can be a carrier of radionuclides on the RCT[4] [1–9, 12].

It is known from [1] that the activity of radionuclides in soil decreases in direct proportion to the depth. ^{137}Cs and transuranic elements are mostly concentrated in the upper (0-5 cm) layer. Here their ^{137}Cs content varies in the range of 41–76 %

It is shown in [2] that forest and peat fires are an uncontrolled burning process. This is a disaster for the population, economy and nature. When extinguishing such fires, a radiation factor is added to the RCT.

It was noted in [3] that emissions of ^{137}Cs fractions during forest fires can reach 3–4 %.

Work [4] emphasizes the importance of accurate forecasting of fire risks for a successful strategy of extinguishing forest fires. It is proposed to use the software of the decision support system. This software consists of a fire hazard assessment module and a radionuclide transfer module in case of a fire. It allows you to work with the parameters of forest fires based on a database and predict the environmental consequences of forest fires on the RCT (the amount of radionuclide emissions, secondary pollution of territories).

In the field research of the south-western regions of the Bryansk region, a mobile radiometric laboratory of the RCT was used. This equipment made it possible to determine the impact of forest and peat fires on the spread of radioactive contamination. In addition, radiation risks for the population were assessed. The results of field gamma-spectrometry were recorded in three localities. The experiment involved the scintillation gamma-ray spectrometer MKS-AT6101S. Calculations for a hypothetical fire were performed using the SAUR AIUS RSCHS 2030 software tool[5].

Results

Analysis of the consequences of large forest fires in the Chernobyl NPP area. In April 2020, large-scale forest fires broke out in the Chernobyl zone. Forests and meadows burned intensely for more than two weeks [5]. From April 6 to April 26, fires were recorded within a radius of 25 km around the reactor [6].

On April 3, the fire engulfed a huge area of forests around the EZ [7] (Fig. 1).

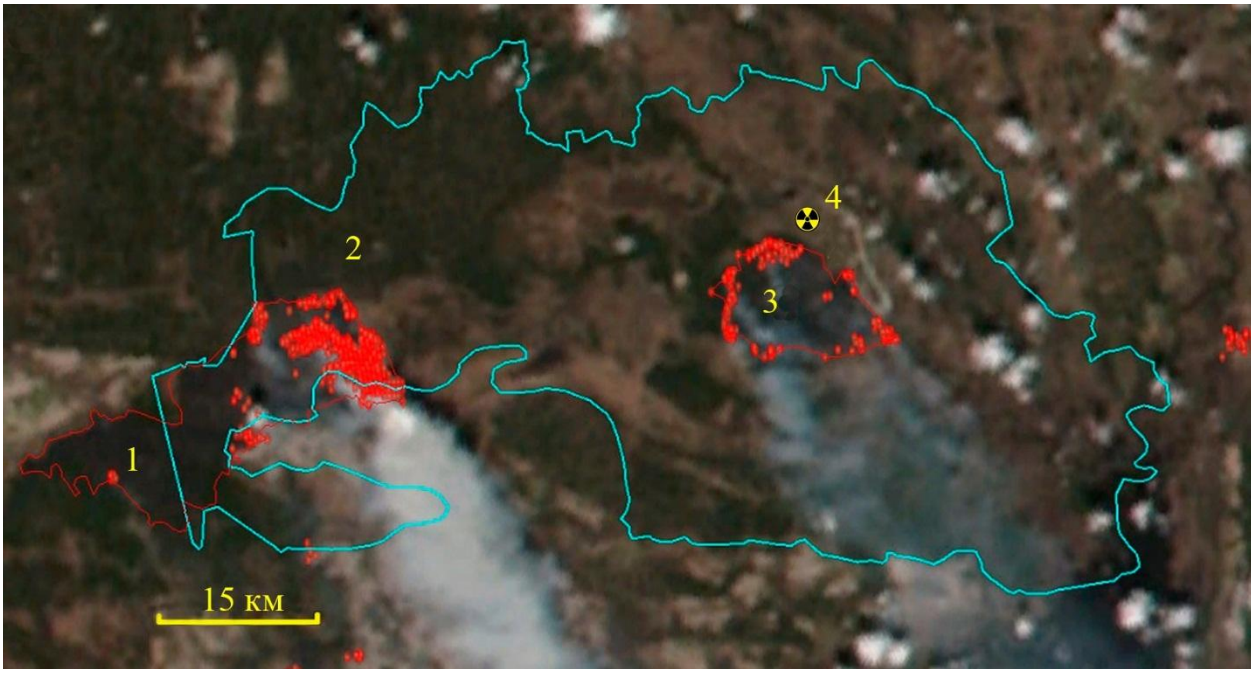

Fig. 1. Satellite image of fire in the EZ (April 2020):
1 — location of a fire on April 3; 2, 3 — the situation on April 8;
4 — location of the Chernobyl nuclear power plant, the blue line is the EZ border [7][6]

[3] Kuzmenkova N. V., Rozhkova A. K., Vorobeva T. A. Radioekologicheskaya otsenka vozdeistviya torfyanykh pozharov na okruzhayushchuyu sredu v zone otseleniya Bryanskoi oblasti. Radioekologicheskie posledstviya radiatsionnykh avarii: k 35-i godovshchine avarii na ChAES : mat-ly mezhdunar. nauch.-prakt. konf. Obninsk. 2021. p. 190–193. (In Russ.).

[4] Idem

[5] Informatsionno-analiticheskaya sistema analiza i upravleniya riskami avtomatizirovannoi informatsionno-upravlyayushchei sistemy Edinoi gosudarstvennoi sistemy preduprezhdeniya i likvidatsii chrezvychainykh situatsii (SAUR AIUS RSChS-2030). OOO "TsIEKS". Available from: http://www.esrc.ru/sites/default/files/contentuploads/docs/cieks_2020.pdf?ysclid=l7q7p6c8cl443523486 (accessed 06.09.2022). (In Russ.).

[6] Квітневі лісові пожежі 2020 року в зоні відчуження Чорнобильської АЕС стали найбільшими в історії. Лісівник. Available from: https://forester.blogspot.com/2020/04/2020_10.html (accessed 06.09.2022).

It was extinguished only after 10 days. The fire, which engulfed about 20 thousand hectares, destroyed a significant amount of forest[7].

More than 1,000 people, 120 fire trucks, helicopters and airplanes took part in the extinguishing. 10 unmanned aerial vehicles (UAVs) were used for aerial reconnaissance[8]. This made it possible to quickly assess the situation and make the right decisions on the deployment of firefighting equipment[9].

Most publications in foreign scientific journals have confirmed the absence of radiation danger to the population. The same was stated in the statement of the International Atomic Energy Agency (IAEA)[10]. The total effective dose of inhalations received from fires in the EZ was ~0.003 % of the permissible level of exposure of the population (1 mSv/year) [5].

After the Chernobyl accident in 1986, the first significant forest fires in the EZ date back to August 1992. They affected 1 thousand hectares of meadows and forest lands, the crown fire covered more than 5 thousand hectares [7]. During ground fire, there was no noticeable (more than 1 km) advance of radioactive contamination, even in the course of smoke propagation. Combustion products from a crown fire are carried much further in strong winds, but they are less radioactive, since the crowns of trees are much less polluted than the forest floor, grass and undergrowth [7].

In 1994, the content of ^{137}Cs in different levels of the pine forest was measured in the western territory of the Red Forest in the EZ: from needles to soil at a depth of 15 cm (Fig. 2 [7, 8]).

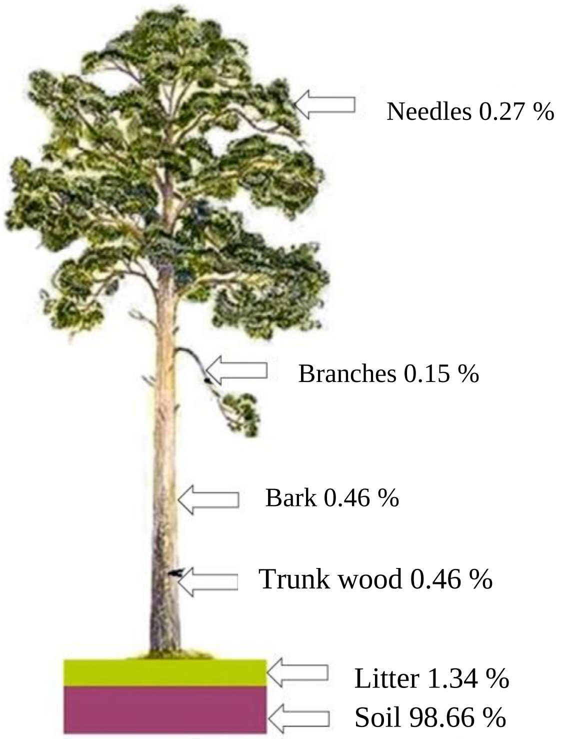

Fig. 2. Distribution of ^{137}Cs in parts of pine and soil. Samples were taken in the EZ (10 and 20 km south of the Chernobyl NPP) [7]

For liquidators, the most radioactively hazardous are ground fires of the Chernobyl NPP EZ, since submicron aerosols containing ^{137}Cs remain in the atmosphere for a long time and can carry it over considerable distances. A 10-fold decrease in the concentration of radioactive aerosols in the smoke plume was observed at a distance of more than 2 km from the fire front [8].

S. I. Voronov and co-authors found out that the Bryansk region forests are significantly polluted by ^{137}Cs. At the same time, more than 40 % of the affected forests belong to the radiation contamination zone (RCZ) with a density of ^{137}Cs radioactive contamination of the soil of more than 5 Ci/km^2. Of these, an indicator of 15-40 Ci/km^2 and more was recorded on 16 %, in some quarters — up to 200 Ci/km^2.

---

[7] Sivkov P. Ekologi zayavili o vtorichnom radioaktivnom zagryaznenii iz-za lesnykh pozharov v zone ChAES. Available from: https://tass.ru/obschestvo/10583913 (accessed 06.09.2022). (In Russ.).

[8] Aviation Code of the Russian Federation of March 19, 1997 No. 60-FZ. State Duma. Federation Council. Available from: http://ivo.garant.ru/#/document/10200300/paragraph/319340:1 (accessed 08.10.2022). (In Russ.).

[9] Peng H. Chernobyl: Massive Wildfire Extinguished with the Help of Drones. Available from: https://enterprise-insights.dji.com/user-stories/chernobyl-wildfire-extinguished-with-drones (accessed 27.08.2022).

[10] IAEA Sees No Radiation-Related Risk from Fires in Chornobyl Exclusion Zone. International Atomic Energy Agency. Available from: https://www.iaea.org/ru/newscenter/pressreleases/magate-ne-vidit-radiacionnyh-riskov-v-svyazi-s-pozharami-v-chernobylskoy-zone-otchuzhdeniya (accessed 06.09.2022). (In Russ.).

In the south-western regions of the Bryansk region, forests of the 1st-3rd classes (according to the classification of natural fire danger[11]) predominate [9].

In accordance with law[12], since 1991, four types of radiation hazard zones have been established on the territory of the Bryansk region:

– zone of exclusion (EZ);

– resettlement zone (RZ);

– areas with the right of resettlement (ARR);

– zone of residence with preferential social and economic status (ZPS).

EZ is characterized by a density of ^{137}Cs radioactive contamination of more than 40 Ci/km^2, RZ — more than 15 Ci/km^2, ARR — from 5 to 15 Ci/km^2, ZPS — from 1 to 5 Ci/km^2.

According to the Russian National Report, in 2020, the forest area in the Bryansk region amounted to 226.9 thousand hectares, including:

– ZPS — 127 thousand hectares;

– ARR — 84.2 thousand hectares;

– RZ — 14.9 thousand hectares;

– EZ — 0.8 thousand hectares [10].

Figure 3 shows the forecast of ^{137}Cs contamination in the Bryansk Region by 2026.

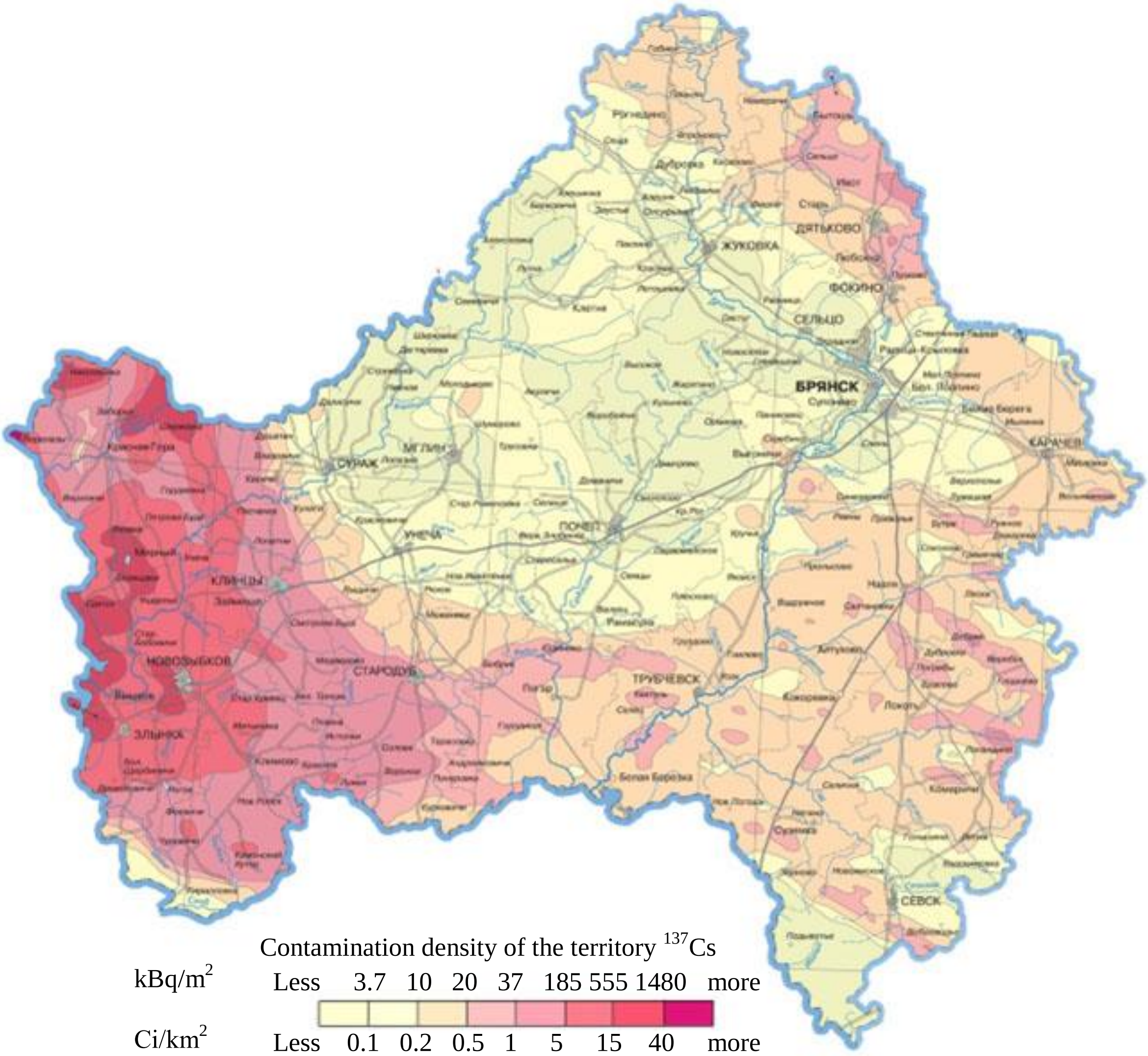

Fig. 3. ^{137}Cs contamination map of the Bryansk region according to the Atlas of the consequences of the Chernobyl accident (forecast for 2026)

[11] Klassifikatsiya prirodnoi pozharnoi opasnosti lesov i klassifikatsiya pozharnoi opasnosti v lesakh v zavisimosti ot uslovii pogody. Federal Forestry Agency. Available from: http://ivo.garant.ru/#/document/12189021/paragraph/9:0 (accessed 06.09.2022). (In Russ.).

[12] O sotsial'noi zashchite grazhdan, podvergshikhsya vozdeistviyu radiatsii vsledstvie katastrofy na Chernobyl'skoi AES. Law of the RSFSR of 15.05.1991 No. 1244-1. Supreme Soviet of the RSFSR Available from: https://base.garant.ru/185213/ (accessed 06.09.2022). (In Russ.).

The most radioactively contaminated areas: Gordeyevsky, Zlynkovsky, Klintsovsky, Krasnogorsky and Novozybkovsky are located in the Bryansk region and occupy a total of 14.3 % of the region's territory. There are 329 settlements on this area (Fig. 4) [11].

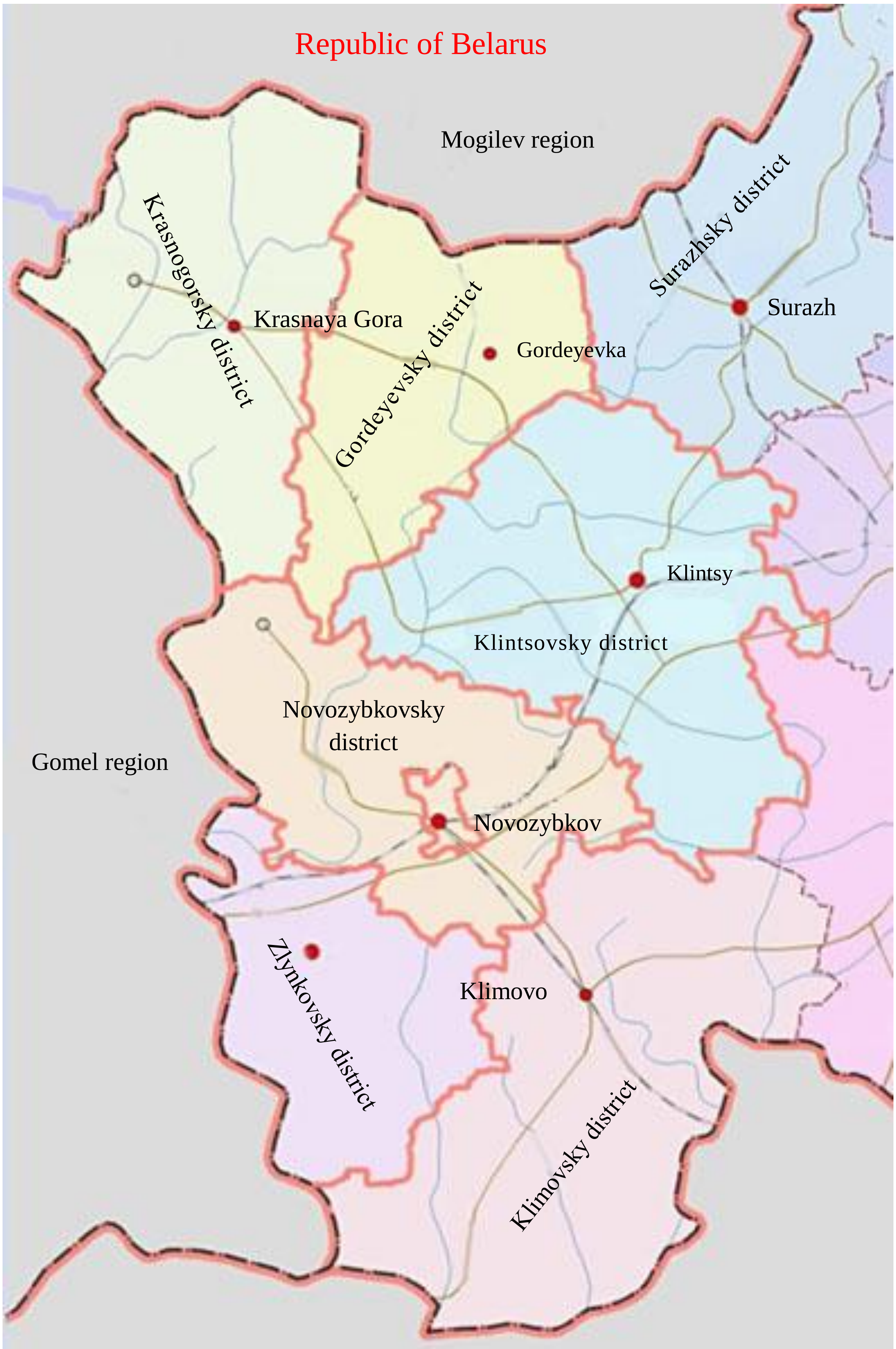

Fig. 4. South-west of the Bryansk region. Administrative municipalities on the RCT[13]

[13] Raiony Bryanskoi oblasti na karte s granitsami. Available from: https://maps-rf.ru/brjanskaja-oblast/rajony.php?ysclid=l5p8uis5n9622087709 (accessed 06.09.2022). (In Russ.).

Work [9] presents a similar forecast for 2046. The data relate to four RCZ of the most polluted areas of the Bryansk region. The content of ^{137}Cs in the forest litter was measured. The researchers have confirmed significant pollution, especially in the Krasnogorsky district and Novozybkovsky city district. The exact figures are given below.

– Gordeyevsky district: ZPS — 3.932 kBq/kg; APP — 9.43 kBq/kg; RZ — 18.1 kBq/kg.

– Zlynkovsky district: ZPS — 4.24 kBq/kg; APP — 8.67 kBq/kg.

– Krasnogorsky district: ZPS — 3.1 kBq/kg; APP — 9.25 kBq/kg; RZ — 26.6 kBq/kg; EZ — 81.49.

– Novozybkovsky city district: ZPS — 4.58 kBq/kg; APP — 9.34 kBq/kg; RZ — 21.48 kBq/kg.

It should be noted that one of the causes of peat fires is waterlogging of the Bryansk region's RCZ.

According to official data[14], 175 forest fires were registered in the Bryansk region in 2020 fire hazard season on a total area of 1,351.49 hectares. On the territory of the Bryansk region, 1,449 peat bogs with an area of 77.2 thousand hectares were taken into account. Almost 90 % of the marshes occupy an area of up to 100 hectares, 11 — more than 1 thousand hectares. The largest are located in the floodplain of the Nerussa river (7,462 hectares, Brasovsky district) and Kozhanovsky (6,984 hectares, Kranogorsky district).

In[15] it is noted that during a peat fire, aerosols containing ^{137}Cs do not spread further than 500 m from the source of ignition, therefore they do not pose any danger to residents of nearby settlements. However, the results of work [12] indicate that a burning peat bog is the most powerful and long-acting source of radioactive contamination. Therefore, it is important to prevent peat and forest fires. This will reduce the transfer of radionuclides and emissions of radioactive fumes.

Expedition surveys of radioactively contaminated territories of the south-western districts of the Bryansk region. In 2019, expedition surveys were conducted in the forests and peat bogs of the border territories of the Bryansk region. The influence of forest and peat fires on the health of the RCT population was studied. Measurements were carried out using a mobile radiometric laboratory (MRL)[16].

The survey route (Fig. 5) was chosen based on the data on the maximum level of radioactive contamination.

[14] Tsublova E. G., Lukashov S. V. Prirodnye resursy i okruzhayushchaya sreda Bryanskoi oblasti. Godovoi doklad ob ekologicheskoi situatsii v Bryanskoi oblasti v 2020 g. Bryansk, 2021. 251 p. Available from: http://www.kpl32.ru/in_doc/20210616_21856_gosdoklad_2020.pdf (accessed 06.09.2022). (In Russ.).

[15] Kuzmenkova N. V., Rozhkova A. K., Vorobeva T. A. Radioekologicheskaya otsenka vozdeistviya torfyanykh pozharov na okruzhayushchuyu sredu v zone otseleniya Bryanskoi oblasti (In Russ.).

[16] Proektirovanie avtomatizirovannoi sistemy monitoringa chrezvychainykh situatsii s radiatsionnym faktorom na radioaktivno zagryaznennykh vsledstvie katastrofy na Chernobyl'skoi AES territoriyakh gosudarstv — uchastnikov Soyuznogo gosudarstva (AS KRO): otchet o NIR. ANO TsAB IBRAE RAN; headed by Gavrilov S. L. Moscow, 2019, 380 p. No. GR AAAA-B20-220013090244-3. (In Russ.).

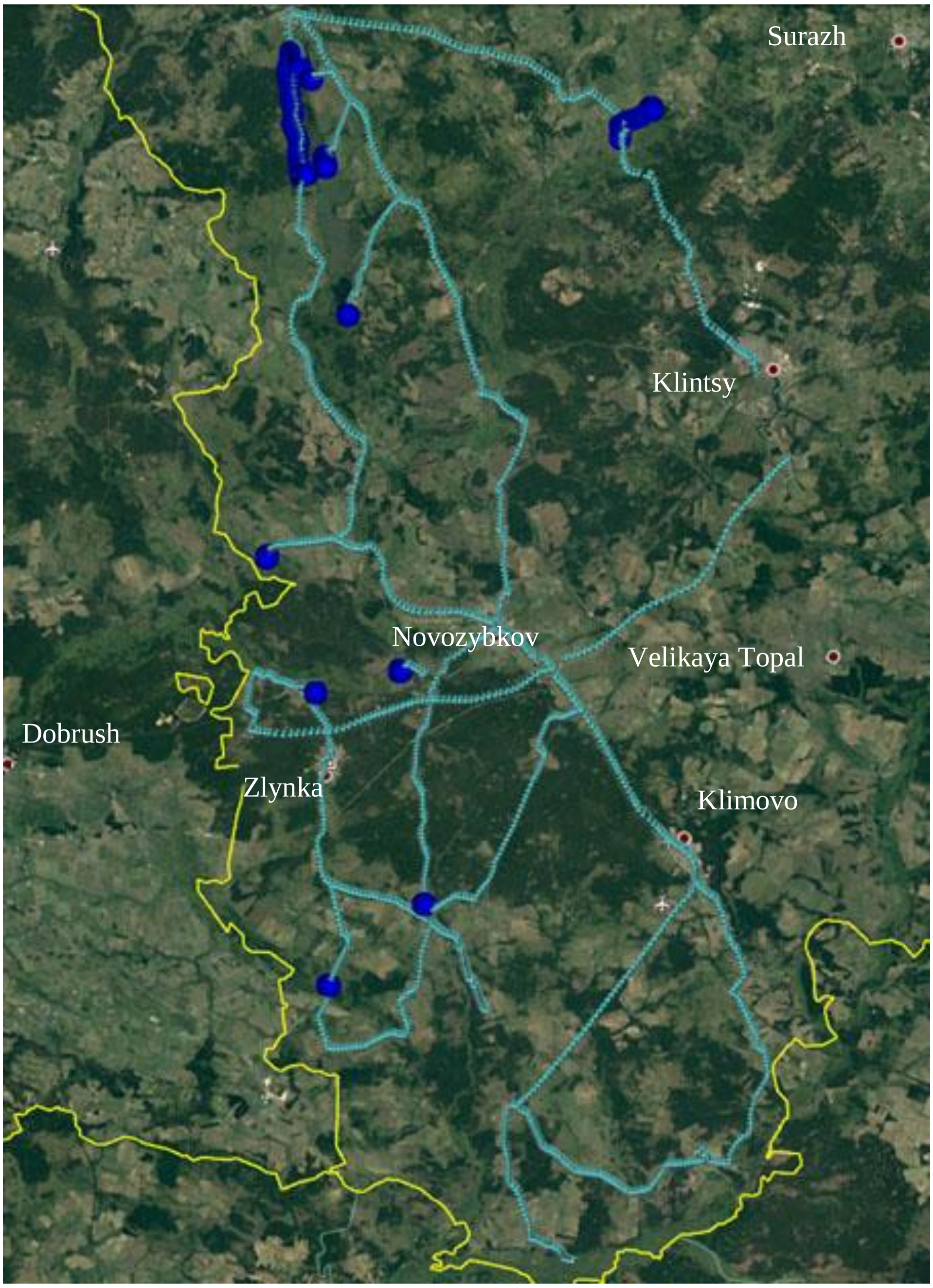

Fig. 5. Radiation survey route map

During the MRL movement through the areas most contaminated with radionuclides, the Gamma Sensor installation conducted continuous gamma-radiation survey. The ambient dose equivalent rate (ADER) of gamma radiation was measured. The measurements were made at 2,757 points.

The MKS-AT6101S spectrometer was used to detect ionizing radiation sources with the identification of radionuclides, and the DKS-96 dosimeter-radiometer was used to confirm the radiation situation data.

At all points of field measurements, gamma radiation ADER did not exceed 1.2 μSv/h (with an average value of 0.2-0.3 μSv/h). This is consistent with the data of the Atlas of the consequences of the Chernobyl accident (0.1–0.3 μSv/h).

For measurements in the Kozhanovskoye, Belimovo, Chaynoye and Oboleshevo marshes, the Becquerel Monitor LB 200 unit manufactured by Berthold technologies was used. Field measurements did not reveal traces of ^{137}Cs at a depth of more than 40 cm

The greatest activity of ^{137}Cs was observed in the upper (0-4 cm) soil layer (up to 65%). This is consistent with the results obtained by Belarusian scientists (41-76 % [1])

To clarify the radiation situation in the south-western regions of the Bryansk region, radiation surveys were conducted by field gamma spectrometry in three areas with an average ADER level of more than 0.6 μSv/h (Novozybkovsky, Zlynkovsky and Koasnogorsky). The results are summarized in Table 1.

Table 1

Results of field gamma-ray spectrometry, ^{137}Cs

Measuring point (locality)	Measured value		Data from the Atlas of the consequences of the Chernobyl accident, kBq/m^2 (Ci/km^2)
	Bq/cm^2	kBq/m^2	
Perevoz village (Novozybkovsky district)	45.7	457	555–1480 (15–40)
Vyshkov urban-type settlement (Zlynkovsky district)	96.8	968	555–1480 (15–40)
Velikoudebnoye village (Krasnogorsky district)	32.2	322	185–555 (5–15)

A scintillation gamma-ray spectrometer MKS-AT6101S was used in the experiment. The device was mounted on a tripod in such a way that there was a distance of 1 meter between the surface of the earth and the registration center of the scintillator crystal. To account for the distribution of activity by depth when calculating surface activity, several soil cores were taken at the measurement site. The results obtained are comparable with the data of the Atlas of the consequences of the Chernobyl accident.

Assessment of possible radioactive contamination in case of a forest fire. Taking into account the data on the activity of ^{137}Cs in the Bryansk region, the possibility of potential radioactive contamination in the event of a forest fire was considered. For the estimated calculation, a point of ignition was chosen in the forest near the village of Vyshkov (geographical coordinates 52º28´45″N, 31º42´39″E)

The following parameters were set as boundary conditions:

— characteristics of a forest fire (type of fire — ground, class of forest fire frequency — deciduous forest, duration of fire — 24 hours, weather fire hazard class — V, i.e. extreme fire hazard);

— weather conditions at the time of the forest fire (wind direction — 90 ° — azimuth; speed — 10 m/s).

The calculation was performed in the SAUR AIUS RSCHS 2030 software environment for a hypothetically occurred forest fire on 14.11.2019 00:00. On the conditional date 15.11.2019 and the time 00:00, the following results were obtained:

– area of the burnt forest — 3.7 hectares;

– fire perimeter — 0.7 kilometer;

– smoke coverage area — 1,437.6 hectares;

– radioactive contamination zone area — 348.0 hectares;

– number of people injured in the fire — 33 people;

– number of victims — up to 1 person.

As a result of such a fire, the density of radioactive contamination of the area may increase by 5-10% (from the initial one). An increase in the radiation dose in this single case will not lead to significant consequences for the population. However, a series of fires is potentially dangerous. It can worsen the situation in the border areas with background pollution.

During the expedition, it turned out that water barriers (rivers, lakes) on the Bryansk region RCT made it difficult for ground-based mobile radiation monitoring equipment to access the forests of the shore front. In this case, the most effective are:

– remote means of radiation monitoring based on UAVs (detection of fires)[17] [13];

– surface means of radiation control (radiation reconnaissance and refinement of radiation control data).

Unmanned aerial vehicles are an indispensable tool in the fight against forest fires. Thermal images are especially important, as they convey a bird's-eye view of the area and help determine the direction of fire propagation. This allows firefighters to quickly make decisions about where units should move and who should be evacuated.

Discussion and Conclusion. The results of scientific and expeditionary research allow us to make a number of statements. In a fire in a radiation-contaminated area, the content of radioactive aerosols in the smoke plume can exceed the permissible values by orders of magnitude, therefore firefighters risk receiving an unacceptably high inhalation dose of radiation.

It should be noted that the radiation situation in the forests of the Bryansk region RCT is changing extremely slowly. The forest floor is most dangerous. It accounts for more than 70 % of the total stock of ^{137}Cs in forest combustible materials. ^{137}Cs is active in the forest floor and in the upper layer (up to 40 cm) of peat bogs, so forest and peat fires pose a risk of radionuclide transfer to nearby settlements. It will remain a threat in the coming years.

Expedition surveys with MRL showed that at all points of field measurements, ADER does not exceed 1.2 μSv/h. The average ADER (0.2–0.3 μSv/h) corresponds to the data of the Atlas of the consequences of the Chernobyl accident. Such a dose is not dangerous for the health of the population of the Bryansk region RCT. Nevertheless, frequent fires significantly increase the likelihood of transferring active ^{137}Cs to residential areas. In this sense, timely monitoring and forecasting of fires is relevant.

The authors have formulated the proposals to improve technical and technological components of the solution of the considered problem.

1. To clarify the radiation situation, it is necessary to use cross-country vehicles. They should be equipped with:

– means of recording the radiation situation;

– hardware and software complex for automatic collection, analysis of information and its fixation in databases.

This will allow you to quickly clarify the radiation situation in the event of a large fire. Predictive models and electronic databases of radioactive contamination make it possible to optimize the routes of special equipment. Such navigation will be based on the results of past measurements of ^{137}Cs activity and up-to-date data updated based on the results of the current route.

2. To provide reliable cellular communication between all operational response units in the emergency zone.

Further research is focused on the creation of quick-deployable radiation monitoring modules and mobile aerial photography complexes using UAVs in an emergency zone. New measuring equipment and software will allow determining in real time the characteristics of radiation fields with geo-linking.

References

1. Dvornik A. A., Dvornik A. M., Korol R. A. Shamal N. V., Gaponenko S. O., Bardyukova A. V. Potential threat to human health during forest fires in the Belarusian exclusion zone. Aerosol Science and Technology. 2018;52(8):923–932. https://doi.org/10.1080/02786826.2018.1482408

[17] Voronov S. I. Kompleksnaya sistema monitoringa za sostoyaniem zashchity naseleniya na radioaktivno zagryaznennykh territoriyakh. Radioekologicheskie posledstviya radiatsionnykh avarii: k 35-i godovshchine avarii na ChAES: mat-ly mezhdunar. nauch.-prakt. konf. Obninsk, 2021. p. 175–177. (In Russ.).

2. Saraseko E. G. Timoshkov V. F., Degtyareva E. I. Elimination of wild fires on the soils of different types. Vestnik Mogilevskogo gosudarstvennogo universiteta im. A. A. Kulyashova. Seriya B. Estestvennye nauki: matematika, fizika, biologiya. 2020;2(56):86–98 (In Russ.).

3. Yoschenko Y., Kashparov V., Levchuk S. Lundin S., Protsak V., Khomutinin Yu., Glukhovsky O., Maloshtan I., Tschiersch J. Formation of Radioactive Aerosol Particles During the Wildland Fires in Chernobyl Zone and their Radioecological Impact. Radioactive Particles in the Environment. 2009:69–89. https://doi.org/10.1007/978-90-481-2949-2_4

4. Dvornik A. A., Dvornik A. M., Kurilenko R. S., Bardyukova A. V., Seglin V. N., Shamal N. V., Korol R. A. Mapping of forest fire hazard depending on weather conditions using geoinformation technologies. Proceedings of the National Academy of Sciences of Belarus. Biological series. 2021;66(3):320–332. https://doi.org/10.29235/1029-8940-2021-66-3-320-332

5. Talerko M., Kovalets I., Lev T. Igarashi Y., Romanenko O. Simulation study of radionuclide atmospheric transport after wildland fires in the Chernobyl Exclusion Zone in April 2020. Atmospheric Pollution Research. 2021;12(3):193–204. https://doi.org/10.1016/j.apr.2021.01.010

6. Meutter P. De, Gueibe Ch., Tomas J. et al. The assessment of the April 2020 Shernobyl wildfires and their impact on ^{137}Cs levels in Belgium and The Netherlands. Journal of Environmental Radioactivity. 2021;237:06688. https://doi.org/10.1016/j.jenvrad.2021.106688

7. Borovoi A. A., Gavrilov S. L., Khvoshchinskii V. A. Chernobyl. Hazard of forest fires. Fire safety. 2022;3(108):37–43. https://doi.org/10.37657/vniipo.pb.2022.65.89.003 (In Russ.).

8. Pazukhin E. M., Borovoi A. A., Ogorodnikov B. I. Forest Fire as a Factor of Environmental Redistribution of Radionuclides Originating from Chernobyl Accident. Radiochemistry. 2004;46(1):93–96. (In Russ.).

9. Marchenko T. A., Radin A. I., Razdaivodin A. N. Retrospective and current state of forest territories of the border areas of the Bryansk region exposed to radioactive contamination. Radiation Hygiene. 2020;13(2):6–18. https://doi.org/10.21514/1998-426X-2020-13-2-6-18 (In Russ.).

10. Bolshov L. A. (Ed.) Rossiiskii natsional'nyi doklad: 35 let chernobyl'skoi avarii. Itogi i perspektivy preodoleniya ee posledstvii v Rossii. 1986–2021. Moscow: Akadem-Print, 2021. 104 p. (In Russ.).

11. Skorobogatov A. M., Apanasyuk O. N., Bulantseva T. A. Impact of radioactive contamination zones regime on municipalities (case of Bryansk oblast). Regional'nye issledovaniya. 2021;4(74):89–103. https://doi.org/10.5922/1994-5280-2021-4-7 (In Russ.).

12. Dusha-Gudym S. I. Transport of radioactive materials by wildland fires in the Chernobyl accident zone: how to address the problem. International forest fire news. 2005;32:119–125.

13. Gavrilov S. L., Pimenov A. E., Shvedov A. M. et al. Experience of using unmanned aerial vehicles for airborne gamma-spectrometric survey of territories. ANRI. 2022;3(110):3–11. https://doi.org/10.37414/2075-1338-2022-110-3-3-11 (In Russ.).

Received 10.12.2022.

Revised 29.11.2022.

Accepted 16.01.2023.

About the Authors:

Apanasyuk, Oleg N., head of the Laboratory for Targeted Programs Development for Integrated Safety and Protection of the Population, Nuclear Safety Institute of the Russian Academy Of Sciences (52, Bolshaya Tulskaya st., Moscow, 115191, RF), ORCID, aon@ibrae.ac.ru

Gavrilov, Sergey L., head of the Scientific and Technical Problems of Complex Systems Development Department, Nuclear Safety Institute of the Russian Academy Of Sciences (52, Bolshaya Tulskaya st., Moscow, 115191, RF), ORCID, gav@ibrae.ac.ru

Shikin, Sergey A., head of the Integrated Radiation Monitoring Systems Development Department, Nuclear Safety Institute of the Russian Academy Of Sciences (52, Bolshaya Tulskaya st., Moscow, 115191, RF), ORCID, shickin@ibrae.ac.ru

Pimenov, Artem E., head of the Laboratory for Advanced Methods of Radiation Situation Monitoring, Nuclear Safety Institute of the Russian Academy Of Sciences (52, Bolshaya Tulskaya st., Moscow, 115191, RF), ORCID, artisl@ibrae.ac.ru

Claimed contributorship

O. N. Apanasyuk: formulation of the basic concept, generalization and analysis of the research results, preparation of the text, formulation of the conclusions. S. L. Gavrilov: academic advising, conducting field studies and calculations, revision of the text, correction of the conclusions. S. A. Shikin: conducting field studies, analysis of the results, revision of the text. A. E. Pimenov: conducting field studies, analysis of the results, revision of the text.

Conflict of interest statement

The authors do not have any conflict of interest.

All authors have read and approved the final manuscript.

TECHNOSPHERE SAFETY

Original article
UDC 621.9.06:628.5
https://doi.org/10.23947/2541-9129-2023-1-28-38

Reduction of Watercrafts Vibroacoustic Activity by Vibration Damping Materials

Aleksandr V. Budovskiy ✉, Yuriy I. Bulygin, Aleksandr V. Pavlikov, Aleksandr V. Tryukhan
Don State Technical University, 1, Gagarin Sq., Rostov-on-Don, Russian Federation
✉ k55355396@gmail.com

Abstract

Introduction. Electric machines, diesel installations, pumping units and fans, as well as working bodies of dredgers (pipelines, scoops, rippers, etc.) are the main sources of noise and vibration on watercrafts. Moreover, the main harmful factors in the operation of floating cranes and dredgers are both the vibration itself and the accompanying phenomena of infrasound and structural noise. One of the most urgent tasks for the introduction of technosphere safety methods on watercrafts is to reduce the harmful effects of vibroacoustic factors on the health of personnel. The research objective is to improve the working conditions of watercrafts drivers by introducing the method of designing vibration protection systems proposed by the authors, taking into account both the external factors (ambient temperature) and the dynamic characteristics of vibration damping materials. The possibility of choosing the most rational vibration damping material based on the engineering calculation of the required vibration insulation is shown.

Materials and Methods. A passive method of vibration control has been applied, in which elastic elements and vibration damping material are used in the watercraft design. The sources of noise and vibration have been identified, and their actual exposure levels have been determined. The analysis of dynamic characteristics and properties of vibration damping materials is carried out. The factors influencing the efficiency of vibration damping are revealed.

Results. A design scheme of the vibration damping model at the workplace of the watercraft driver has been developed. An analytical database of dynamic characteristics and properties of vibration damping materials has been created. An engineering method for calculating the effectiveness of vibration insulation has been adapted to watercrafts. The calculations of the effectiveness of vibration insulation using various vibration damping materials of different thicknesses have been performed, on the basis of which the advantages of vibration damping flooring made of elastomeric plate VEP20 have been proved.

Discussion and Conclusion. The engineering methodology developed in Excel for calculating the effectiveness of vibration insulation is automated and has a user-friendly interface. This allows you to calculate and reasonably select multilayer structures taking into account the ambient temperature, as well as the dynamic characteristics of vibration damping materials depending on the spectrum of noise and vibration. The results obtained can be used in the design of vibration protection systems for watercraft drivers.

Keywords: vibration damping materials, vibration damping, watercrafts, dredgers, vibration acoustic factor, loss coefficient.

For citation. A. V. Budovskiy, Yu. I. Bulygin, A. V. Pavlikov, A. V. Tryukhan. Reduction of Watercrafts Vibroacoustic Activity by Vibration Damping Materials. Safety of Technogenic and Natural Systems, 2023, no.1, pp. 28–38. https://doi.org/10.23947/2541-9129-2023-1-28-38

Introduction. The difficulty of determining the optimal level of vibration insulation is associated with the identification of sources of vibroacoustic activity and depends on the watercraft design features. In addition, the effectiveness of vibration insulation depends on the dynamic properties of vibration damping materials themselves. In turn, the dynamic characteristics of vibration damping materials are influenced by environmental conditions (temperature) and vibration spectra.

In order to reduce the watercrafts vibroacoustic activity, it is necessary to solve a set of interrelated tasks:

– to identify the main sources of noise and vibration, as well as their actual exposure levels;

– to develop vibration damping models and design schemes for vibration protection system of the watercraft driver at the workplace;

– to conduct an analytical review of scientific research on the determination of the dynamic characteristics of materials that affect the effectiveness of vibration damping;

– to determine the exact dynamic characteristics of vibration damping materials, including the coefficient of loss of vibrational energy, taking into account the spectrum of vibrations and temperature[1].

The solution to the above tasks will allow us to propose a reasonable methodology for the engineering calculation of vibration insulation based on vibration-damping materials, taking into account the specifics of the object of study.

Materials and Methods. To reduce vibration levels, methods of vibroacoustic protection of the watercraft driver were used. They consisted in the use of an elastic damping element in the design under development.

A dredger for mining operations was selected as the object of research — a floating dredging unit PZU-8M (Fig. 1). It is used by KT "Krym-Investstroy and Company" during the development of the Sasyk sand-gravel mixture deposit in the Crimea River. In machines of this type, the source of noise and vibration is the equipment mounted on pontoons (Fig. 1).

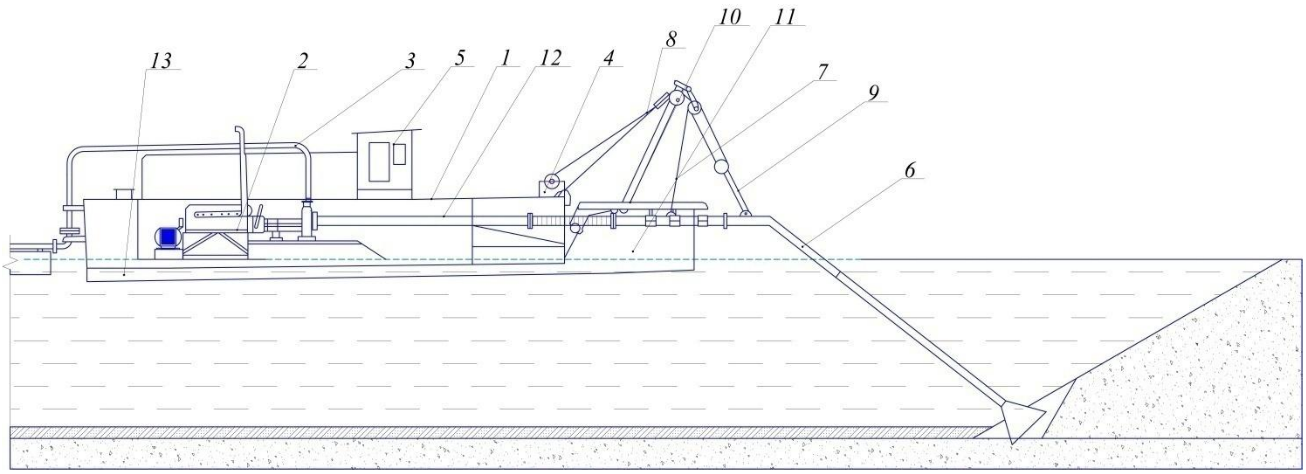

Fig. 1. Diagram of the PZU-8M floating dredging unit: 1 — body; 2 — 3D6SN engine; 3 — dredging pipe; 4 — hoist winch of the ripper frame; 5 — control cabin;
6 — suction pipe; 7 — jib boom; 8 — suspension of the jib boom; 9 — tackle pulley of the suspension of the suction pipe frame; 10 — lifting frame of the ripper; 11 — side pontoon; 12 — pressure pipeline; 13 — central pontoon

[1]Avdonin V. V. Vibropogloshchayushchie kompozitsionnye pokrytiya. Dissertation. Saransk, 2015. 123 p. (In Russ.).

There is a problem of obtaining reliable information about noise and vibration levels on this equipment. Often, these data may be found in the protocols of the results of a special assessment of working conditions (SAWC) or in special literature (guidance document, GOST), as well as in scientific and technical literature (dissertations, articles, reports)[2] [1, 2]. However, the degree of their reliability varies, which necessitates planning and conducting noise and vibrations measurements directly on the object.

For example, the actual noise levels of the 3D6SN diesel pump installed on the PZU-8M dredger platform are given in the guidance document[3] and shown in Figure 2.

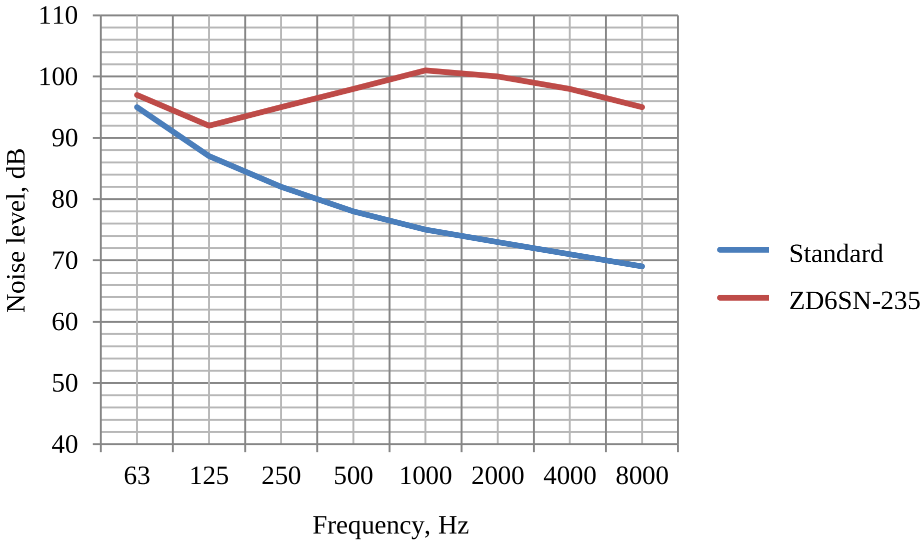

Fig. 2. Comparison of the actual sound pressure level of the diesel pump ZD6SN with the sanitary and hygienic norms[4]

Judging by the data in Figure 2, the required noise insulation reaches 26 dB at a frequency of 1000 Hz, which is one of the reasons for the high levels of noise and vibration transmitted from the diesel pump to the driver's cabin.

In the case under consideration, KT "Krym-Investstroy and Company" provided the authors with the protocols with the results of measurements of sound pressure and vibration acceleration levels at the workplace, which were obtained as part of SAWC conducted in the organization in March-April 2017. Since the measurement protocols present equivalent noise levels measured three times in accordance with the method, it is necessary to decompose the sound pressure level into the spectrum according to Osipov[5] to obtain a complete spectral noise characteristic.

As a result of the analysis of the protocol data on noise and vibration levels, spectral noise characteristics were obtained (Fig. 3). These values of the actual sound pressure levels at the workplaces of the driver and the assistant driver of the PZU-8M dredger revealed an excess of sanitary and hygienic standards, which corresponded to 3.2 harmful class of working conditions. The actual values of the vibration parameter corresponded to 3.1 class of working conditions, and an excess of 6.3 dB over the adjusted levels was also found (Fig. 4).

[2]Shcherbakova O. V. Vibroizolyatsiya strukturnogo shuma na sudakh. Dissertation. Novosibirsk, 2014. 20 p. (In Russ.).
[3]RD 31.81.81-90. Rekomendatsii po snizheniyu shuma na sudakh morskogo flota. Approved by the decision of the Ministry of the Maritime Fleet and the Ministry of Justice of 04.04.1991. Leningrad, 1991. 67 p. (In Russ.).
[4]On approval of the Methodology for conducting a special assessment of working conditions, the Classifier of harmful and (or) hazardous production factors, the report form for conducting a special assessment of working conditions and instructions for completing it: Order of the Ministry of Labor and Social Protection of the Russian Federation No. 33n of January 24, 2014. Available from: https://www.consultant.ru/document/cons_doc_LAW_158398/ (accessed 15.02.2023). (In Russ.).
[5]Osipov G. L. (Ed.) Zvukoizolyatsiya i zvukopogloshchenie. Textbook. Moscow: Astrel', 2004. 450 p. (In Russ.).

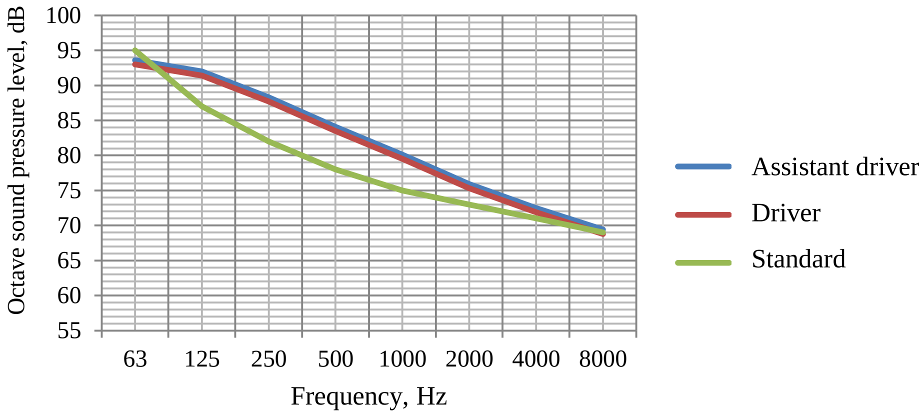

Fig. 3. SAWC results of the dredger driver and the driver assistant on the noise factor (Authors' figure)

Thus, in the future, we will consider reliable sound pressure and vibration acceleration levels measured by the device "Noise meter-vibrometer "Ecofizika 110A" in accordance with the methodology[4] in the SAWC framework, (Fig. 3, 4).

Means of protection against vibration and noise can affect the excitation source itself or on the path of its propagation. It is necessary to try to implement technical solutions for noise and vibration protection at the design stage of machines. When this is not done, you have to do it already at the operational stage.

Vibration damping (vibration-absorbing) coatings are among the means of protection against vibration and noise transmitted to the dredger driver's cabin. Their main purpose is to reduce the vibroacoustic activity of noise and vibration sources.

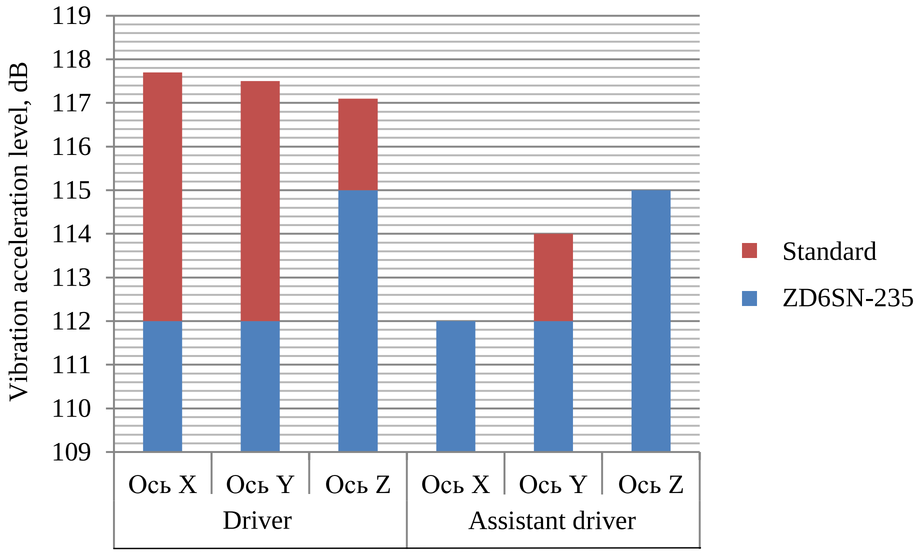

Fig. 4. SAWC results of the dredger driver and the driver assistant on the vibration factor

Results. *Design scheme of the vibration damping model*. Figure 5 shows the design scheme of the vibration damping system at the workplace of the dredger operator. Since the mass of the vibration damping mat $m_П$ is small in comparison with the mass of the platfor m m_1, the influence of its movement on the vibrations of the platform is neglected. The main structure with a mass of m_1 does not rely on vibration insulators with reduced rigidity. In addition, we do not take into account the effect on vibration insulation of vibrations from water. Vibration dampener (mat) is connected to the main mass by vibration insulators with reduced stiffness C_2 and dampers with reduced viscous resistance drag coefficient r.

The design scheme of the vibration damping system at the workplace of the dredger operator is described analytically by a system of differential equations (1)–(3) (Fig. 5).

According to this design scheme, the following relations of the parameters involved in the model equations are valid:

$$C_2 = E \cdot \frac{h^3}{12(1-\mu^2)}, m_2 = m_п + m_ч, r = 2m_2 \cdot f_i \cdot η_Σ, F(t) = m_п \cdot g \cdot a, \quad (1)$$

where E — modulus of elasticity, Pa; μ — Poisson's ratio; $m_ч$ — mass of a person (driver), kg; η_Σ — total coefficient of loss of vibrational energy; $F(t)$ — external force of influence, N.

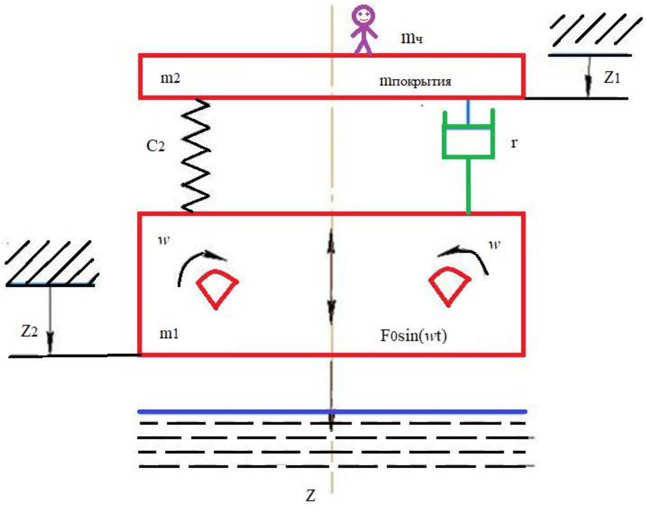

Fig. 5. Design scheme of the vibration damping system at the dredger operator workplace

Differential equations of motion have the form:

$$m_1 z_1'' + r z_1' + C_2 z_1 - r z_2' - C_2 z_2 = F_0 \sin(\omega t) \tag{2}$$

$$m_2 z_2'' - r z_2' - C_2 z_1 + r z_2' - C_2 z_2 = 0, \tag{3}$$

where z_1, z_2 — vibration displacement of the platform and vibration damping flooring, m; F_0 — amplitude of the external disturbing force, N; ω — circular rotation frequency, rad/s.

System of differential equations (2) and (3) can subsequently be solved both analytically and numerically.

However, for the purposes of engineering calculation, it seems to the authors that simplified dependencies are quite acceptable when there is no need to accurately determine the vibration damping parameters.

Algorithm for calculating the vibration insulation effectiveness. The efficiency of vibration damping in structures and structural elements is determined through the coefficient of loss η, which is characterized by the ratio of the energy absorbed in the system during the oscillation cycle ($W_{погл}$) to the maximum potential energy in the system ($W_{пот}$):

$$\eta = \frac{1}{2\pi} \cdot \frac{W_{погл}}{W_{пот}}. \tag{4}$$

To calculate the efficiency of vibration damping flooring at the workplace of the PZU-8M dredger operator, we use the coefficient of loss of vibrational energy, which is determined for a single-layer structure by formula[6]:

$$\eta = \frac{\frac{E_1 \cdot h_1^3}{12(1-\mu_1^2)} \cdot \eta_1 + \frac{E_2 \cdot h_2^3}{12(1-\mu_2^2)} \cdot \eta_2}{\frac{E_1 \cdot h_1^3}{12(1-\mu_1^2)} + \frac{E_2 \cdot h_2^3}{12(1-\mu_2^2)}}, \tag{5}$$

where E_1 and E_2 — elastic modulus of steel tubular platform and vibration damping flooring, Pa; η_1 and η_2 — effective coefficients of vibrational energy losses of steel and flooring; h_1 and h_2 — thickness of the steel sheet of the platform and vibration damping flooring, mm; μ_1 and μ_2 — Poisson's ratios of steel and flooring material.

The calculated decrease in octave sound pressure levels is determined by formula:

$$\Delta L = 10 \cdot lg \frac{\eta}{\eta_{основн}}, \tag{6}$$

where $\eta_{основн} = \eta_{плтаформы} = 10^{-4}$.

[6]Chukarin A. N. Vibroakusticheskie osnovy rascheta metallorezhushchikh stankov na stadii ikh proektirovaniya. Dissertation. Rostov-on-Don, 1995. 29 p. (In Russ.).

Analytical base of dynamic characteristics and properties of vibration damping materials. The difficulty of determining the coefficient of loss of vibrational energy of materials η is due to the absence of proven dependences η on temperature T and on the frequency spectrum f in the literature. Only in source[1] there is some information about the dynamic characteristics of some materials and substances. The analysis of the scientific literature shows that there is also a limited number of dissertation studies on this issue, for example, in [3] only the features of vibration damping materials used in construction are considered. The lack of sufficient information about the spectrum of dynamic characteristics of vibration damping materials makes it necessary to plan experimental studies in the future to determine η. At this stage of the study, as a result of the analysis of available literature sources, the dynamic characteristics of some materials used as vibration-insulating flooring in workplaces were collected and presented in Table 1 [4–7].

Let us calculate the expected reduction of noise and vibration levels at the workplace of the dredger operator depending on the thickness of the damping elements according to formulas (4)–(6). From the reference data for steel, we have: $E_1=2\cdot10^{11}$ Pa, $\eta_1=10^{-4}$, $\mu_1=0.28$, the thickness of the steel sheet covering the dredger platform is $h_1=1.5$ mm. Dynamic characteristics of vibration damping materials are selected from Table 1. Figure 6 provides the calculation results. The analysis of the values calculated using formula (6) of the expected decrease in sound pressure levels and vibration acceleration when using vibration damping materials allowed us to draw a number of conclusions.

Table 1

Fragment of the created database of dynamic characteristics of vibration damping materials

Material	Effective coefficient of vibrational energy loss, η	Modulus of elasticity $E\cdot10^{-8}$, Pa	Poisson ratio, μ
Felt	0.2	5	0
Linoleum 1	0.21	7	0.4
Rubber 8797	0.2	0.1	0.4
Vibration damping elastomeric plates[7]			
VEP 10	0.25	0.11	0.025
VEP 20	0.3	0.14	0.07
VEP 4	0.13	0.11	0.06
Elastomeric vibration damping plates Nowelle[8]			
Nowellemod 1	0.25	0.1	0.03
Nowellemod2	0.13	0.1	0.06
Nowellemod3	0.24	0.11	0.09
Nowellemod4	0.26	0.07	0.09

[7] Vibrogasyashchie elastomernye plastiny. TU 2534-002-61734928-2013. Electronic fund of legal and regulatory documents. Available from: https://docs.cntd.ru/document/437156319 (accessed 15.02.2023). (In Russ.).

[8] Elastomernye vibrodempfiruyushchie plastiny Nowelle. TU 2534-001-32461352-2015. Electronic fund of legal and regulatory documents. Available from: https://docs.cntd.ru/document/437156318 (accessed 15.02.2023). (In Russ.).

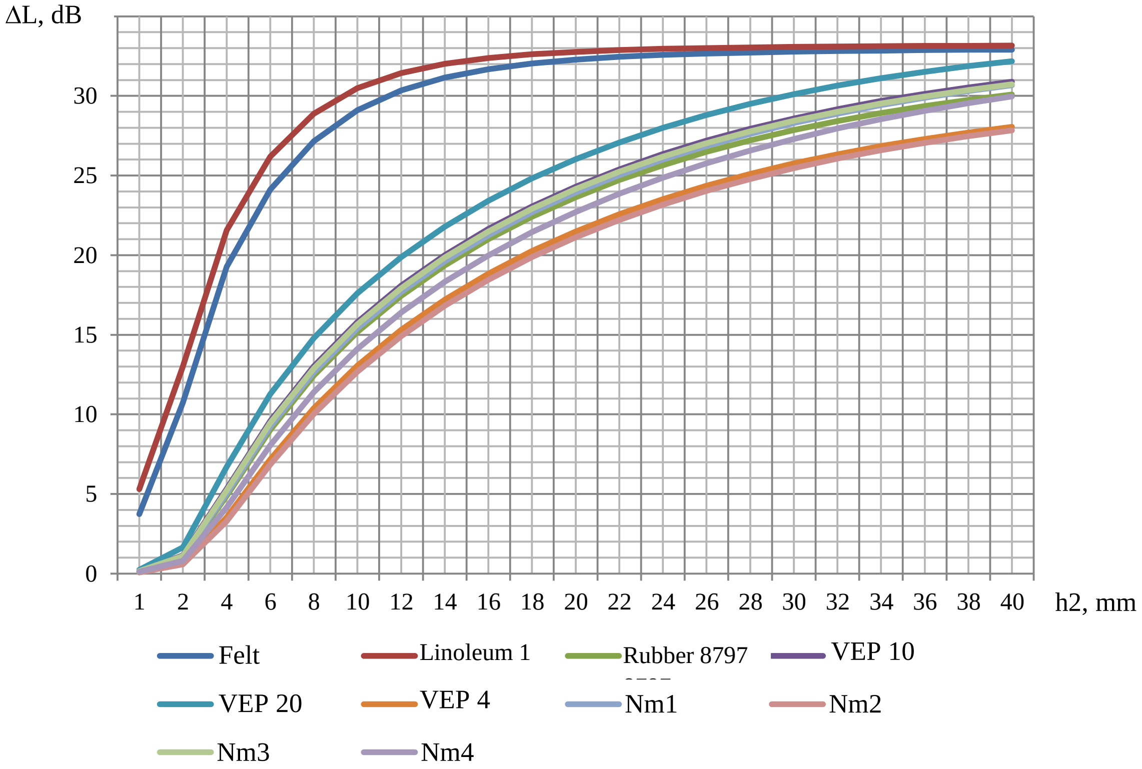

Fig. 6. Graph of the dependence of sound pressure level decrease on vibration damping material thickness h_2, mm

Materials such as felt and linoleum 1, with a relatively small coating thickness (up to 40 mm), provide more effective noise and vibration insulation compared to other materials. However, in the future, an increase in the thickness of non-rubber coating (from 40 to 60 mm and above) does not affect the effectiveness of workplace insulation (Fig. 7).

On the contrary, the results of calculation of the vibration damping efficiency show that with a coating thickness of more than 49 mm, the efficiency of materials made of elastomeric plate VEP20 increases and continues to grow, compared with materials such as felt and linoleum (Fig. 7). Moreover, with a thickness of vibration damping flooring VEP20 h_2=4 mm, a decrease in sound pressure and vibration acceleration levels is achieved up to sanitary and hygienic standards.

Thus, the calculations of the effectiveness of vibration insulation when using various vibration damping materials of different thicknesses have shown the advantages of vibration damping flooring made of elastomeric plate VEP20 compared with other materials.

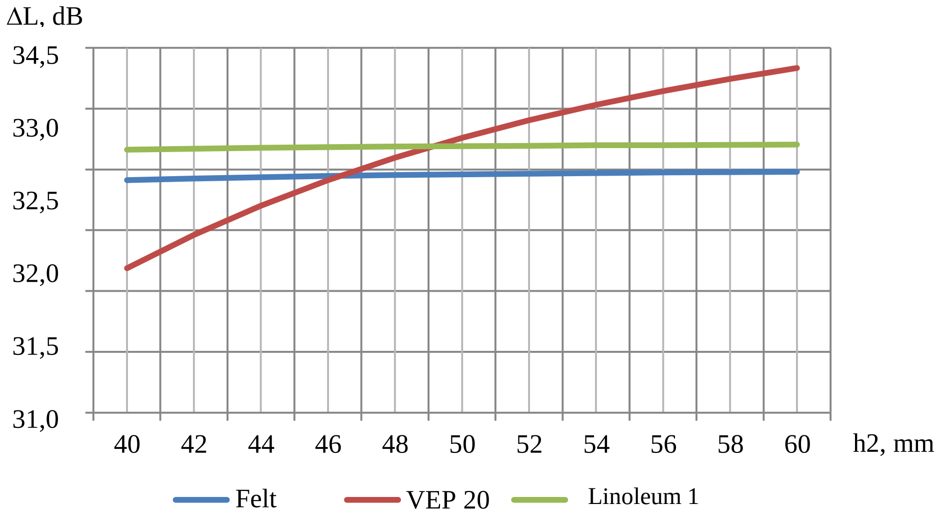

Fig. 7. Comparison of the effectiveness of sound pressure levels reduction due to vibration damping of the dredger platform with a rubber plate, felt and linoleum1, where h_2 is the vibration damping flooring thickness, mm

Significance of vibration damping materials properties. It should be noted that the above calculation of vibration and noise insulation is made for a special case when the dynamic characteristics do not change from temperature, noise and vibration spectrum. In real operating conditions, under the influence of external temperature and the frequency spectrum of vibrations, the values of dynamic elastic modulus and vibrational energy loss coefficients of damping materials change significantly, which, in turn, are determined by their chemical structure and molecular mobility, intra- and intermolecular interaction.

It follows from dependence (7) that at low ambient temperatures (below 0 °C), polymers are in a glassy state, which means that their dynamic elastic modulus reaches a value of 10^9 Pa. Conversely, at high temperatures (28 °C and above), when polymer materials are in a highly elastic state, the values of elastic modulus decrease to 10^5—10^6 Pa.

The effective coefficient of loss of vibrational energy of polymers depends on the value:

$$\omega\tau_1 = \frac{2\tau_1\pi}{T}, \qquad (7)$$

where τ_1 — relaxation time; T — oscillation period.

The value of the effective loss coefficient of the polymer directly depends on its temperature. For this reason, its value will increase with decreasing ambient temperature. At low temperatures, the polymer material behaves in the same way as at high oscillation frequencies. With an increase in temperature or with a decrease in frequency, ωT_i decreases, the loss of vibrational energy first increases, then, after passing through the maximum (at ωT_i=1), decreases.

At high ambient temperatures or at low frequencies, the modulus of elasticity and the effective loss coefficient are quite small.

Conducting experimental studies of the dynamic characteristics of vibration damping materials is of great importance in the design of integrated protection systems for watercraft drivers [8–9]. Thus, in the absence or insufficient efficiency of microclimate normalization systems in the watercraft cabin, it is possible to worsen the damping properties of materials and the effectiveness of vibration damping of the coating (flooring, mat), which is under the influence of temperatures in either a heating or cooling microclimate[9] [10].

Automation of the engineering methodology for calculating the effectiveness of vibration insulation by means of Excel. To quickly change and select the main parameters of the vibration damping coating, a control program was developed in Microsoft Excel (Fig. 8, 9). Based on the database of dynamic characteristics of vibration damping materials, the program automatically determines the total coefficient of vibrational energy loss of all flooring layers, as well as a decrease in the sound pressure level.

[9]Maslenskiy V. V. Uluchshenie uslovii truda operatorov tekhnologicheskikh i mobil'nykh mashin v usloviyakh nagrevayushchego mikroklimata. Author’s thesis. Rostov-on-Don, 2021. 20 p. (In Russ.).

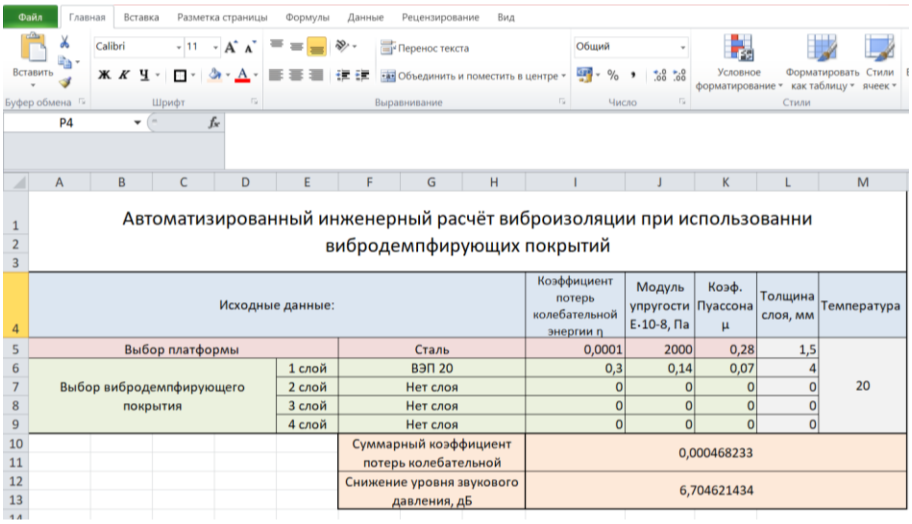

Fig. 8. Interface of the program for automated calculation of vibration insulation efficiency in MS Excel

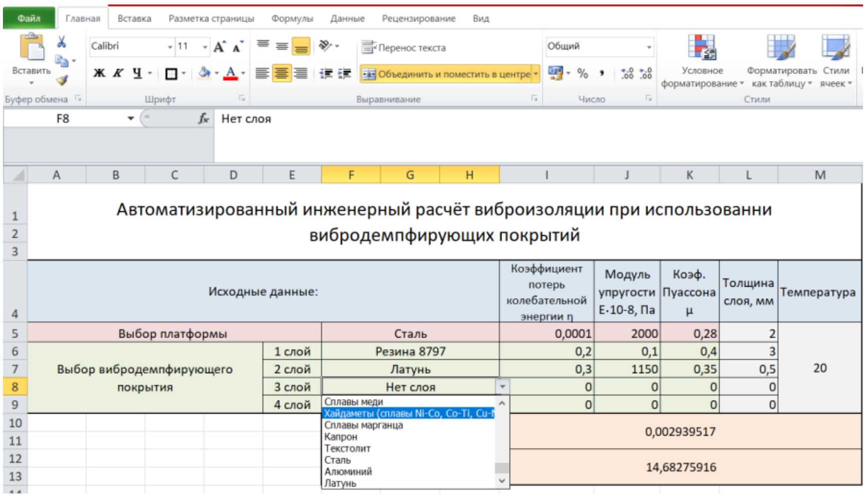

Fig. 9. Use of vibration damping materials database in the design of vibration protection in MS Excel

At the initial stage of preparation for the calculation, the operator must have the following data: the number of flooring layers (the maximum number is 4), the thickness of each layer, the temperature of the medium. Further, by selecting the material of each layer, the vibration protection designer achieves the maximum reduction in the sound pressure level at the specified parameters.

Discussion and Conclusion. The authors have automated the calculations of vibration insulation efficiency in Excel. The calculation module of the above program is provided with data from the analytical database of dynamic characteristics and properties of vibration damping materials, which is easily replenished. This allows you to calculate and reasonably select multilayer structures taking into account the ambient temperature, as well as the dynamic characteristics of vibration damping materials depending on the spectrum of noise and vibration. The method of calculation and selection of vibration damping material for vibration protection systems of the driver proposed by the authors can be used not only at the design stage of new watercrafts, but also during the operation of the existing structures.

References

1. Yegelskaya E. V., Korotkiy A. A. Power-plant vibroacoustics impact on noise levels in floating crane cabins. Vestnik of Don State Technical University. 2012;1–2(62):33–37. (In Russ.).

2. Shcherbakova O. V., Romanchenko M. K. Research of requirements of sanitary norms, recommended for vibration and noise on a river transport. Zhurnal universiteta vodnykh kommunikatsii. 2010;1:70–73. (In Russ.).

3. Smirnov V. A., Smolyakov M. Yu. Sravnitel'nyi analiz dinamicheskikh kharakteristik elastichnykh plastmass i rezinovykh vibrodempfiruyushchikh materialov. Stroitel'nye materialy. 2018;6:36–40. (In Russ.).

4. Kirpichnikov V. Yu., Syatkovsky A. I., Shlemov Yu. F. High-effective tools for low-frequency shock-absorbing using flexible element made from polymer film. Shipbuilding. 2020;1(848):44–47. (In Russ.).

5. Volodin P. N., Brostilov S. A., Bekbauliev A. O., Yurkov N. K. Zashchita REA ot mekhanicheskikh vozdeistvii putem vibrodempfirovaniya nesushchikh konstruktsii i soputstvuyushchie etomu negativnye factory. Robototekhnika i sistemnyi analiz: coll. papers. Penza. 2015;1:86–89. (In Russ.).

6. Lesnyak A. N., Pshenitsyn A. A., Spiridonov A. Yu. Application efficiency for vibration damping covers. Shipbuilding. 2015;3(820):39–41. (In Russ.).

7. Skripchenko D. S., Ovsyannikov S. N. Methods of Tests Conduction for Determining the Dynamic Elasticity Modulus, Dynamic Shear Modulus, and Loss Factor of Sound Insulation Materials. Construction Materials. 2017;6:55–58. (In Russ.).

8. Yaitskov I. A., Chukarin A. N., Finotchenko T. A. Theoretical research of noise and vibration spectra in cabins of locomotive and diesel shunting locomotive. International Journal of Applied Engineering Research. 2017;12(21):10724–10730.

9. Abdrakhmanov N. Kh., Fedosov A. V., Khamitova A. N. et al. Main aspects of vibroacoustic factors assessment. Safety of Technogenic and Natural Systems. 2021;3:3-22. (In Russ.).

10. Meskhi B., Bulygin Yu., Shchekina E., Maslensky V. Elements of microclimate normalization system in the cabin of TORUM grain mandy combine. IOP Conference Series: Earth and Environmental Science. 2019;403:012089. 0.1088/1755-1315/403/1/012089

Received 25.12.2022

Revised 23.01.2023

Accepted 26.01.2023

About the Authors:

Budovskiy, Aleksandr V., student of the Life Safety and Environmental Protection Department, Don State Technical University (1, Gagarin sq., Rostov-on-Don, 344003, RF), ORCID, k55355396@gmail.com

Bulygin, Yuriy I., professor of the Life Safety and Environmental Protection Department, Don State Technical University (1, Gagarin sq., Rostov-on-Don, 344003, RF), Dr. Sci. (Eng.), ORCID, bulyur_rostov@mail.ru

Pavlikov, Aleksandr V., assistant of the Life Safety and Environmental Protection Department, Don State Technical University (1, Gagarin sq., Rostov-on-Don, 344003, RF), ORCID, sanya.pavlikov@mail.ru

Tryukhan, Aleksandr V., postgraduate student of the Life Safety and Environmental Protection Department, Don State Technical University (1, Gagarin sq., Rostov-on-Don, 344003, RF), ORCID, tryukhan.alexandr@mail.ru

Claimed contributorship

Yu. I. Bulygin: formulation of the basic concept, goals and objectives of the study, revision of the text, correction of the conclusions, A. V. Pavlikov: collection and analysis of the research results, A. V. Budovsky: calculations, preparation of the text, A. V. Tryukhan: revision of the text, formulation of the conclusions.

Conflict of interest statement

The authors do not have any conflict of interest.

All authors have read and approved the final manuscript.

TECHNOSPHERE SAFETY

Original article
UDC 331.453
https://doi.org/10.23947/2541-9129-2023-1-39-46

Ensuring Occupational Safety at Railway Transport Operation by Upgrading the Systems of Vibration Damping Plates and Rail Plates

Elena I. Golovina ✉, **Dmitriy A. Sokolov**
Voronezh State Technical University Voronezh, Russian Federation
✉ u00111@vgasu.vrn.ru

Abstract

Introduction. Noise and vibration in railway transport is a dangerous type of pollution for both the workers and the environment. It is important to carry out a comprehensive analysis of the effects of noise and vibration pollution on railway transport workers, the environment, and to consider available methods to minimize harmful effects created during the movement of trains. Safety can be achieved by ensuring regulatory noise and vibration levels. The work objective is to assess the safety of work during the operation of railway transport by improving the system of vibration damping pads and rail plates.

Materials and Methods. In the course of the study, an analysis of the occurrence of noise and vibration, an assessment of their negative impact on railway transport workers and the environment was carried out. The available methods of noise pollution minimization are considered, the classification of noise and vibration control methods is described. The methods and means required by the regulatory documents on labor safety during the operation of railway transport were used in the work.

Results. Based on the results of the study, it follows that there is a need to strengthen measures for comprehensive protection and minimization of harmful factors. The result of the study was the proposal to improve one of the applied methods of noise minimization — the installation of a vibration damping pad, for the production of which secondary raw materials in the form of rubber crumbs are used. The paper calculates the economic efficiency of one of the proposed methods of minimizing noise pollution and describes the positive effect after its application, considers available options for improving the sound absorption of rails.

Discussion and Conclusion. Based on the results of the study, the positive economic effect of one of the proposed ways to improve the noise minimization method was revealed.

Keywords: noise pollution, vibration, environment, vibration damping plates, noise pollution minimization, vibration minimization.

Acknowledgements. The authors would like to thank Professor, Dr. Sci. (Eng) Vyacheslav Yakovlevich Manokhin for mentoring, and also express their gratitude to anonymous reviewers.

For citation. E. I. Golovina, D. A. Sokolov. Ensuring Occupational Safety at Railway Transport Operation by Upgrading the Systems of Vibration Damping Plates and Rail Plates. Safety of Technogenic and Natural Systems, 2023, no.1, pp. 39–46. https://doi.org/10.23947/2541-9129-2023-1-39-46

Introduction. Comprehensive analysis of noise and vibration pollution from railway transport shows a long-term negative impact on human health [1]. This effect is dangerous due to the occurrence of various diseases — vibration disease, diseases of the auditory nerve (neuritis, auditory dissynchrony) [2]. The share of noise in the factor assessment of the working conditions of drivers and assistant drivers of locomotives is more than 35% [3]. When conducting a special assessment of working conditions, the degree of harmfulness and danger under the action of vibroacoustic factors is established according to R 2.2.2006–05, taking into account their temporary characteristics (constant, non-constant noise, vibration, etc.)[1]. Creation of a comfortable working environment for people working in railway transport is achieved by minimizing the impact of such factors.

When assessing the impact of noise pollution and vibration within the framework of a special assessment of working conditions, a consistent methodology is used, which includes: identification of factors that negatively affect workers; research and measurement of factors; attribution of working conditions to a certain class, based on the degree of harmfulness [4]. When assessing working conditions, attention is paid to the nature of noise (constant or non-constant) and its tone characteristics. When an employee is exposed to constant noise, the assignment of working conditions to a class or subclass under the influence of vibroacoustic factors is carried out based on the measurement results of sound pressure levels in octave ranges with average geometric frequencies 31.5; 63; 125; 250; 500; 1000; 2000; 4000; 8000 Hz (Table 1) [5].

Table 1

Working conditions classes depending on noise levels, local, general vibration, infra- and ultrasound in the workplace according to R 2.2.2006–05[2]

Factor name, indicator, unit of measurement	Working conditions class					
	Acceptable	Harmful				Hazardous
	2	3.1	3.2	3.3	3.4	4
	Exceeding the MPL to ...dB/time (inclusive):					
Noise, equivalent sound level, dBA	MPL	5	15	25	35	35
Local vibration, equivalent corrected level (value) of vibration velocity, vibration acceleration (dB/time)	MPL	3/1.4	6/2	9/2.8	12/4	12/4
Total vibration, equivalent corrected level of vibration velocity, vibration acceleration (dB/time)	MPL	6/2	12/4	18/6	24/8	24/8
Infrasound, total sound pressure level, dB/Lin	MPL	5	10	15	20	20
Air ultrasound, sound pressure levels in 1/3 octave frequency bands, dB	MPL	10	20	30	40	40
Contact ultrasound, vibration velocity level, dB	MPL	5	10	15	20	20

[1] R 2.2.2006-05. Guide on Hygienic Assessment of Factors of Working Environment and Work Load. Criteria and Classification of Working Conditions. Commission on State Sanitary and Epidemiological Rationing; Chief State Sanitary Doctor of the Russian Federation. Bulletin of normative and methodological documents of the State Sanitary and Epidemiological Supervision. 2005. No. 3(21). 114 p. (In Russ.).

[2] R 2.2.2006-05. Guide on Hygienic Assessment of Factors of Working Environment and Work Load. Criteria and Classification of Working Conditions. (In Russ.).

Working conditions assessment by vibroacoustic factors at the workplaces of drivers and assistant drivers, track and station workers is carried out similarly to stationary workplaces where there is equipment that is a source of noise and vibration. The maximum permissible noise levels in the workplace are determined taking into account the severity and intensity of work activity according to SN 2.2.4/2.1.8.562–96[3].

The work objective is to assess the safety of work during the operation of railway transport by upgrading the systems of vibration damping plates and rail plates.

The main source of noise in railway transport is the noise emitted by the train during movement, which is created by track machines and technical equipment [1]. Vibration is transmitted from the wheelsets to the body of the car and tends to spread into the environment [5]. Increased noise and vibration are considered to be the criteria, the compliance of which with regulatory values is technically the most difficult to achieve [6].

The results of long-term clinical observations and examinations of large groups of people of various specialties, whose work is associated with exposure to intense noise, allow us to consider noise sickness an independent form of professional pathology[4]. Noise regime, which significantly exceeds the standards, with continuous exposure has a negative effect on health: the hearing organs, nervous and vegetative systems suffer [7]. Noise level from railways depends on many factors. This is influenced, for example, by the technical condition of the tracks and rolling stock, the type of brakes used, the volume of traffic or the terrain. Carriage and repair and equipment depots, which are located near residential areas, cause significant harm to human health and the integrity of natural systems. Noise and vibration that occur during the movement of trains also harm humans and the environment. A significant excess of noise level standards brings discomfort to residents, can be a significant cause of deterioration of well-being and decreased performance. Prolonged and systematic exposure to noise pollution and vibration can be the beginning of the development of diseases of the nervous and vegetative-vascular systems. The number of people exposed to a high degree of sleep disturbance is very large. Most people are exposed to constant noise of 50-60 dB at night, which in the absence of other daytime noise sources is one of the main factors of insomnia and systematic neuroses.

In noise minimization methods classification, the following directions are used: minimizing or eliminating noise at the source, minimizing noise from the source to the object (sound insulation, sound absorption, minimization) and protecting people with special means. Noise protection can be implemented by means of collective protection (acoustic screens, fences, casings, vibration damping pads), or by means of individual protection (overhead headphones, earplugs).

Materials and Methods. Current methods of noise control are technical methods (timely maintenance of equipment and railway tracks, grinding rails, etc.), architectural planning and acoustic methods (installation of noise shields, casings, vibration damping plates).

To date, there are many alternative methods that contribute to noise exposure reduction through the use of additional technical solutions: highly elastic gaskets for rail fasteners, ballast mats, elastic supports for the track on plates with a ballast tank, systems called "mass-spring". Mass-spring systems are used when presenting the most stringent requirements for protection against structural noise and in the presence of constructive implementation possibilities.

The results of theoretical studies have shown the effectiveness of the "mass-spring" design scheme. The most effective structures are those that contain monolithic concrete or concrete elements [8]. When designing an elastic

[3] SN 2.2.4/2.1.8.562-96. Shum na rabochikh mestakh, v pomeshcheniyakh zhilykh, obshchestvennykh zdanii i na territorii zhiloi zastroiki. Sanitary Standards. State Committee on Sanitary and Epidemiology Surveillance of the Russian Federation. Consortium "Codex". Available from: https://docs.cntd.ru/document/901703278 (accessed 18.01.2023). (In Russ.).

[4] Terenteva L. S. Geoekologicheskaya otsenka akusticheskogo zagryazneniya primagistral'nykh territorii: na primere g. Voronezha: dis. cand. sci. (geogr.). nauk. Voronezh, 2008. 152 p. (In Russ.).

support for mass-spring systems, the chosen design solution determines the final efficiency of the vibration insulation system.

Let us consider the actual constructive methods of noise control in more detail. A belt support, as a type of construction, is used in "mass-spring" systems (Fig. 1). The main advantage of such a support is effective vibration compensation that occurs during train movement due to the relatively large area of the bases. With the introduction of a belt support, it is possible to obtain a reduction in the frequencies of the upper structure of the track that negatively affect a person with long-term exposure at a lower cost. The positive effect is the reduction of vibration and noise.

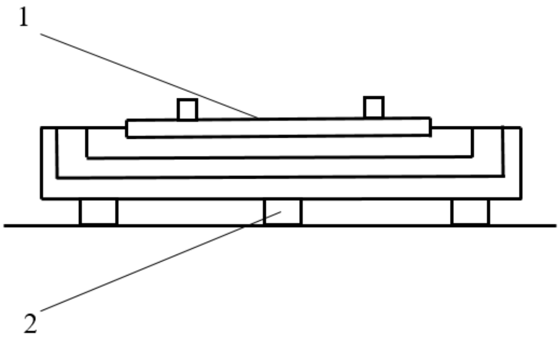

Fig. 1. Variant of belt supports installation scheme: 1 — railbed; 2 — belt supports

The materials used in the mass-spring system must have a number of properties: resistance to short-term, peak loads, have a fine-mesh, static structure, which makes it possible to maintain the useful efficiency of the supports during operation.

Point supports can only be used with a specific design. Slabs of monolithic concrete are lifted; the supports are installed through special mounting holes (Fig. 2). It is worth noting that the support area is extremely small, when designing supports of such a design, it is necessary to take into account the horizontal forces that arise during the movement of the train. To limit horizontal shifts in accordance with the specified parameters, it is necessary to find the optimal ratio between the shear modulus, the elasticity of the material, the thickness and the area of the support.

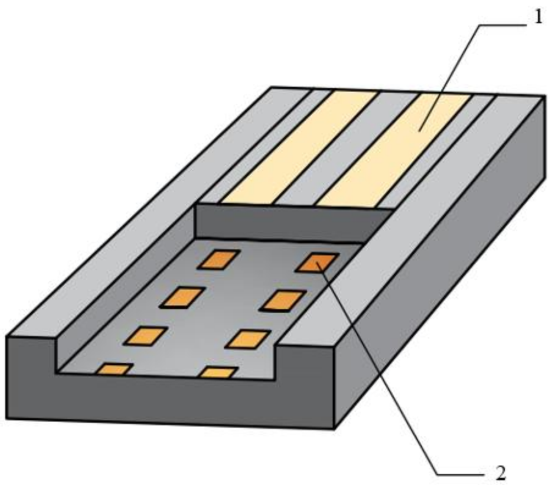

Fig. 2. Variant of point support installation scheme: 1 — railbed; 2 — point supports

After installation, point supports can provide protection against structural noise and reduce natural frequencies. The use of such systems makes it possible to achieve noise minimization up to 30 dB or more. The main difficulty in using this method is a complicated installation, depending on the design of the plates, the high cost of installation and routine maintenance.

One of the effective and relatively low-cost methods of noise reduction from the "wheel-rail" system in the source is to reduce the sound emission of the rail. This is achieved by installation of vibration damping plates [1].

The vibration damping plate is an overlay that is installed on rails to absorb noise. Their advantage is that they prevent the spread of noise to the surrounding area. Due to their structural composition, they absorb vibrations arising in the "wheel-rail" system, and thereby prevent the formation of noise in the rail. In case of train movement, when the wheel comes into contact with the rail, noise with a variable spectrum is generated. The rail damper operates according to the vibration absorption system at frequencies with the highest noise level. Fig. 3 provides one of the variants of the vibration damping plate scheme.

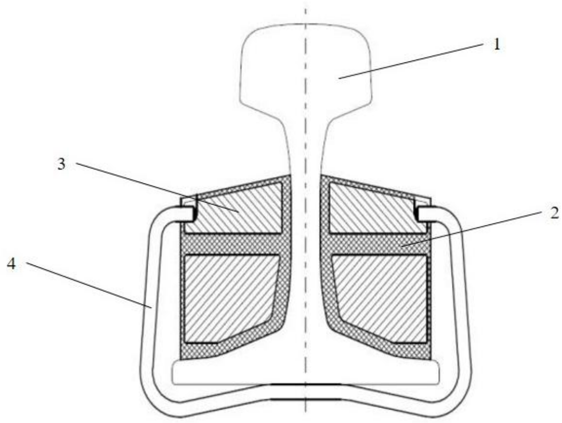

Fig. 3. Variant of the vibration damping plate installation scheme: 1 — rail; 2 — plate; 3 — plate filling; 4 — plate attachment

In a number of frequency ranges (low and high), the plate structure is not suitable for noise reduction. On the other hand, in the case of frequencies characteristic of most of the generated noise, the plate is the most effective minimization method. The plate, which prevents the spread of vibration, also contributes to a qualitative reduction of vibration exposure.

The authors propose to modernize the existing methods of reducing noise and vibration pollution by using more economical materials of plates and mats without a complete reconstruction of the railbed.

Results. Rail plates usually reduce the noise level by about 3-4 dB, while improving the design — by 5-8 dB. Based on the analysis of the studies, the authors have constructed a graph with the measurement results (Fig. 4)[5]. Several ways of design improvement are proposed to obtain a better result of noise minimization through the use of modern structures, such as a continuous welded rail, elastic rail fastening, anti-vibration mats and flexible gaskets under the rails. It should be borne in mind that such improvements are available only when replacing or laying a new railway track. The disadvantage of the presented activities is the high cost and complexity of the installation.

[5] GOST 32203 — 2013. Railway rolling stock. Acoustics. Measurement of outward noise. VNIINMASh; Federal Agency for Technical Regulation and Metrology. Moscow, 2014. 20 p. (In Russ.).

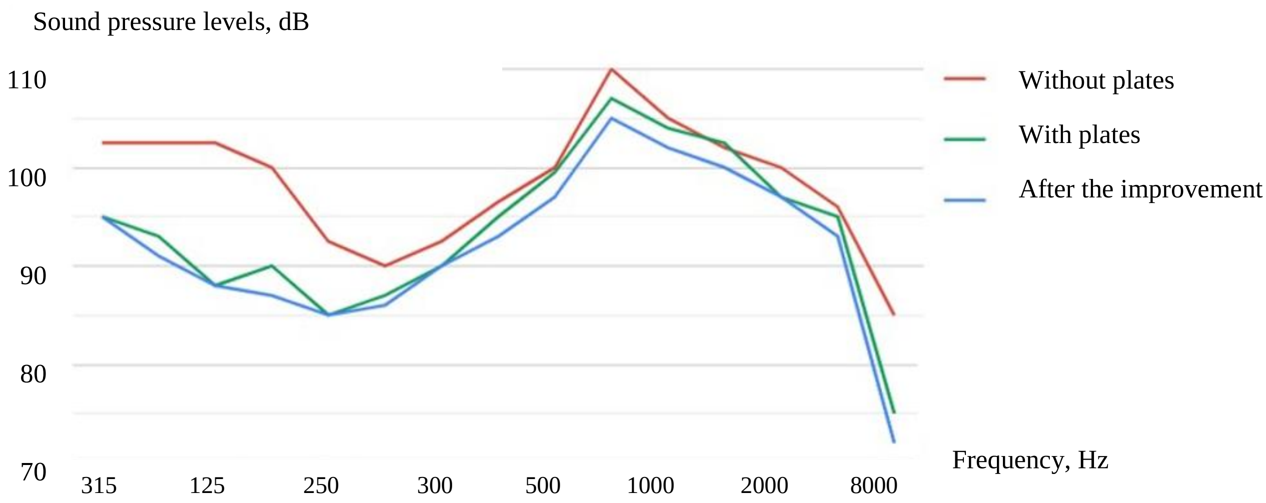

Fig. 4. Graph with measurement results

When carrying out measurements, the influence of noise from other vehicles and industrial facilities on the measurement results should be excluded. By analyzing the available options, a budget and relatively simple improvement option was found — the use of a mat system made of recycled synthetic fiber waste that will repeat the shape of the rails. It consists of 3 or 5 parts that are placed between and next to the rails, while the combination significantly reduces the noise from railway traffic (Fig. 5). It is worth noting that when using raw materials for the manufacture of mats from recycled materials, it will be possible to reduce the cost of mats up to 20–30 % or more. It is worth noting that the use of materials in the production of which more than 60 % rubber crumb is used, can also be used as a substitute for filling the lining of the vibration damping plate.

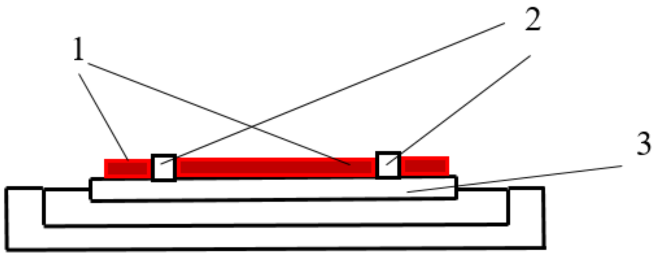

Fig. 5. Variant of the mat system installation scheme: 1 — mat system; 2 — rails; 3 — railbed

When considering the use of the mats system, it is worth identifying all sides of the financial issue. An economic assessment of the effectiveness of environmental protection costs is necessary for the most rational use of limited material and financial resources of an enterprise or organization [9]. It serves to evaluate the advantages (or disadvantages) already obtained, to determine the most appropriate option for the environmental project, as well as to determine the amount of costs necessary to achieve optimal environmental and economic results. When developing a choice for the introduction of new equipment or technology aimed at cleaner production, safety for human health and the environment, as well as the environmental friendliness of the technologies and materials used, should be taken into account.

To create a model for calculating economic efficiency in the implementation of a new method for reducing noise and vibration, we use the methodology described in [10], according to which the main calculations will be performed point by point. The economic assessment of measures to minimize and protect against noise is calculated as the calculation of the annual economic effect when using measures. The economic effect for the year is found by calculating the difference between the result obtained when applying protection measures and the annual costs of these measures [11].

Based on the analysis of open sources, we assume that a sheet of vibration damping mat costs from 3.5 thousand rubles for a sheet of one m^2 in size. As a result of calculations, a model of economic efficiency from the mat system introduction is presented in Table 2.

Table 2

Economic efficiency model when using an improvement in the method of minimizing noise and vibration effects

Economic effect of noise protection measures, P, thousand rubles/year	Spending on noise protection measures made up for one year, PZ, thousand rubles/year	Economic effect for the year, E, thousand rubles/year
909	264	645

Discussion and Conclusion. To minimize harmful vibrocoustic effects, the authors propose a measure to improve one of the methods used — the installation of vibration damping plates. For their production, secondary raw materials can be used in the form of rubber crumbs in an amount of more than 60% of the volume of the material. Such an improvement option has an advantage in places where scheduled repairs of the plates are planned, as well as where the plates have not yet been installed.

By upgrading, it is possible to achieve a noise reduction of 5–8 dB, cheaper material and easier installation of plates. The annual economic effect of the introduction of this method of improving working conditions during the operation of railway transport is about 645 thousand rubles.

References

1. Sokolov D. A. Characteristics of noise pollution and vibration of railway transport. Minimizing the impact of noise and vibration on railway transport workers. Student i nauka. 2022;1(20):65–67. (In Russ.).

2. Chebotarev A. G., Paltsev Yu. P. Vibroacoustic factors of the working environment in underground and surface mining of solid minerals. Russian Mining Industry. 2012;5(105):50–54. (In Russ.).

3. Ponomarev V. M., Vasileva D. N. Issledovaniya urovnei zvuka v kabinakh lokomotivov v usloviyakh ekspluatatsii. Nauka i tekhnika transporta. 2016;2:29–34. (In Russ.).

4. Gotlib Ya. G., Alimov N. P., Azarov V. N. Issues of noise reduction to evaluate labor conditions. Alternative energy and ecology. 2013;13(135):70–83. (In Russ.).

5. Yarusov N. I., Okulova V. V. Shum kak vrednyi proizvodstvennyi factor. Bezopasnost' v professional'noi deyatel'nosti. 2021:294–298. (In Russ.).

6. Manokhin V. Ya., Drozdova L. F., Golovina E. I., Sokolov D. A. Analysis and assessment of safety during operation of the shot blasting machine in the foundry. Safety of Technogenic and Natural Systems. 2022;2:36–42. https://doi.org/10.23947/2541-9129-2022-2-36-42 (In Russ.).

7. Salnikova L. A., Sokolov D. A., Golovina E. I. Analiz vliyaniya shuma i zapylennosti na zhelezobetonnom proizvodstve. Gradostroitel'stvo. Infrastruktura. Kommunikatsii. 2022;1(26):48–50. (In Russ.).

8. Kanev N. G. Prognoz vibratsii rel'sovogo transporta pri proektirovanii vibroizolyatsii fundamentov zdanii. Fundamenty. 2020;2:51–52. (In Russ.).

9. Petrova E. E. Analiz effektivnosti prirodookhrannykh zatrat v investitsionnom analize. Science Vector of Togliatti State University. 2010;4(14):252–255. (In Russ.).

10. Suetina T. A., Safina D. M. Methodology for assessing the economic efficiency of investments in the implementation of lean manufacturing measures. Rossiyskoe predprinimatelstvo. 2018;19(10) 3085–3094. (In Russ.).

11. Ushakova E. O. Metodika opredeleniya ekonomicheskoi effektivnosti zatrat na prirodookhrannye meropriyatiya. Geo-Sibir. 2006;6:185–190 (In Russ.).

Received 09.12.2022.

Revised 26.12.2022.

Accepted 26.12.2022.

About the Authors:

Golovina, Elena I., associate dean for academic affairs, Engineering Systems and Structures Faculty, associate professor of the Technosphere and Fire Safety Department, Voronezh State Technical University (84, 20 letiya Oktyabrya st., Voronezh, 394006, RF), ORCID, u00111@vgasu.vrn.ru

Sokolov, Dmitriy A., student of the Technosphere and Fire Safety Department, Voronezh State Technical University (84, 20 letiya Oktyabrya st., Voronezh, 394006, RF), ORCID, dmitriysokolov598@gmail.com

Claimed contributorship

E. I. Golovina: academic advising, formulation of the basic concept, goals and objectives of the study. D. A. Sokolov: conducting the experiment, analyzing the research results, preparing and formatting the text of the article, formulation of the conclusions.

Conflict of interest statement

The authors do not have any conflict of interest.

All authors have read and approved the final manuscript.

TECHNOSPHERE SAFETY

Original article
UDC 614. 841
https://doi.org/10.23947/2541-9129-2023-1-47-55

Application of Geo-Positioning and Monitoring Technologies for Blocking and Extinguishing Fires in Steppe and Grain Areas

Oleg V. Denisov✉, **Kristina V. Khokhlova**, **Maksim V. Gribashov**

Don State Technical University, 1, Gagarin Sq., Rostov-on-Don, Russian Federation

✉ ovd63@mail.ru

Abstract

Introduction. The relevance of this study is determined by the increasing need to ensure reliable protection of steppe and agricultural territories from possible fires with the help of innovative monitoring methods, the use of fire equipment, fire water supply systems and modern fire extinguishing means. Despite the introduction of new, modern and safe for the environment and people technical solutions aimed at preventing and extinguishing fires, there is still a need to improve the technologies used in the field of fire safety, which is a serious problem for the country. The work objective is to assess the technical feasibility of effective application of geo-positioning technologies and monitoring based on a set of special devices, model calculation of conditions for reliable fire blocking on steppe and agricultural territories, in particular, in fields with grain areas.

Materials and Methods. The main research methods are the analysis of sources of normative-methodological and scientific-technical information, mathematical modeling, extrapolation to computational and graphic materials, physical experiment.

Results. The data are presented for the development and implementation in the practical activities of fire departments of new technical solutions and technologies for monitoring and extinguishing steppe fires and fires in grain areas, the creation and development of material, technical, methodological and information base for the system of blocking geoecological fires.

Discussion and Conclusion. The analysis of the causes of fires in steppe and agricultural territories allowed us to outline the main methods of their monitoring. Based on the study of prototypes, changes in the technical and layout characteristics of the main elements, a rational solution (know-how) for extinguishing fires in steppe and grain areas is proposed — a tractor-soil-thrower-fire-break maker. At the same time, it is concluded that it is also possible to increase the efficiency of multifunctional tracked or wheeled robotic complexes due to elements of navigation systems (geo-positioning) and monitoring using automatic process control systems.

Keywords: steppe fires, grain areas fires, geo-positioning technologies, fire monitoring.

Acknowledgements. The authors express their gratitude to the deputy head of the Second Fire and Rescue Unit of the Federal Fire-Fighting Service of the State Fire-Fighting Service of the Main Directorate of Russia for the Rostov region, Lieutenant Colonel S. N. Kovalenko and Director of Syntex LLC A. A. Tokarev for the critical comments to the article made earlier. The authors also express their gratitude to its anonymous reviewers.

For citation. O. V. Denisov, K. V. Khokhlova, M. V. Gribashov. Application of Geo-Positioning and Monitoring Technologies for Blocking and Extinguishing Fires in Steppe and Grain Areas. Safety of Technogenic and Natural Systems, 2023, no. 1, pp. 47–55. https://doi.org/10.23947/2541-9129-2023-1-47-55

Introduction. The analysis of scientific and technical literature revealed a lack of available data on the technical features of extinguishment of steppe fires. Most of these fires (up to 80 % according to various sources) are anthropogenic in nature (violations of fire safety rules when handling open fire and when operating faulty, outdated or not properly maintained equipment). Natural factors of such fires are also known (fires often occur because of a lightning strike during a thunderstorm).

A steppe fire is a naturally or artificially caused fire in steppes. It is produced to displace unwanted plants and destroy dead vegetation in order to improve the herbage. According to the mechanism of fire propagation, a steppe fire is similar to a forest ground fire, but its spread rate is higher, which is due to a number of factors, namely the greater combustibility of dry steppe grasses and a high speed of surface wind in the steppe. Such fires cause significant damage to the natural environment (vegetation and wildlife); can pose danger to people and economic objects[1,2] [1, 2].

The causes of fires in steppe and grain areas can also be accidents of ground and air transport, grain harvesting equipment, terrorist acts, military actions and careless handling of open fire. The most fire-hazardous situation develops in late spring and early summer, when the weather is dry and hot. Such fires are characterized by the emergence of one or more islands of fire, which quickly spread to large areas. They have a high speed, reaching 30 km/h at certain moments. This factor is due to the large amount of dry vegetation, ripe cereals and other flammable materials. Steppe fires and grain areas fires pose a huge danger not only to people, but also to farm animals. The fire, which is coming from all sides, exerts strong psychological pressure, thereby can provoke mass panic, which often leads to numerous victims.

The analysis of the use of technical means in extinguishing natural and man-made fires that have occurred in Russia over the past three years has shown that construction and agricultural machinery is actively used for preventive work and extinguishing fires, eliminating their consequences[3] [3, 4].

The relevance of the study is also due to the increasing need for the use of advanced equipment and modern devices that ensure fire safety in the steppes and grain areas, when fighting natural fires is complicated by the presence of warehouses with chemicals, for example fertilizers, on the ground [3, 5].

Materials and Methods. Dump trucks and bulldozers are most often used to clear debris, create mineralized strips during steppe and wildfires. The effectiveness of the use of construction and agricultural machinery as special

[1]Technical Regulations on Fire Safety Requirements. Federal Law No. 123-FZ of 22.07.2008. Electronic Fund of Legal and regulatory and technical documents. Available from: https://docs.cntd.ru/document/902111644?section=status (accessed 31.05.2022). (In Russ.).

[2]On Fire Safety. Federal Law No. 69-FZ of 21.12.1994. Collection of Legislative Acts of the Russian Federation. 2014. No. 5. Article 1. (In Russ.).

[3]Denisov O. V., Khokhlova K. V., Popko G. A. K razrabotke meropriyatii po preduprezhdeniyu i tusheniyu lokal'nykh pozharov na poligonakh tverdykh bytovykh otkhodov. Aktual'nye problemy nauki i tekhniki: mat. Vserossiiskoi nauch.-prakt. konf. Rostov-on-Don, 2021. P. 136-137. (In Russ.).

equipment, as well as aerospace exploration and monitoring technologies to ensure fire safety has been proven in practice.

It is possible to increase the efficiency of a multifunctional tracked or wheeled robotic complex due to the elements of navigation systems, the actual technical positioning devices. An example is the Global Russian Navigation Satellite System (GLONASS). This system can broadcast civilian signals anywhere in the country and the world free of charge and without restrictions, with automatic control of monitoring processes. Since the beginning of the 2000s (since the adoption of the federal target program "Global Navigation System"), GLONASS is actively used in preventing and extinguishing geoecological fires.

According to expert estimates, the use of systems and technologies for geo-positioning and monitoring of protected areas will reduce efforts and costs for predicting fire-hazardous situations by 15 %, costs by 20%, as well as reduce the number of personnel required, fire equipment, water or extinguishing agents used. All this together will increase the efficiency of work and provide an opportunity to extinguish fires at night.

Geo-positioning and monitoring technologies will help to increase efficiency due to the task map for differentiated mineralization, plowing and irrigation of steppe territories, presented in Figures 1, 2. Externally, the equipment performing these works does not differ from the usual one.

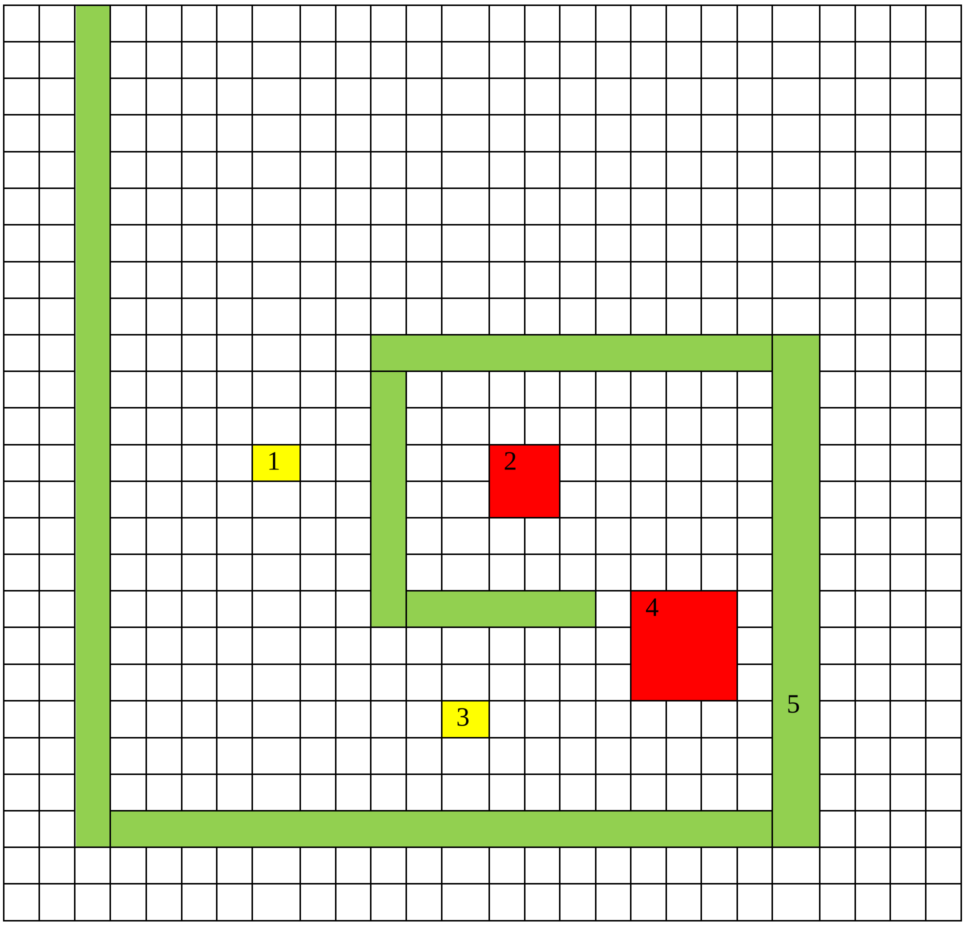

Fig. 1. Simplified map-scheme of the task of monitoring and geoecological zoning of steppe territories and grain areas:1 and 3 — zones with dangerous critical parameters of the environment;
2 and 4 — suspected combustion zones; 5 — the route of the equipment in accordance with the task map

Fig. 2. Work of the equipment for plowing of a given territory [3]

The concept of precise operation of special fire equipment, which is a technology of geo-positioning and monitoring, is based on detailed knowledge of protected areas. It means that in such territories there are areas that are heterogeneous in terms of fire protection, soil and air humidity, ambient temperature, wind direction and speed. These parameters need to be constantly monitored, that is, to carry out their system monitoring. A variant of such a technical complex is shown in Figure 3.

The main task of fire services is to maximize the use of the potential of each local steppe area, optimize the fire equipment and personnel used and, as a result, increase the efficiency of fire extinguishing.

Fig. 3. Weather monitoring system [3]

Accurate cartography for the prevention and extinguishing of fires in steppe and grain areas is necessary in order to calculate, according to the local moistening of the soil layer, how much water or extinguishing agents (EA) will be needed to extinguish fires. Thus, it is possible to estimate the costs of moistening or extinguishing [6, 7]. When using this method, the data on differentiated moistening or extinguishing of areas can also be quickly mapped.

Such cartography is the basis for decision-making, for example, when choosing the type and quantity of necessary firefighting equipment for a given steppe area or grain field. Cartography of steppe and grain areas allows you to:

– save money by local moistening or precise extinguishing of only those areas where it is necessary;

– save time, fuel and lubricants. It is believed that it is possible to scan up to 20 hectares per hour;

– accurately identify fire-hazardous or burning areas;

– use map archives for many years, accumulating experience. Fire-hazardous areas practically do not change over time.

To extinguish steppe fires, fire equipment on tracked or wheeled vehicles is used. It has a wide spectrum of action, has several types. Each type of special tracked firefighting equipment is capable of solving a large number of complex tasks. For this purpose, various types of extinguishing agents are used. Basically, this is water and foam, but in the upgraded machine proposed by the authors, fire extinguishing powders and gases will be additionally used. To supply each of these substances to the fire source, special fire equipment is needed.

Firefighting equipment is designed to extinguish fires of varying complexity with hydraulic guns and hand fire nozzles, as well as to collect and store water and a foaming agent solution, supply water with a certain flow rate, irrigate the cabin during fire extinguishing.

After analyzing several prototypes, as well as changes in the technical and layout characteristics of the main elements of the equipment, a rational solution (know-how) for extinguishing fires in steppe and grain areas is proposed — a tractor-soil-thrower-fire-break maker. The complex of technical solutions includes modifying of the soil-thrower itself, which allows you to partially separate the dry combustible vegetable fraction from the mineral one. In addition, it was found that it is also possible to increase the efficiency of a multifunctional tracked or wheeled robotic complex due to the elements of navigation systems (geo-positioning) and monitoring based on automatic process control systems. It is also assumed, that an improved wheeled or tracked tractor-soil-thrower-fire-break maker equipped with a geonavigation system can also be used to prevent landscape fires, to actively extinguish the edge of steppe or forest ground fires with the help of a mineralized layer of soil and with a minimum volume of dry combustible plant fraction.

Figure 4 shows the main elements of the device. Tractor (1) with enclosing contour (2) consists of frame, suspension mechanism (3), wave-spherical discs forming a crushed soil shaft in front of the milling cutters installed at the level of the bottom of the furrow, support wheels regulating the level of the bottom of the furrow, drive (4) of soil-thrower-fire-break maker (5), bucket-pusher (6) for cutting tree roots and protecting the milling cutters from large obstacles, supporting all-metal wheels to limit the depth of the milling cutters.

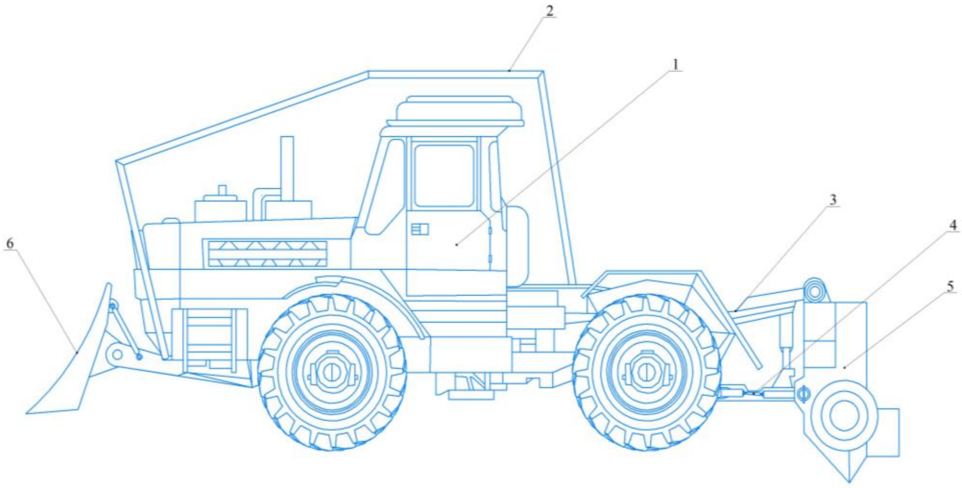

Fig. 4. Wheeled tractor with attachments — soil-thrower-fire-break maker

Protective casing (know-how) consists of two main parts — the protective casing itself and the soil pipeline, made with the possibility of changing its position and separating the combustible plant fraction. In this case, the protective casing is a part of the cylinder surface around the milling cutters. The lower half of the surface of the protective casing is missing, providing the possibility of taking the necessary volume of crushed soil, and the upper part passes into an elliptical or cylindrical surface of the mineral-soil pipeline having a branch for the dry plant fraction. The position and other geometric characteristics of the mineral-soil pipeline can be changed (including automatically) by means of a mechanism for adjusting the angle of its installation by means of a control unit, hydraulic pumps and a number of hydraulic cylinders from the cab of a mobile transport and energy vehicle (tractor, car).

The problem of ensuring fire safety in steppe areas will always be relevant. To improve the process of organizing the extinguishing of fires in steppe and grain areas, it is necessary to carry out many measures, not limited only to the use of heavy special, construction, agricultural machinery for the elimination of fires and their consequences.

The authors have also considered other situations requiring the use of special equipment, in which various machines were studied that performed well in extinguishing natural and man-made fires. As a result, it was determined that such a technique can be widely used both in extinguishing fires in steppe and grain areas, and in fires in fertilizer warehouses.

To calculate the effectiveness of the use of special, construction, agricultural machinery in fires of steppe and grain areas, its tactical and technical characteristics are highlighted and its capabilities are determined.

Results. The most important conditions for ensuring fire safety of steppe and grain areas, along with social ones, are technical and environmental conditions.

Analytical and modeling research methods are used to assess the effectiveness of the use of advanced special, construction, and agricultural machinery in geoecological fires under consideration[4] [6, 7].

Using the example of an average fire in the grain area, we apply a model calculation of the conditions for reliable blocking of steppe fires.

[4]Uspensky I. A. Analiz instrumentov razrabotki tsifrovykh dvoinikov kak sredstv optimizatsii operatsii agropromyshlennogo kompleksa. Perspektivnye tekhnologii v sovremennom APK Rossii: traditsii i inovatsii: mat. 72-i mezhdunar. nauch.-prakt. konf. Ryazan, 2021. P. 437-440. (In Russ.).

Let us assume a conditional situation in which the combustion is located near the object of protection. Let us assume that there are about 200 fire-hazardous points in the grain area. The distance from combustion to the place of blocking is 20 meters. The speed of movement of the combustion source carrier is in the range from 3 to 30 m/min. Since the distribution density of the experimentally obtained data was no more than 5 %, it was decided to represent this array by an approximating function. The graphical interpretation is shown in Figures 5 and 6.

Using the principles of "protection by distance and time", we use dimensionless speed and time, risks for personnel engaged in measures to prevent and extinguish steppe fires and fires in grain areas.

The graphs show that with an increase in the speed of movement of the fire front in the grain areas, due to natural factors, and the time of rapid detection and response, the probability of penetration of fire front into critically dangerous points of the object of protection arises.

In this model, such accompanying factors as technical readiness and the condition of special extinguishing agents, the nature of the fire, its changing parameters were not considered. They can influence the probability of successful blocking of the combustion source as well.

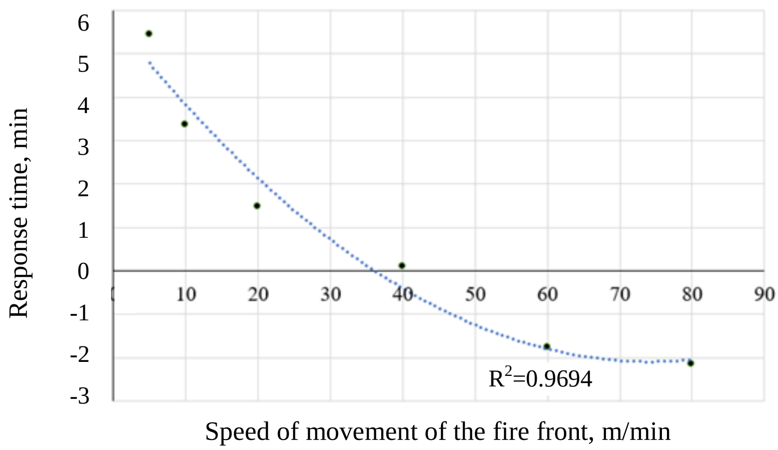

Fig. 5. Graphical dependence of the obtained results on the "protection by distance" principle

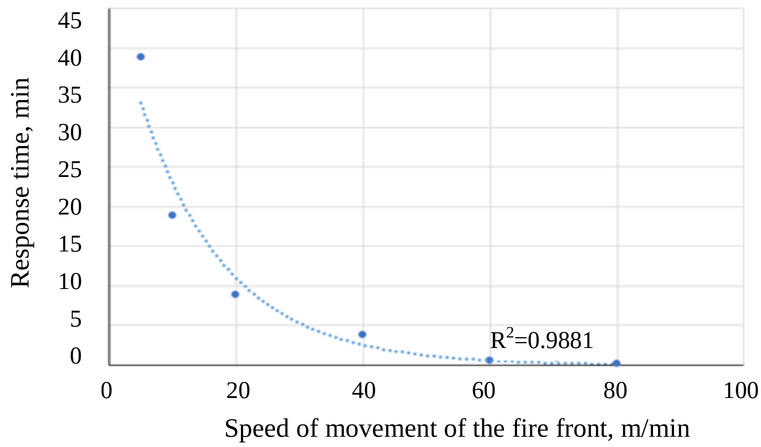

Fig. 6. Graphical dependence of the obtained results on the "protection by time" principle

Due to the developed conditions for reliable blocking of steppe and grain areas fires, developed by one of the authors earlier [3], it is possible to determine the controlled parameters of the fire safety model based on geo-positioning technologies and monitoring of natural parameters.

Discussion and Conclusion. The results of the conducted research show that the problem of fires in steppe and grain areas is very relevant. This is due to the high level of fire and environmental risks of heterogeneous origin [6]. All this allowed us to draw the following conclusions:

– as a result of studying the statistics of fires in steppe and grain areas in the Russian Federation, it was found that over the past 20 years there has been an increase in them;

– based on analytical and modeling research methods, it has been proved that there are effective solutions for reliable blocking of geoecological fires, taking into account the response time, the speed of propagation of the fire front and other factors;

– the design and layout of the main elements of the tractor-soil-thrower-fire-break maker (know-how) are briefly described, which allow you, through constructive analysis, to technically implement reliable blocking of fires in steppe and grain areas;

– it is established that it is possible to increase the effectiveness of fire prevention and extinguishing on the basis of navigation systems and automatic control of monitoring processes in conjunction with mobile transport and energy vehicle (tractor, car) equipped with a ground throwing device.

This area of scientific research is promising and has a high innovative and practical value for improving the fire safety system.

References

1. Shishov S. G. Kharakteristika landshaftnykh pozharov i ikh vliyanie na pozharobezopasnost' ob"ektov khraneniya boepripasov. Molodezh'. Obrazovanie. Nauka. 2019;1(14):178–204. (In Russ.).

2. Andreev S. S., Popova E. S. Ecologic-geographical estimation of climatic comfortness of Rostov-on-Don. European Journal of Natural History. 2013;5:32–34.

3. Denisov O., Andreeva E. An innovative approach to the elimination of combustion foci at MSW landfills (on the example Rostov region). E3S Web of Conferences: Environmental Education and Training of Ecologists. 2021;273(78):04006. 10.1051/e3sconf/202127304006

4. Bulygin Yu., Andreeva E., Shoniya D. The role of hazardous factors of chemical and physical nature in welders` occupational risks management. E3S Web of Conferences: Environmental Education and Training of Ecologists. 2021;273:12028. 10.1051/e3sconf/202127312028

5. Andreeva E. S., Klimov P. V., Shtenske K. S. Atmospheric air pollution as one of the factors of noncarcinogenic risk to the health of the human population in Rostov-on-Don. Geography and Natural Resources. 2021;42(1):32-36. https://doi.org/10.1134/S1875372821010030

6. Basilaia M., Bogdanova I., Dymnikova O. Cosmoharmonic principles of environmental safety. E3S Web of Conferences. Innovative Technologies in Environmental Science and Education. 2019;135:01079. 10.1051/e3sconf/201913501079

7. Pustovaya L. E., Chebysheva V. A. Analysis and assessment of the safety level of port facilities using the example of a sulfur storage warehouse. Safety of Technogenic and Natural Systems. 2021;2:43–49. (In Russ.).

Received 18.12.2022.

Revised 09.01.2023.

Accepted 09.01.2023.

About the Authors:

Denisov, Oleg V., associate professor of the Life Safety and Environmental Protection Department, Don State Technical University (1, Gagarin sq., Rostov-on-Don, 344003, RF), Cand. Sci. (Eng.), ORCID, ovd63@mail.ru

Khokhlova, Kristina V., student of the Life Safety and Environmental Protection Department, Don State Technical University (1, Gagarin sq., Rostov-on-Don, 344003, RF), ORCID, cristy2020@yandex.ru

Gribashov, Maksim V., Master's degree student of the Life Safety and Environmental Protection Department, Don State Technical University (1, Gagarin sq., Rostov-on-Don, 344003, RF), ORCID, gribashov10@gmail.com

Claimed contributorship

K. V. Khokhlova, M. V. Gribashov: formulation of the basic concept, goals and objectives of the study, calculations, preparation of the text, formulation of the conclusions; O. V. Denisov: academic advising, development of technical solutions, analysis of the research results, revision of the text, correction of the conclusions.

Conflict of interest statement

The authors do not have any conflict of interest.

All authors have read and approved the final manuscript.

MACHINE BUILDING

Original article

UDC 004.413.4:[625.1/.5+004.9]

https://doi.org/10.23947/2541-9129-2023-1-56-69

Integral Risk Assessment in Steel Ropes Diagnostics Using Computer Vision

Aleksey V. Panfilov, Nikolay N. Nikolaev ✉, Aleksandr R. Yusupov, Anatoliy A. Korotkiy

Don State Technical University (Rostov-on-Don, Russian Federation)

✉ nnneks@yandex.ru

Abstract

Introduction. Currently, the technical condition of ropes of cable-working machines is evaluated periodically according to regulatory documentation. At the same time, methods of visual and instrumental control are used, which depend on the skills and physical capabilities (vision) of the personnel performing the work. There is no unified system of continuous assessment of the technical condition based on a set of factors that does not depend on the human factor. As a result, emergencies occur even when all routine maintenance is carried out on time. To correct this situation, it is proposed to use a computer vision system and neural networks, which allows determining its suitability for further operation by risk levels based on the totality of detected and identified defects, with the interpretation of their results in the color scheme: green — acceptable, yellow — increased, red — high. The work objective is to propose an integral method for risk assessment of operating machines with rope traction when defects and their combinations are detected in a steel rope using computer vision while excluding the influence of the human factor.

Materials and Methods. Training of the neural network was carried out on the basis of statistical data of defects obtained from the results of technical inspections of machines with rope traction, on sections of the rope, multiples of its six and thirty nominal diameters according to GOST 33 718. Indexing of risks in the color scheme was carried out according to GOST 55 234.3 to develop a strategy for steel ropes maintenance. A certificate of registration of a computer program was obtained for the neural network program code. The neural network processes visual and measurement control data based on computer vision.

Results. An integrated risk assessment system has been created for the diagnosis of steel ropes using computer vision, which allows you to detect defects in steel ropes timely, assess the existing risk of further operation and give recommendations to specialists of operating organizations in real time. This will dramatically reduce the risk of accidents, injury and death of people at facilities using steel ropes.

Discussion and Conclusion. The proposed integrated risk assessment system can be applied in any facility that uses rope traction. These are elevators for various purposes, funiculars, cable cars, cranes and many other machines. It should be noted that the estimated commercial cost of the system is low; therefore, the system is available to a wide range of consumers.

Keywords: integrated system, risk assessment, steel rope, computer vision, neural network, recommendation system.

Acknowledgements. The authors would like to thank their colleagues from DSTU for their help in developing the system and to express gratitude to the Innovation Promotion Fund for financial support of the research.

For citation. A. V. Panfilov, N. N. Nikolaev, A. R. Yusupov, A. A. Korotkiy. Integral Risk Assessment in Steel Ropes Diagnostics Using Computer Vision. Safety of Technogenic and Natural Systems, 2023, no.1, pp. 56–69. https://doi.org/10.23947/2541-9129-2023-1-56-69

Introduction. Timely assessment of technical condition of facilities directly responsible for safety of various technological operations is the most important task. This will reduce or eliminate emergencies with injury, loss of life and damage to material objects [1, 2]. Such critically important technical facilities from the point of view of risk assessment include: elevators (passenger, hospital and cargo); cable cars (passenger and cargo); mine hoisting installations; oil and gas drilling rigs; lifting cranes; hoists; ship lifting devices; skip hoists; rope mechanisms of offshore platforms; mechanisms on offshore pipelayers and others.

To carry out continuous monitoring of the parameters of steel ropes technical condition, a recommendation system of integrated risk assessment of the continuation of steel ropes work in mechanisms with the use and interpretation of computer vision system data has been developed.

The urgency of the problem is confirmed by the available statistics of accidents at facilities using cable traction, which occur despite the existing system of periodic inspections and flaw detection of steel ropes [3–5].

The work objective is to propose an integral method of risk assessment of operating machines with cable traction when defects are detected in a steel rope and combined with the use of computer vision during routine maintenance.

Tasks to be solved to achieve this goal in the course of this study:

1. Describe the existing regulations on visual and measuring control of steel ropes on machines with cable traction.
2. Propose a method of visual and measuring control using computer vision in a steel rope.
3. Show that computer vision is an artificial intelligence technology.
4. Define the intelligent decision support system (IDSS) in relation to the proposed method of risk assessment of operating machines with rope traction when defects are detected and combined with the use of computer vision in a steel rope during routine maintenance.
5. Apply one of the known methods of risk analysis for an integral assessment of the technical condition of steel ropes.
6. Propose an algorithm and a computational procedure for an integral risk assessment of operating steel rope with defects at a fixed length equal to six and thirty nominal rope diameters.

The starting point for the creation of the product was the emerging problems with elevators (and other cable cars) and the possibility of using video information analytics, which is based on deep learning algorithms for pattern recognition. This will significantly increase the objectivity of the information received about the parameters of technical condition of the steel rope, balancing devices, fastenings of the ends of the seals and ensure the level of safety of the operation of machines on cable traction, while eliminating the human factor [6, 7].

Materials and Methods. Steel ropes are subjected to daily, periodic and special inspections in all types of lifting structures. Operating instructions is the document used by the personnel during repair and maintenance work. In its absence, it is necessary to use Safety Rules or GOST standards.

Elevator electricians, crane operators, machinists, mechanicians, electricians and other categories of service personnel carry out visual inspections of steel ropes periodically or immediately before starting work. Inspections are carried out in the following order:

1. Familiarization with the entries in the journal (journal of the elevator daily inspection; watch — for the lifting crane; changeable journal — for suspended cable cars, etc.).
2. Inspection of the sections of rope wound on the drum, as well as those passed through the rope-carrying pulley, block, resting on shoes, fixed in couplings, couches and clamps.

The operator (driver) of the lifting structure has a log in which the results of inspections are recorded.

The frequency of flaw detection of steel ropes for specific lifting structures and their frequency are shown in Table 1.

Table 1

Frequency of inspections and flaw detection of steel ropes[1]

No.	Name of the lifting device	Purpose of the steel rope	Frequency of flaw detection (month)	Note
1	Hoisting crane	cargo boom traction guy	12 12 12 36	* ** * **
2	Cable crane	track traction cargo guy support cable suspensions holding the crane (support)	subsequent every 24 12 12 36 not subject not subject not subject	the first one at commissioning
3	Lifts and winches for lifting people	cargo traction	6 12	
4	Removable lifting bodies		not subject	
5	Removable lifting devices		not subject	
6	Electric hoists	cargo	12	*
7	Elevators	traction tail	6 not subject	
8	Lifts (towers)		not subject	

No.	Name of the lifting device	Purpose of the steel rope	Frequency of flaw detection (month)	Note
9	Overhead passenger (cargo) cable cars	track, traction, carrier and traction tension	the second one is after 36, the next one every 12 not subject	the first one at commissioning
10	Inclined rail-rope lifts (funiculars)	traction tension (tail) safety	the second one is after 36, the next one every 12 not subject not subject	the first one at commissioning
Note: low rotation ropes, regardless of their purpose, are subject to flaw detection every 12 months; * during intensive operation in an aggressive environment and elevated temperature; ** for ropes operated without replacement on cranes with expired service life.				

Rules[1] require periodic (in some cases, daily) visual and dimensional examination (VDE) of steel ropes with the detection of external defects, information about which is entered in the inspection log.

Defects in steel ropes arise as a result of:

– external influences with mechanical equipment or the external environment in the elevator shaft, including the formation of an electric arc discharge;

– inadequate quality of the supplied steel rope as a component product;

– improper quality of steel ropes installation;

– malfunctions of mechanical parts of the elevator, the indicator of which is the rope.

It can be stated that their defects in steel ropes are an "indicator" of technical condition of all mechanical equipment of the lifting structure, namely: wear of the pulley groove; rope slipping on the pulley, including as a result of excessive lubrication; misalignment of the winch attachment; backlash in the elements of the transmission mechanisms of the drive, etc. [8-12]. Possible malfunctions of the mechanical parts of the elevator, depending on the defective indicators, are presented in Table 2.

The VDE method is proposed[2], which makes it possible to carry out an integral assessment of the technical condition of a steel rope, implemented in the form of a software and hardware complex, which is a computational recommendation system for decision-making for service personnel when they perform maintenance work on machines with cable traction. This allows you to get the necessary safety level, while eliminating the subjectivity of the human factor, namely, physiological limitations associated with vision.

The proposed method provides for the creation, development and implementation of artificial intelligence, namely, a set of technological solutions that allow simulating human cognitive functions (vision and self-learning), including the search for solutions to identify the discovered defects in steel ropes with the results of human intellectual activity.

[1] Ob organizatsii bezopasnogo ispol'zovaniya i soderzhaniya liftov, pod"emnykh platform dlya invalidov, passazhirskikh konveierov (dvizhushchikhsya peshekhodnykh dorozhek), eskalatorov, za isklyucheniem eskalatorov v metropolitenakh. Government of the Russian Federation. Electronic fund of legal and regulatory documents. Available from: https://docs.cntd.ru/document/436745439?section=text (accessed 23.01.2023). (In Russ.).

[2] Korotkiy A. A. et al. Sposob vizual'no-izmeritel'nogo kontrolya stal'nogo kanata. Patent 2775348, Russian Federation, D07B 1/00; B66B 7/1215; G05B 99/00. No. 2021107842, 2022. 16 p. (In Russ.).

Table 2

Possible malfunctions of the elevator mechanical equipment depending on defects types

No.	Rejection rate	"Indicator" of a possible malfunction
1	Breaks of external wires	– Wear of the pulley groove – Misalignment of the rope-carrying pulley during installation or maintenance – Contact with external elements when moving in the mine – Inadequate quality of the supplied steel rope
2	Surface wear of the rope	– Wear of the pulley groove – Misalignment of the rope-carrying pulley during installation or maintenance
3	Surface corrosion	Impact of corrosion factors (oxygen, electrochemical, chemical)
4	Local reduction of rope diameter	– Inadequate quality of the supplied steel rope – Core damage – Damage to internal strands
5	Local increase of rope diameter	– Inadequate quality of the supplied steel rope – Swelling of the fiber core from excess moisture
6	Waviness	– Inadequate quality of the supplied steel rope – Defects in the installation or improper maintenance of balancing devices, places of sealing their ends
7	Temperature impact (electric arc discharge or lightning strike)	Exposure to electric current during installation, improper maintenance and during operation
8	Twist	– Overload – Incorrect reeving – Incorrect laying of the new rope on the drum
9	Elongation (residual)	– Inadequate quality of the supplied steel rope – Overload – Core damage – Damage to internal strands
10	Defects of balancing devices, places of sealing of their ends	Defects in installation and improper maintenance

Artificial intelligence technologies, in accordance with "National Strategy ..."[3] (subparagraph "a" of paragraph 5), include technologies based on the use of computer vision and intellectual decision support.

Artificial intelligence should be understood as a set of technological solutions that allows you to simulate human cognitive functions (including self-learning and finding solutions without a predetermined algorithm) and perform specific tasks with results comparable to or superior to the results of human intellectual activity.

The claimed method includes a set of technological solutions consisting of computer vision, information and communication infrastructure, software (including the implementation of machine learning methods), processes and services for data processing and solution search.

For an integral assessment of the steel rope technical condition, an intelligent decision support system (IDSS) using artificial intelligence (AI) methods was used (Fig. 1, 2).

[3] O razvitii iskusstvennogo intellekta v Rossiiskoi Federatsii (vmeste s «Natsional'noi strategiei razvitiya iskusstvennogo intellekta na period do 2030 goda»). President of the Russian Federation. Electronic fund of legal and regulatory documents. Available from: https://docs.cntd.ru/document/563441794/titles/64U0IK (accessed 23.01.2023). (In Russ.).

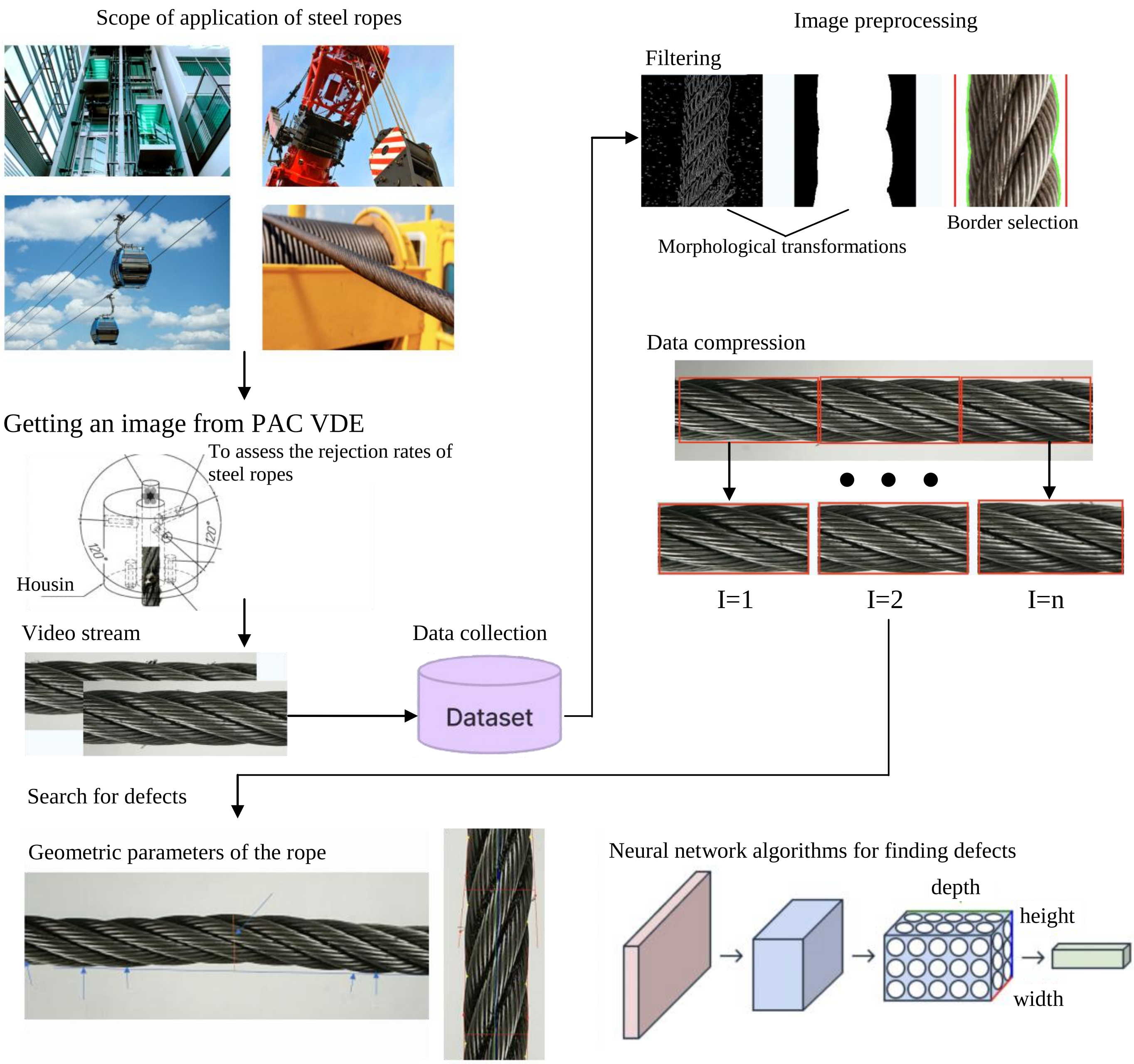

Fig. 1. Functional diagram of the method of visual and dimensional examination of a steel rope (Authors' figure)

An intelligent decision support system replaces a human consultant. It provides support to decision makers by collecting and analyzing factual data on detected defects, provides suggestions of possible options for action and their assessment. The purpose of artificial intelligence methods embedded in an intelligent decision support system is to allow a computer to perform these tasks, mimicking human capabilities as much as possible.

The proposed IDSS implementation is based on expert systems that encode knowledge and simulate cognitive behavior of human experts using predicate logic rules.

An expert system is a computer system that simulates the ability of a human expert to make decisions. Expert systems are designed to solve complex problems by reasoning with the help of a body of knowledge, presented mainly in the form of "if-then" rules, and not with the help of ordinary procedural code. The expert system is divided into two subsystems — the output mechanism and the inference mechanisms. The knowledge base represents facts and rules.

The inference mechanisms apply rules to known facts to infer new facts. Inference mechanisms may also include explanation and debugging capabilities.

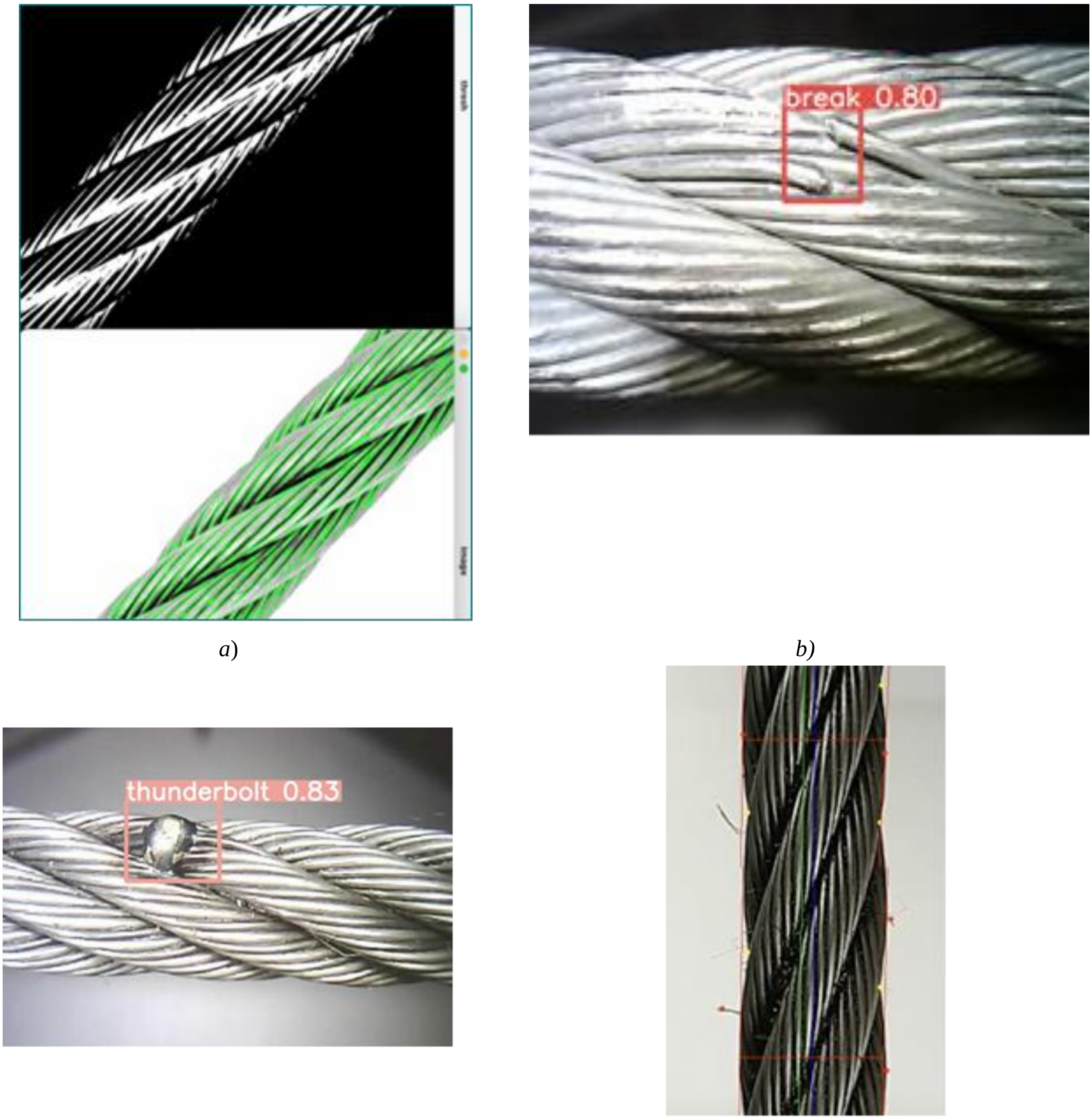

a) *b)* *c*) *d*)

Fig. 2. Detection of defects by means of computer vision:
a — determination of external wires wear; *b* — wire breakage;
c — temperature effect; *d* — local decrease/increase in diameter
(Authors' figure)

The created method makes it possible to automate processes when assessing the safety of using steel rope on cable traction machines. This makes it possible to provide users (staff) with a visual recommendation system for decision-making in the form of a web application that is not influenced by the human factor. This ensures increased security and reduced costs. This method automates and combines two control methods: visual and instrumental [14-16].

An expert system for risk assessment can be implemented based on well-known methods, such as[4]: Delphi method; failure mode and effects analysis (FMEA); failure mode effects and criticality analysis (FMECA); reliability-centered maintenance (RCM); risk indices; scenario analysis; structured method "What if?" (SWIFT); fuzzy logic methods, etc.

Regardless of the methodology used, risk assessment is carried out using a risk assessment matrix or a similar tool (for example, see GOST R 58 771[4] or GOST R 55 234.3[5], or GOST 12.0.230.5[6]).

The axes of the matrix can be both the probability and consequences of risk, as well as any other technical parameters of mechanical equipment that characterize their importance or criticality.

According to the results of such an assessment, risk is usually assigned one of three levels — high (red), medium (yellow) or low (green).

It is possible to increase the number of levels. The names of the colors are given as part of the most common scheme.

Standardization recommendations[7] also provide for the use of a color scheme in risk assessment.

To assess risk levels and develop maintenance and culling strategies based on a recommendation decision-making system, we apply the RIMAP approach — procedures for monitoring technical condition and maintenance based on a risk-oriented approach (recommended by GOST 55 234.3[5]). The approach allows us to successfully combine all known methods of risk assessment and decision-making.

The application of the RIMAP approach solves the following tasks:

- identification of hazards;
- determination of the mechanisms of defects and failures;
- determination of the probability of failure;
- determination of the consequences of failure;
- risk level assessments.

The main danger for rope systems is the risk of rope breakage, as well as the destruction of the sealing points of the rope ends.

Table 3 shows the rejection rates of steel ropes and the mechanisms of damage development.

Next, you need to determine the probability of failure. This requires initial data on various defects listed in Tables 2 and 3.

[4] GOST R 58771-2019. Risk management. Risk assessment technologies. NPO RusRisk, Technical Committee for Standardization "Risk Management", Federal Agency for Technical Regulation and Metrology. Available from: https://docs.cntd.ru/document/1200170253 (accessed 23.01.2023). (In Russ.).

[5] GOST R 55234.3-2013. Practical aspects of management of risk. Risk-Based Inspection and Maintenance Procedures. ANCO "NITS KD", Technical Committee for Standardization TC 010 "Risk Management", Federal Agency for Technical Regulation and Metrology. Electronic fund of legal and regulatory documents. Available from: https://docs.cntd.ru/document/1200108150 (accessed 23.01.2023). (In Russ.).

[6] GOST 12.0.230.5-2018. Occupational safety standards system. Health management systems. Risk assessment methods to ensure the safety of work. Federal Agency for Technical Regulation and Metrology, Interstate Council for Standardization, Metrology and Certification. Electronic fund of legal and regulatory documents. Available from: https://docs.cntd.ru/document/120016046 (accessed 23.01.2023). (In Russ.).

[7] R 50.1.090-2014. Risk management. Key risk indicators. NP RusRisk, Technical Committee for Standardization TC 010 "Risk Management", Federal Agency for Technical Regulation and Metrology. Electronic fund of legal and regulatory documents. Available from: https://docs.cntd.ru/document/1200120834 (accessed 23.01.2023). (In Russ.).

Table 3

Rejection indicators of steel ropes and mechanisms of damage development

Designation	Name of the defect type	Rejection standards according to regulatory and technical documents	Mechanisms of damage development
A (at length 6d) B (at length 30d)	Breaks of outer wires	According to the operating manual of the rope (depending on the type and brand)	Fatigue wear, mechanical wear, corrosion (oxygen, electrochemical, chemical)
C	Surface wear of the rope	Reduction of the diameter of the outer wires by 40% or more	Mechanical wear
D	Surface corrosion	Rope diameter reduction by 7% or more	Corrosion (oxygen, electrochemical, chemical)
E	Local reduction of rope diameter	Reduction by 3-6% of the rope diameter from the nominal one	Core damage, damage to internal strands
F	Local increase in rope diameter	Increase by 3-6% of the rope diameter from the nominal one	Swelling of fiber core from excess moisture
G	Waviness	When the directions of spiral waviness coincide with the direction of the rope lay and the waviness step and the rope lay step are equal at db = 1.08 dk (where db and dk, respectively, are the diameter of the waviness and the diameter of the rope). In other cases, at db≥1.33dk	Bending of sheave grooves of small radii
H	Temperature effect	If soot, scorching, or a characteristic color change is detected on the surface of the rope	Static electric discharge, lightning strike, heating
I	Twist	1) When reeving 1:1 — 0.5 turns per 10 meters 2) When reeving 2:1 — 0.5 turns per 20 meters 3) For ropes with an organic core — 1 turn per 10 meters	Overload, incorrect reeving, incorrect laying of a new rope on the drum
J	Elongation (residual)	With a residual elongation of more than 0.5% of the working length after wear-in	Overload, core damage, damage to internal strands
K	Defects of balancing devices, rope sealing sites	Deviation of position and shape from the original arrangement of elements	Overload, wear of parts and elements

To obtain a reliable sample of data based on the available rope defect results, the Monte Carlo method was used, with the help of which a sample of 1000 rope sections was generated, multiples of its 6 nominal diameters, allowing considering all combinations and variations of defects. The estimation of the total probability of failure for the sample was carried out in accordance with the algorithm shown in Figure 3. The resulting sample was used to train a neural network in order to implement the risk indexing method of the RIMAP approach.

Since the output data is discrete, the neural network must solve the classification problem. A multilayer perceptron is selected as the type of neural network.

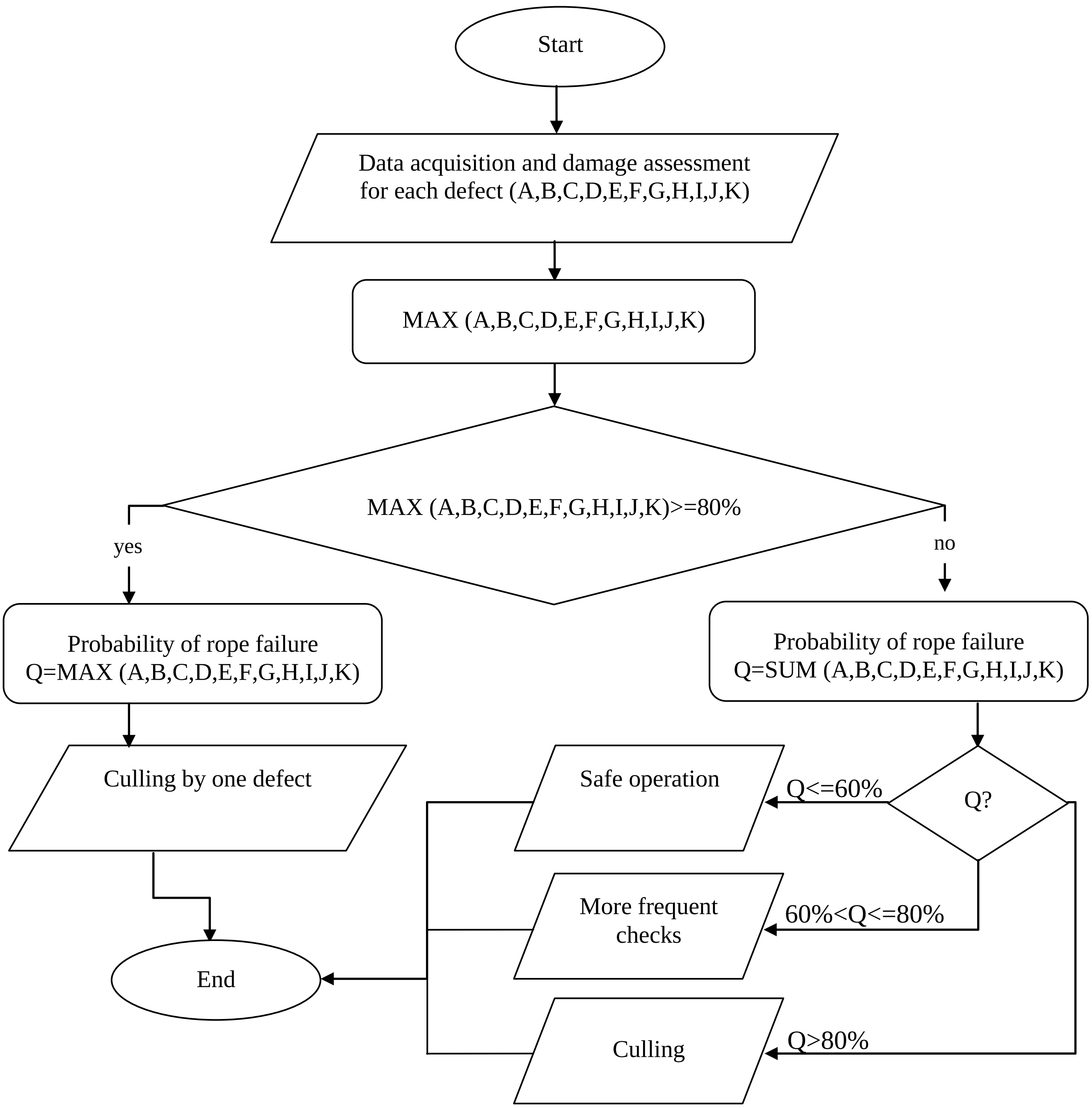

Fig. 3. Algorithm for estimating the total damage to the rope section (Authors' figure)

During the training, 20 neural networks were obtained, from which the top five were automatically selected (Fig. 4).

Among the neural networks obtained, the MLP 11-9-3 network can be distinguished, which has the best performance on the test sample of 96 %, and on the training and control samples — 98 %.

Summary of active networks (Spreadsheet in Risk_Estimation)								
Index	Net. name	Training perf.	Test perf.	Validation perf.	Training algorithm	Error function	Hidden activation	Output activation
1	MLP 11-4-3	95,85714	95,33333	98,00000	BFGS 36	SOS	Tanh	Identity
2	MLP 11-14-3	96,28571	94,66667	96,00000	BFGS 50	SOS	Logistic	Tanh
3	MLP 11-7-3	96,42857	95,33333	98,00000	BFGS 16	SOS	Exponential	Logistic
4	MLP 11-14-3	97,57143	94,66667	97,33333	BFGS 92	SOS	Logistic	Identity
5	MLP 11-9-3	98,14286	96,00000	98,00000	BFGS 155	SOS	Logistic	Tanh

Fig. 4. The best neural networks out of 20 trained ones (Authors' figure)

These are the best indicators, therefore, for further work in the intelligent decision support system, we will use the specified neural network. This neural network has 11 neurons in the input layer (according to the number of defects at the input), 9 neurons in the hidden layer, as well as 3 neurons in the output layer (according to the number of possible risk assessments of further operation of the steel rope). A logistic function is used as the activation function of the neurons of the hidden layer, and a tangential function is used for the output layer.

Analysis of the sensitivity of the MLP 11-9-3 neural network to changes in influencing wear indicators showed that changes in the indicators J (elongation), I (torsion), E (local decrease in rope diameter) and G (waviness) have the greatest impact (Fig. 5).

	Sensitivity analysis (Spreadsheet in Risk_Estimation) Samples: Train										
Networks	J	I	E	G	A	F	K	H	C	D	B
1.MLP 11-4-3	4,09029	3,78539	3,538596	2,999158	2,547528	2,325594	1,647709	1,675373	1,173743	1,138040	1,004637
2.MLP 11-14-3	3,10473	2,80809	2,788032	2,397576	1,973580	1,837489	1,595495	1,540505	1,102962	1,130396	1,012868
3.MLP 11-7-3	3,28691	2,97724	2,869449	2,475196	2,139719	2,020911	1,700607	1,700192	1,151866	1,085886	1,003372
4.MLP 11-14-3	7,30974	6,61641	6,316661	5,374687	4,347702	3,728140	2,721447	2,575235	1,506436	1,705318	1,137510
5.MLP 11-9-3	11,24972	10,23045	9,817238	8,400586	7,023844	5,798566	5,965579	5,509112	2,803276	2,617175	1,092058
Average	5,80828	5,28351	5,065995	4,329440	3,606475	3,142140	2,726167	2,600083	1,547656	1,535363	1,050089

Fig. 5. Sensitivity analysis of the MLP 11-9-3 neural network (Authors' figure)

A certificate of registration of a computer program was obtained for the neural network program code[8].

Results. An integrated risk assessment system has been created for the diagnosis of steel ropes using computer vision, which allows detecting defects in steel ropes in a timely manner, assessing the existing risk of further operation and giving recommendations to specialists of operating organizations in real time. This will dramatically reduce the risk of accidents, injury and death of people at facilities using steel ropes.

This system is the core of the product — a software and hardware complex (PAC) (Fig. 6) automating the processes of assessing the safety of using steel ropes, defects in balancing devices and places of sealing their ends on machines using cable traction, which is a visual recommendation system for decision-making for specialists. At the same time, the human factor is eliminated, which ensures increased safety and reduced costs.

The main functional purpose of PAC is the automatic detection of defects in steel ropes, balancing devices and fasteners of the ends of rope seals by special optical means (photo and video fixation), followed by processing of the received digital information by photo and video analytics based on machine learning, including an integral assessment of suitability for further operation by risk analysis methods, which is translated into the risk assessment color scheme on users' mobile devices.

[8] Korotkiy A. A. et al. Integral'naya otsenka tekhnicheskogo sostoyaniya stal'nogo kanata : progr. dlya EVM. Cert. No. 2022683712. Inzhenerno-konsul'tatsionnyi tsentr «Mysl'». No. 2022683761, 2022. (In Russ.).

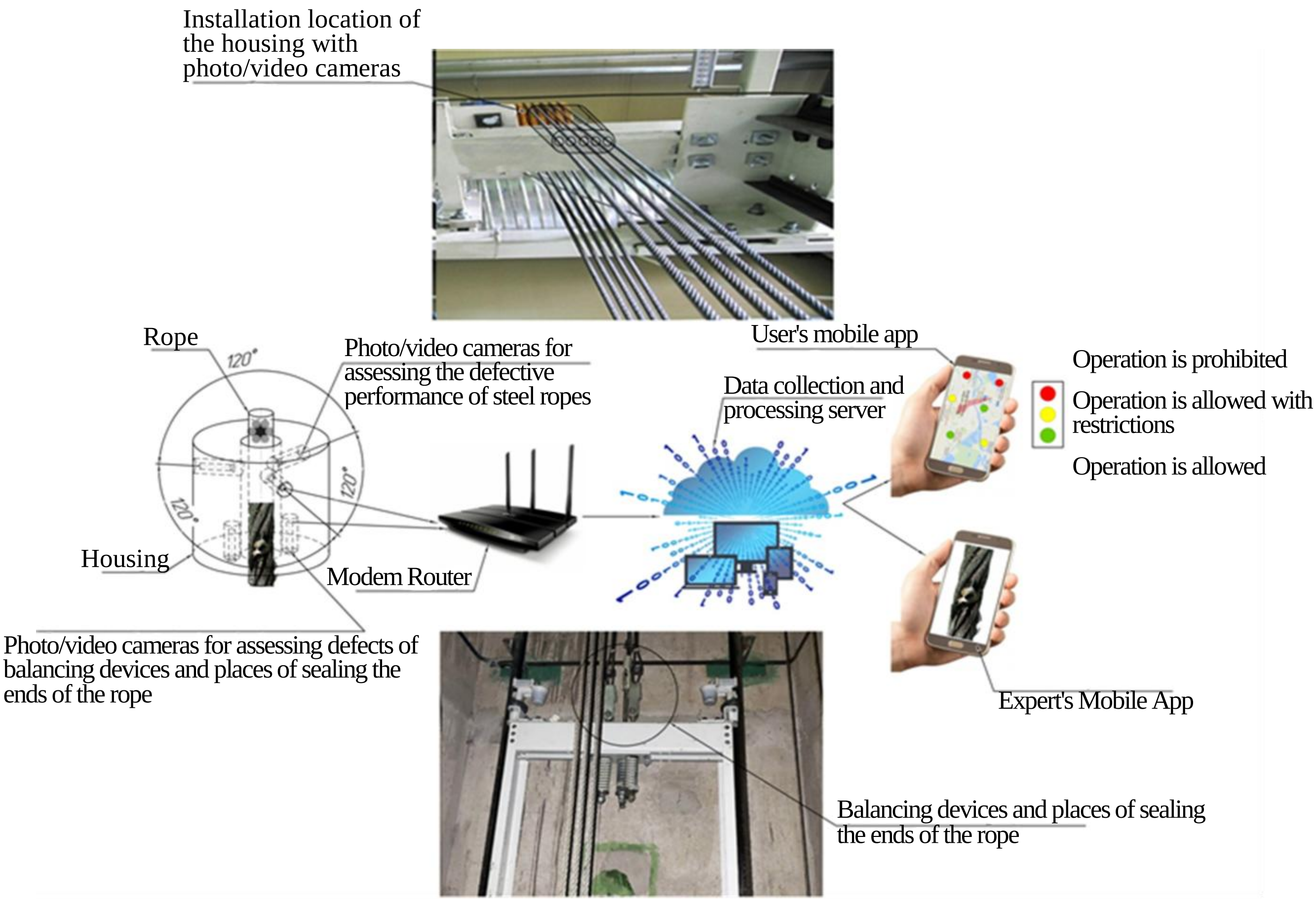

Fig. 6. PAC functional scheme (Authors' figure)

Discussion and Conclusion. Integral risk assessment in the diagnosis of steel ropes using computer vision, taking into account its advantages over the traditional visual and instrumental control system will be in demand by the industry of cable traction machines. This market is the target for the use of the product created by the authors. For example, the number of passenger elevators in operation on the territory of the Russian Federation is 450 thousand units. More than 50 thousand organizations are engaged in elevator maintenance. Each elevator requires a hardware part of the complex, i.e. the volume of the consumer market is 450 thousand pcs. The software part is necessary for each service organization, i.e. 50 thousand licenses. The mobile application is necessary for the specialists of each service organization, which must have at least three specialists, i.e. 150 thousand licenses. Taking into account the technological and economic advantages (the price is about 55 thousand rubles), the developed system will take a strong position in the industry of cable cars.

References

1. Martinod R., Estepa D., Paris C., Trujillo A. Journey Safety Assessment to Urban Aerial Ropeways Transport Systems Based on Continuous Inspection During Operation. Journal of Transportation Saropefety & Security. 2015;7:279-290. 10.1080/19439962.2014.942018

2. Ferrarese M., Loner E., Pulina M. Demand, business profitability and competitiveness in the cableway system: A multidimensional framework. Research in Transportation Economics. 2021;90:101041. https://doi.org/10.1016/j.retrec.2021.101041

3. Piskoty G., Affolter Ch., Sauder M., Nambiar M., Weisse B. Failure analysis of a ropeway accident focussing on the wire rope's fracture load under lateral pressure. Engineering Failure Analysis. 2017;82:648-656. https://doi.org/10.1016/j.engfailanal.2017.05.003

4. Peterka P., Krešák J., Vojtko M., Mantič M. Failure analysis of the journal bearing pulley of the cargo cable way. Engineering Failure Analysis. 2020;111:104329. https://doi.org/10.1016/j.engfailanal.2019.104329

5. Mapelli C., Barella S. Failure analysis of a cableway rope. Engineering Failure Analysis. 2009;16(5):1666-1673. 10.1016/j.engfailanal.2008.12.011

6. Panfilov A. V., Deryushev V. V., Korotkiy A. A. Recommended Safety Systems for Risk-Oriented Approach. Occupational Safety in Industry. 2020;5:48–55. (In Russ.).

7. Panfilov A. V., Bakhteev O. A., Deryushev V. V., Korotkiy A. A. Adaptive remote monitoring and control system for the operation of hazardous facilities based on a risk-based approach. Safety of Technogenic and Natural Systems. 2020;2:19–29. https://doi.org/10.23947/2541-9129-2020-2-19-29 (In Russ.).

8. Panfilov A. V., Korotkiy A. A., Ivanov B. F., Panfilova E. A. About criteria and standards for discharge of ropes of passenger ropeways. Scientific and Technical Journal of Bryansk State University. 2021;1:53–65. (In Russ.).

9. Shakti P. J., Mohd I., Subbaratnam B., Naresh K. Dynamic behavior of ropeway string. IOP Conf. Series: Materials Science and Engineering 998. 2020:012068. 10.1088/1757-899X/998/1/012068

10. Kattimani M. A., Ibrahim M., Ahmed M. A., Salam M. A. Modelling and analysis of helical ropeway string. Journal of Emerging Technologies and Innovative Research. 2022;9(6):357-365. Available from: https://www.researchgate.net/publication/361612084_MODELLING_AND_ANALYSIS_OF_HELICAL_ROPEWAY_STRING

11. Fontanari V., Menapace C., Pedrotti E. Study of the lightning damage produced in a full-locked wire rope of an aerial cableway. Engineering Failure Analysis. 2019;103:530-539. 10.1016/j.engfailanal.2019.05.002

12. Wahid A., Mouhib N., Ouardi A., Sabah F., Chakir H., Lghorba M. E. Experimental prediction of wire rope damage by energy method. Engineering Structures. 2019;201:109794. https://doi.org/10.1016/j.engstruct.2019.109794

13. Peterka P., Kačmáry P., Krešák J., Šimoňák J., Bindzár P., Mitrík D. Prediction of fatigue fractures diffusion on the cableway haul rope. Engineering Failure Analysis. 2016;59:185-196, https://doi.org/10.1016/j.engfailanal.2015.10.006

14. Collini L., Degasperi F. MRT detection of fretting fatigue cracks in a cableway locked coil rope. Case Studies in Nondestructive Testing and Evaluation. 2014;2:64-70. https://doi.org/10.1016/j.csndt.2014.09.001

15. Yanfei Kou, Jiujiang Guo, Jingjing Li, Shaoni Jiao, Jiquan Liu, Zhiwei Yan, Kun Zhu A New Detection Method of the Surface Broken Wires of the Steel Wire Rope Using an Eddy Current Differential Probe. IEEE Access. 2022;10:63619–63625. https://doi.org/10.1109/ACCESS.2022.3183097

16. Kumar K., Goyal D., Banwait S. S. Effect of Key Parameters on Fretting Behaviour of Wire Rope. Archives of Computational Methods in Engineering. 2020;27:549–561. https://doi.org/10.1007/s11831-019-09326-y

Received 11.01.2023

Revised 16.01.2023

Accepted 16.01.2023

About the Authors:

Panfilov, Aleksey V., associate professor of the Operation of Transport Systems and Logistics Department, Don State Technical University (1, Gagarin sq., Rostov-on-Don, 344003, RF), Cand. Sci. (Eng.), associate professor, ScopusID, ORCID, panfilov@ikcmvsl.ru

Nikolaev, Nikolay N., associate professor of the Operation of Transport Systems and Logistics Department, Don State Technical University (1, Gagarin sq., Rostov-on-Don, 344003, RF), Cand. Sci. (Eng.), associate professor, ResearcherID, ScopusID, ORCID, nnneks@yandex.ru

Yusupov, Aleksandr R., senior lecturer of the Robotics and Mechatronics Department, Don State Technical University (1, Gagarin sq., Rostov-on-Don, 344003, RF), ORCID , temple_black@mail.ru

Korotkiy, Anatoliy A., head of the Operation of Transport Systems and Logistics Department, Don State Technical University (1, Gagarin sq., Rostov-on-Don, 344003, RF), Dr. Sci. (Eng.), professor, ScopusID, ORCID, korot@novoch.ru

Claimed contributorship

A. V. Panfilov: formulation of the basic concept, goals and objectives of the study; N. N. Nikolaev: data preparation, text preparation, conclusions formulation; A. R. Yusupov: data preparation, text preparation, illustrations preparation; A. A. Korotkiy: academic advising, analysis of the research results, revision of the text, correction of the conclusions.

Conflict of interest statement

The authors do not have any conflict of interest.

All authors have read and approved the final manuscript.

CHEMICAL TECHNOLOGIES, MATERIALS SCIENCES, METALLURGY

Original article
UDC 614. 841
https://doi.org/10.23947/2541-9129-2023-1-70-75

Structural Organization of Steel to Ensure Special Equipment Safety

Viktor N. Pustovoit, Yuri V. Dolgachev, Ivan V. Ivankov
Don State Technical University, 1, Gagarin Sq., Rostov-on-Don, Russian Federation
✉ fipm-dstu@mail.ru

Abstract

Introduction. At present, great success has been achieved in the field of creating effective protective materials. Various non-metallic, metal-ceramic, a0nd also composite materials act as armor elements. However, most of the armor elements of vehicles and personal protective equipment (PPE) are steels that, along with high ballistic resistance, have a high mass. In this regard, the relevance of the article is related to the possibility of lightening typical protective elements when using a material that has a structural organization like a natural ferrite-martensite composite (NFMC). The work objective is to evaluate the prospects of using steel with an oriented structure as an effective protective material when exposed to high-speed concentrated impact of high power in comparison with the steel materials used.

Materials and Methods. The features and disadvantages of effective armor steels are revealed, a comparative analysis is carried out with steel oriented as NFMC. The assessment of 14G2 steel microstructure state with different hardening temperatures (730 °C and 760 °C) was carried out by the method of microstructural analysis. In relation to the topic of the study, the prospects for the use of low-carbon ferritic-martensitic steel were shown based on the laws of fracture mechanics and their comparison with the experimental data obtained on a sample of 14G2 steel with dimensions of 150×44×7 mm after testing for bullet resistance by cartridges with a steel core and armor-piercing cartridges with a tungsten core made of SVD rifles and AK-74 assault rifles of 7.62 mm and 5.45 mm caliber, respectively.

Results. The possibilities of resistance to fracture of steel with an oriented ferritic-martensitic structure are evaluated in comparison with typical homogeneous and heterogeneous steel materials. The resistance of such steel is related to the nature of the development of fracture, expressed in the deceleration of the crack during delamination at the ferrite-martensite boundaries. When a delamination is formed, a crack expends energy on delamination and changes its direction, which subsequently leads to a complete stop of the fracture process.

Discussion and Conclusion. The disadvantages of armor elements made of homogeneous and heterogeneous steel materials, associated with a high effective thickness of the protective element and the laborious process of obtaining a steel sandwich, respectively, can be solved by using oriented ferritic-martensitic steel. The data presented indicate a higher fracture resistance due to a special crack propagation mechanism, which is relevant in the development of armored vehicles. This makes it possible to reduce the total mass of combat vehicles associated with a decrease in the effective thickness of protective elements while maintaining the required class of resistance to high-speed impact loading, which will increase their mobility and reduce fuel consumption.

Keywords: steel composite, ferrite, martensite, high-speed impact, fracture resistance, heat treatment, ensuring the safety of special equipment.

For citation. V. N. Pustovoit, Yu. V. Dolgachev, I. V. Ivankov. Structural Organization of Steel to Ensure Special Equipment Safety. Safety of Technogenic and Natural Systems, 2023, no.1, pp. 70–75. https://doi.org/10.23947/2541-9129-2023-1-70-75

Introduction. A characteristic trend in the development of military equipment is the permanent improvement of protective materials. So, instead of thick sheet metal, they are moving to the creation of multilayer metal, as well as non-metallic and metal-ceramic compositions. At the same time, the process of creating effective protective materials pursues two goals — reducing the mass of the protective element and increasing its ballistic resistance. These mutually exclusive factors make it possible to increase the mobility of combat transport systems and ensure safety from the effects of various firearms and fragmentation types of injuries. To simultaneously achieve the above goals, it is proposed to use steel with a structure organized as a natural ferrite-martensitic composite (NFMC) as an effective protective material.

Materials and Methods. The development of the above materials began with the desire to increase the resistance to high-speed high-power impact of hot-rolled homogeneous steel sheets with different carbon content and different degrees of alloying. So, in work on obtaining bullet-resistant steel material[1], the advantages of alloy carbon steel of the composition, % are reflected: carbon — 0.44–0.48; silicon — 1.2–1.6; manganese — 0.3–0.6; chromium — 1.3–1.7; nickel — 1.4–1.8; molybdenum — 0.2–4; iron — the rest. This steel, after quenching and low tempering, has a hardness of about 55-57 HRC and, with a plate thickness of 4.0 mm, provides the 3rd class of protection against a 7.62 mm steel PS bullet (cartridge 57-H-231) of the AKM assault rifle and a 5.45 mm PS bullet (cartridge 7H6) of the AK-74 assault rifle. Such a material has a small effective thickness (8-9 % less than typical steels), but its destruction occurs by the mechanism of brittle destruction (usually an armor plate split occurs). In addition, the production of such steel requires careful control of chemical composition. An increase in viscosity and a change in the nature of destruction require a decrease in the material hardness. However, if the hardness is below 48 HRC, when tested with bullets with a heat-strengthened core, the material is penetrated, although the destruction is viscous.

To eliminate this drawback, two- and more layered steel compositions were created. They are made by explosion welding, pack rolling or surfacing methods [1, 2]. The basic principles of the development of two-layer materials are reduced to obtaining a high hardness of the front layer (about 58-60 HRC) and a high viscosity of the back layer with a hardness of at least 50 HRC. Tests of double-layer steel compositions have shown that when firing from an SVD rifle (caliber 7.62 mm, cartridge 7-B3-3, armor-piercing incendiary bullet B32), sheets are not broken at thicknesses of 10.2–10.6 mm. However, with a higher resistance of these materials, the effective thickness, compared with homogeneous steel armor plates, is almost 2-2.5 times greater.

The use of three-layer compositions with a low-carbon steel interlayer [3] makes it possible to reduce thickness of the armor plate to 8.9 mm. However, a significant disadvantage is the complex technological process of obtaining multilayer armor plates. For reliable adhesion, labor-intensive explosion welding, hot rolling with compression up to 70 %, and in some cases, a combined method with subsequent heat treatment is used.

This paper shows the advantages of a protective material in the form of steel with a structure organized as NFMC.

[1] Kamaev E. A., Sakharov S. A. Vysokoprochnaya bronevaya listovaya stal'. Patent 2185459 C1, Russian Federation, C22C 38/44, No. 2001124667/02, 2002. (In Russ.).

Results. The well-known technology for NFMC production[2] consists in controlled rolling in the intercritical temperature range (A_1–A_3) of steels with a carbon concentration of 0.1-0.2 % to orient in the direction of rolling the ferritic and austenitic phases with a compression ratio of at least 30 % and subsequent quenching. However, rolling in this temperature range is quite time-consuming, as it requires the presence of powerful rolling equipment. In addition, with a low degree of compression, it is not possible to obtain a strict orientation of the ferrite-martensitic structure.

At the same time, obtaining a ferrite-martensitic composite is possible in a less labor-intensive way. Strict orientation of the structure can be obtained by using the following technological mode[3]: hot rolling with at least 70 % of compression, followed by cooling to an intercritical temperature range (A_{C1}–A_{C3}), exposure in this interval for phase refining, quenching followed by low tempering. Such processing does not require powerful rolling equipment and can be carried out in a conventional rolling shop. At the same time, it is necessary to control the sulfur content at the upper level of the grade composition (0.04–0.05 %) to form a sufficient amount of sulfides (Fe, Mn)S, which are stretched into thin plates during rolling (Fig. 1 *a*) and are substrates on which excess ferrite is formed (Fig. 1 *b*), forming elongated plate formations along the rolling direction. The perlite structural component is also oriented (Fig. 1 *b*).

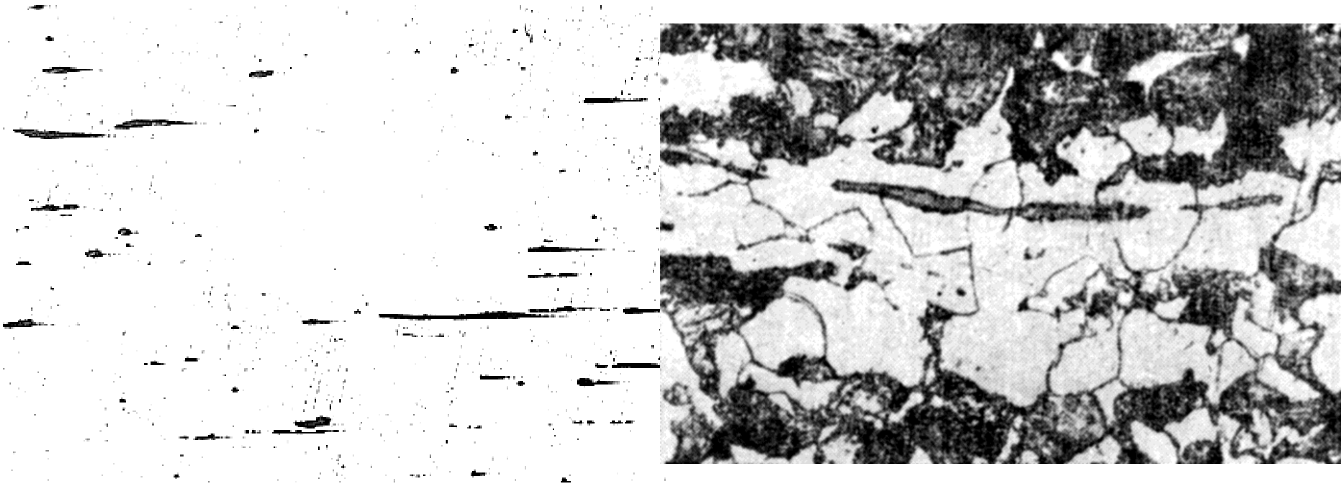

a *b*

Fig. 1. 14G2 steel with a ferritic-martensitic composite structure: *a* — sulfides elongated along the rolling direction, ×100; *b* — ferrite nucleation on a sulfide substrate, ×300

Varying the quenching temperature from the intercritical interval, it is possible to obtain different ratios of the volume fractions of ferrite and martensite[4], as well as different concentrations of carbon in martensite and, consequently, different hardness of martensite plates. As a result of this process, an oriented ferrite-martensitic structure is obtained, providing anisotropy of the material properties (Fig. 2).

[2] Supov A. V. et al. Termicheskaya i termomekhanicheskaya obrabotka stali i chuguna. Metallovedenie i termicheskaya obrabotka stali i chuguna. Spravochnik. Moscow: Intermet Inzhiniring, 2007. Vol. 3. 919 p. (In Russ.).

[3] Pustovoit V. N. et al. Sposob polucheniya estestvennogo ferritno-martensitnogo kompozita. Patent No. 2495141, Russian Federation, C21D 8/00, C21D 8/02, No. 2012119557/02, 2013. 7 p. (In Russ.).

[4] Lavrinenko V. Yu., Posalina A. E. Issledovanie vliyaniya predvaritel'noi termicheskoi obrabotki na poluchenie dvukhfaznoi ferritno-martensitnoi struktury stalei 20 i 20G2R. Novye tekhnologii v uchebnom protsesse i proizvodstve: mat-ly XX mezhdunar. nauch-tekh. konf. Ryazan, 2022. P. 111–115. (In Russ.).

Fig. 2. 14G2 steel with NFMC structure after quenching from 780 °C (29 % martensite), ×360

Theoretical calculations [4] show that layering (artificial or natural) increases fracture toughness of the material and reduces the crack propagation rate.

For NFMC structure, it should be noted that martensitic layers in the ferritic matrix have a finite length (discrete fibers) and some misorientation of ferrite and martensite layers. In this case, as noted in [5], high fracture resistance is provided when the volume fraction of the hardening phase is ~20-25 %, a certain length of fibers from the hardening phase (martensite) is greater than a certain critical value (*lкр* ≥80 microns), and the misorientation of ferritic and martensitic layers is no more than 15.

Test results [6] of steel plates with NFMC structure (dimensions 150×44×7 mm) with steel-core cartridges and armor-piercing tungsten-core cartridges from the SVD rifle and AK-74 rifle of 7.62 98m and 5.45 mm caliber showed that a sample with a small thickness of ferritic layer and low-carbon martensite (quenching from 760 °C) was almost always destroyed. At the same time, a sample with a greater thickness of the ferritic layer and a higher carbon martensite (quenching from 730 °C) showed high ballistic resistance (Fig. 2). This sample did not collapse after being shot by armor-piercing bullets; the metal was deformed by 2-3 mm with the projectile ricocheting, while a small crack formed on the back side.

High ballistic resistance of steel with such a structure is associated with a special mechanism for the development of destruction in the material. When, during the movement of the crack, it approaches the ferrite-martensite boundary, stratification occurs in the ferrite (Fig. 3), as a result of which the crack changes the direction of movement and spends energy on ferrite stratification. The subsequent development of the fracture leads to a change in the crack trajectory with ferrite stratification, stopping the movement of the crack and stress relaxation at its apex.

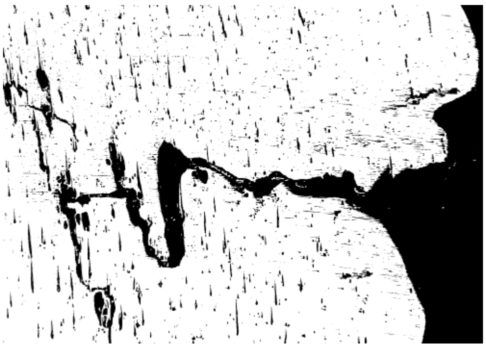

Fig. 3. Direction of movement of a crack in a material with NFMC structure having a vertical orientation of layers, ×50

This result is consistent with the data of works [4, 7, 8], which indicate that discontinuities may form in the layered material along the interface during the fracture process, transferring the crack to a position less favorable for its propagation and leading to the deceleration of the fracture.

Discussion and Conclusion. Thus, the test results show that the use of steel with NFMC structure provides a high level of ballistic resistance with a lower effective thickness and complexity of manufacturing this material. This indicates its advantages over homogeneous steels and multilayer steel compositions. A special method of braking destruction with high-speed local exposure to high power provides a higher threshold of survivability of protection, and reducing the effective thickness increases the mobility of combat vehicles and personnel by reducing the total mass of protection.

References

1. Tsukanov V. V., Mileykovsky A. B., Nigmatulin O. E., Savichev S. A. Advanced steels for protection of special military machines. Military Enginery. Scientific and Technical Journal. Counter-terrorism technical devices. Issue 16. 2018;1–2(115–116):86–94. (In Russ.).

2. Gladyshev S. A., Grigoryan V. A. Bronevye stali. Moscow: Intermet Inzhiniring, 2010. 334 p. (In Russ.).

3. Shishkin T. A., Pervukhin L. B. Combined method of manufacturing armored steel. Izvestia VSTU. 2020;11(246):53–57. (In Russ.).

4. Krausz A. S. Fracture Kinetics of Crack Growth. Springer Netherlands, 2011. 196 p.

5. Wood W. A. The Study of Metal Structures and Their Mechanical Properties. Elsevier Science, 2014. 400 p.

6. Pustovoit V. N., Dolgachev Yu. V, Dombrovskii Yu. M. Ballistic Resistance of Steel with the Structure of a Natural Ferrite-Martensitic Composite. Safety of Technogenic and Natural Systems. 2022;3:54–59. https://doi.org/10.23947/2541-9129-2022-3-54-59 (In Russ.).

7. Pustovoit V. N., Duka V. V., Dolgachev Yu. V. The scenario of crack growth in steel with the structure of a ferrite-martensitic composite. Izvestia VSTU. 2017;10(205):118–121. (In Russ.).

8. Pustovoit V. N., Dolgachev Y. U., Dombrovskii Y. M., Duka V. V. Structural Organization and Properties of a Natural Ferrite-Martensite Steel Composite. Metal Science and Heat Treatment. 2020;62(5-6):369-375. 10.1007/s11041-020-00570-9

Received 09.01.2023.
Revised 16.01.2023.
Accepted 16.01.2023.

About the Authors:

Pustovoit, Viktor N., professor of the Materials Science and Metal Technology Department, Don State Technical University, (1, Gagarin sq., Rostov-on-Don, 344003, RF), Dr. Sci. (Eng.), professor, ORCID, fipm-dstu@mail.ru

Dolgachev, Yuri V., associate professor of the Materials Science and Metal Technology Department, Don State Technical University, (344003, Russian Federation, Rostov-on-Don, Gagarin Square, 1), Cand. Sci. (Eng.), associate professor, ORCID, yridol@mail.ru

Ivankov, Ivan V., Master's degree student of the Materials Science and Metal Technology Department, Don State Technical University, (344003, Russian Federation, Rostov-on-Don, Gagarin Square, 1), ORCID, yanya.ivankov.99@gmail.com

Claimed contributorship

V. N. Pustovoit — formation of the basic concept, goals and objectives of the study, scientific guidance, preparation of the text, formation of conclusions; Yu. V. Dolgachev — testing, processing, analysis and discussion of the results of the study; I. V. Ivankov — preparation of samples for metallographic analysis, revision of the text.

Conflict of interest statement

The authors do not have any conflict of interest.

All authors have read and approved the final manuscript.